NIPER/BDM-0074
Distribution Category UC-122

Chemical Systems for Improved Oil Recovery: Phase Behavior, Oil Recovery, and Mobility Control Studies

Topical Report

By
F. Llave
B. Gall
H. Gao
L. Scott
I. Cook

September 1995

Work Performed Under Contract No. DE-AC22-94PC91008

Prepared for
U.S. Department of Energy
Assistant Secretary for Fossil Energy

Jerry Casteel, Project Manager
Bartlesville Project Office
P.O. Box 1398
Bartlesville, OK 74005

Prepared by
BDM-Oklahoma, Inc.
P.O. Box 2565
Bartlesville, OK 74005

DISCLAIMER

DISCLAIMER

Portions of this document may be illegible in electronic image products. Images are produced from the best available original document.

ACKNOWLEDGMENT

This work was sponsored by the U.S. Department of Energy under M&O contract agreement DE-AC22-94PC91008. The authors wish to thank Drs. Arfon H. Jones and Rebecca S. Bryant of BDM-Oklahoma. for their guidance and advice in conducting the study, Kathleen M. Bertus, and Deanna Evans also of /BDM-Oklahoma and Ligin Zhu and Pei-Chi Chung, DOE/AWU Summer Internees, for their assistance in all phases of the experimental work performed for this project. The authors also wish to acknowledge Dr. Liviu Tomutsa and his staff of the CT Imaging Group for their expertise, advice, and assistance while conducting the CT-monitored experiments.

Table of Contents

Page

1.0 INTRODUCTION 1

2.0 EXPERIMENTAL PROCEDURES 3

2.1 Phase Behavior 3

2.2 Salinity and Alkane Scans 3

2.3 Phase Inversion Temperature (PIT) Measurements 3

2.4 Interfacial Tension (IFT) Measurements 4

2.5 Coreflooding Experiments 4

2.6 Computer-Aided Tomography Imaging Techniques 4

2.7 Polymer Studies 4

2.7.1 Materials 4

2.7.2 Polymer Preparation 5

2.7.3 Viscosity Measurements 5

2.7.4 Polymer Flow in Porous Media 5

3.0 RESULTS AND DISCUSSION 7

3.1 Surfactant Phase Behavior Studies 7

3.2 Coreflooding Experiments 16

3.3 Mobility Control Studies 28

3.3.1 Polyacrylamide Polymers 29

3.3.1.1 Polymer Stability Studies 29

3.3.1.2 Flow Through Berea Sandstone Core 30

3.3.2 Flow Characteristics of Xanthan Biopolymer 33

3.3.3 Relative Permeability Curves and Mobility Control Design 35

3.3.3.1 Calculation Methods 35

3.3.3.2 Mobility Calculations for Polymers Used in this Study 37

3.3.3.3 Summary of Mobility Study 41

3.3.4 CT-Monitored Coreflood for Initial Mobility/Oil Recovery Study 42

3.4 Simulation of Corefloods with UTCHEM Simulator 47

3.4.1 Simulation Run 50

3.4.2 Summary 50

4.0 SUMMARY AND CONCLUSIONS 53

5.0 REFERENCES 57

APPENDIX 59

TABLES

		Page
1	Summary of Coreflooding Experiments	17
2	Chemical Formulations Used in the Mobility Control Studies	28
A-1	*Brine Compositions Used in the polymer Stability Tests*	59

FIGURES

1	Phase inversion temperature (PIT) for 1.0 wt% DM-530 + 1.0 wt% TRS/IBA [1:1] with n-decane	8
2	Phase inversion temperature (PIT) for 0.8 wt% DM-530 + 1.2 wt% TRS/IBA [1:1] with n-decane	8
3	Phase inversion temperature (PIT) for 0.6 wt% DM-530 + 1.4 wt% TRS/IBA [1:1] with n-decane	9
4	Phase inversion temperature (PIT) for 0.4 wt% DM-530 + 1.6 wt% TRS/IBA [1:1] with n-decane	9
5	Phase inversion temperature (PIT) for 0.2 wt% DM-530 + 1.8 wt% TRS/IBA [1:1] with n-decane	10
6	Phase inversion temperature (PIT) for 2.0 wt% DM-530 with n-decane	10
7	Alkane scan for TRS/IBA + DM-530 system at ambient temperature.	12
8	Alkane scan for TRS/IBA + DM-530 system at 40 °C.	12
9	Middle phase behavior limits for TRS/IBA + DM-530 system.	13
10	Phase inversion temperature (PIT) for 1.0 wt% DM-530 + 1.0 wt% TRS/IBA [1:1] with n-heptane	14
11	Phase inversion temperature (PIT) for 1.0 wt% DM-530 + 1.0 wt% TRS/IBA with n-heptane and 500 ppm polymer	14
12	Phase inversion temperature (PIT) for 1.0 wt% DM-530 + 1.0 wt% TRS/IBA with n-heptane and 1000 ppm polymer.	15
13	Effect of polymer loading on phase behavior of DM-530 + TRS/IBA system with n-heptane	15
14	Effect of brine permeability on oil saturation reduction and recovery efficiency of an optimized chemical system.	18
15	Comparison of oil saturation (Socf) vs. brine permeability. Experiments using (a) straight chemical slug , (b) 3-Ø slug, and (c) large pore volume ASP slug.	18
16	Oil cut vs. pore volume injected in different permeability cores	20
17	Oil recovery vs. pore volume injected in different permeability cores.	20
18	Final oil saturation (Socf) vs. permeability for chemical floods started at initial oil saturation and at residual oil saturation after waterflood	21
19	Oil saturation (Socf) and oil cut vs. pore volume injected for coreflood no. 6.	22
20	Oil saturation (Socf) and oil cut vs. pore volume injected for coreflood no. 1.	22
21	Oil saturation (Socf) and oil cut vs. pore volume injected for coreflood no. 8.	23
22	Oil saturation (Socf) and oil cut vs. pore volume injected for coreflood no. 2.	24
23	Oil saturation (Socf) and oil cut vs. pore volume injected for coreflood no. 4.	24
24	Oil saturation (Socf) and oil cut vs. pore volume injected for coreflood no. 3.	25
25	Oil saturation (Socf) and oil cut vs. pore volume injected for coreflood no. 7.	27
26	CT-monitored flow profile of experiment(a) oil saturated core, (b) 0.25 PV untagged 3-Ø chemical slug injected, (c) 0.6 PV untagged polymer slug injected, and (d) 3.0 PV untagged brine injected, end of experiment	26
27	Relative change in viscosity for different polymer and salinity concentrations after aging for one month at (a) 23 and (b) 50 °C.	29

FIGURES - Continued

		Page
28	Flow characteristics of Alcoflood 935 in high permeability Berea sandstone core	31
29	Flow characteristics of Alcoflood 1135 in high permeability Berea sandstone core	31
30	Comparison of flow behavior of two polyacrylamide polymers in similar Bereasandstone core	31
31	Flow characteristics of Alcoflood 1135 in different permeability core	32
32	Flow characteristics of Flocon 4800C in high permeability Berea sandstone core	33
33	Comparison of Xanthan biopolymer flow characteristics in porous media with similar permeability	34
34	Differences in flow characteristics of polyacrylamide polymer and Xanthan biopolymer. Slope of the power fit curve for Xanthan biopolymer is approximately 50% of that for the polyacrylamide polymers	34
35	Oil and water relative permeability curves for high permeability Berea sandstone core	36
36	Total mobility in high permeability Berea sandstone core as a function of oil viscosity	37
37	Oil and water relative permeability as a function of aqueous phase saturation for 260-mD Berea sandstone core	38
38	Comparison of total mobility for 1.3 cP oil as a function of core permeability	38
39	Comparison of total mobility for 17 cP oil as function of core permeability	38
40	Polymer mobility in 700-mD Berea sandstone core as a function of fluid frontal velocity	39
41	Polymer mobility in 260-mD Berea sandstone core as a function of fluid frontal velocity	39
42	Mobility characteristics of Alcoflood 935 polymer in high permeability Berea sandstone core	40
43	Mobility characteristics of polyacrylamide polymer MO3000H-SF prepared in low ionic strength water and in sodium carbonate solutions	41
44	Mobility characteristics of Xanthan biopolymer in high permeability Berea sandstone core as a function of fluid frontal velocity	42
45	Oil production for a chemical flood using an alkaline-surfactant-polymer system in high permeability Berea sandstone core	43
46	CT images of porosity and oil saturation distributions after various stages of a coreflood experiment in high permeability Berea sandstone core	45
47	Oil saturation distribution of a 38 cP oil after polymer injection of an alkaline-surfactant-polymer chemical system with poor mobility control characteristics	46
A-1	Initial viscosity of 2000 ppm polyacrylamide polymer, Alcoflood 935, in different salinity brines	60
A-2	Apparent viscosity of 2000 ppm polyacrylamide polymer, Alcoflood 935, in different salinity brines after aging at ambient temperature	60
A-3	Apparent viscosity of 2000 ppm polyacrylamide polymer, Alcoflood 935, in different salinity brines after aging at 50 °C	60
A-4	Initial viscosity of 1500 ppm polyacrylamide polymer, Alcoflood 935, in different salinity brines	61
A-5	Apparent viscosity of 1500 ppm polyacrylamide polymer, Alcoflood 935, in different salinity brines after aging at ambient temperature	61
A-6	Apparent viscosity of 1500 ppm polyacrylamide polymer, Alcoflood 935, in different salinity brines after aging at 50 °C	61
A-7	Initial viscosity of 1000 ppm polyacrylamide polymer, Alcoflood 935, in different salinity brines	62

FIGURES - Continued

		Page
A-8	Apparent viscosity of 1000 ppm polyacrylamide polymer, Alcoflood 935, in different salinity brines after aging at ambient temperature	62
A-9	Apparent viscosity of 1000 polyacrylamide polymer, Alcoflood 935, in different salinity brines after aging at 50 °C	62
A-10	Initial viscosity of 500 ppm polyacrylamide polymer, Alcoflood 935, in different salinity brines.	63
A-11	Apparent viscosity of 500 polyacrylamide polymer, Alcoflood 935, in different salinity brines after aging at 50 °C	63
A-12	Apparent viscosity of 500 polyacrylamide polymer, Alcoflood 935, in different salinity brines after aging at 50 °C	63
A-13	Apparent viscosity at ambient temperature of polyacrylamide polymer, Alcoflood 935 used in the polymer mobility control study. Viscosities agree with initial viscosity values measured in the polymer degradation studies.	64
A-14	Apparent viscosity at ambient temperature of polyacrylamide polymer, Alcoflood 1135 used in the polymer mobility control study.	64
A-15	Apparent viscosity at ambient temperature of Xanthan biopolymer, Flocon 4800C used in the polymer mobility control study	65

ABSTRACT

Selected surfactant systems containing a series of ethoxylated nonionic surfactants in combination with an anionic surfactant system have been studied to evaluate phase behavior as well as oil recovery potential. These experiments were conducted to evaluate possible improved phase behavior and overall oil recovery potential of mixed surfactant systems over a broad range of conditions. The importance of maximizing the production of oil initially mobilized by surfactant chemical systems resulted in an evaluation of mobility control polymers for selected experimental conditions. Both polyacrylamide polymers and Xanthan biopolymers were evaluated. In addition, studies were initiated to use a chemical flooding simulation program, UTCHEM, to simulate oil recovery for laboratory and field applications and evaluate its use to simulate oil saturation distributions obtained in CT-monitoring of oil recovery experiments.

The phase behavior studies focused on evaluating the effect of anionic-nonionic surfactant proportion on overall phase behavior. Two distinct transition behaviors were observed, depending on the dominant surfactant in the overall system. The first type of transition corresponded to more conventional behavior attributed to nonionic-dominant surfactant systems. This behavior is manifested by an oil-water-surfactant system that inverts from a water-external (highly conducting) microemulsion to an oil-external (nonconducting) one, as a function of temperature. The latter type which inverts in an opposite manner can be attributed to the separation of the anionic-nonionic mixtures into water- and oil-soluble surfactants. Both types of transition behavior can still be used to identify relative proximity to optimal areas. Determining these transition ranges provided more insight on how the behavior of these surfactant mixtures was affected by altering component proportions. Efforts to optimize the chemical system for oil displacement experiments were also undertaken. Phase behavior studies with systems formulated with biopolymer in solution were conducted. The results indicated that the overall solution behavior showed only a slight difference/shift in the presence of the polymer.

Oil recovery experiments were conducted on a select chemical formulation to evaluate the effect of the following variables: (1) effective brine permeability, (2) slug formulation, (3) slug content, (4) slug size, (5) initial oil saturation, and (6) injection strategy, on oil recovery potential. The results of the study showed a definite limiting effect of decreasing core permeability on the effectiveness of chemical treatments for oil displacement. The results showed that experiments conducted in low permeability Berea sandstone cores yielded much higher final oil saturations than those obtained in high permeability cores, under comparable displacement conditions. These results were comparable to those obtained by others researchers for the range of permeabilities tested. Permeability had a more profound impact on oil recovery than the chemical slug size, up to a reasonable, economic limit. Increasing the treatment size was only one of the means to overcome the limiting effects of low permeability on oil recovery. The results from the CT-monitored experiment lend excellent support to the observations made with regards to the effect of permeability on oil recovery potential. Experiments in high permeability cores showed very good frontal sweep, indicative of favorable oil displacement, while the experiments in low permeability cores exhibited the opposite, with significant fluid bypass indicated. CT-aided monitoring has emerged as a valuable tool in evaluating the treatment effectiveness and future displacement experiments need to be fully complemented with the routine use of these types of tools.

The coreflooding results also showed that the proportion of the oil/brine/surfactant in the middle-phase slug also affected the oil displacement. Chemical proportions at near optimal conditions were much more effective in reducing oil saturation levels compared to the systems with higher oil proportions (above optimal). The results followed the trend of: Optimal >Under Optimal >>Above Optimal. The results of the experiments conducted to evaluate the type of slug used indicated that final oil saturations from the straight chemical slug experiments were considerably higher compared to those using middle-phase slugs at comparable brine permeability. Although both sets of experiments were formulated to be optimal, the straight chemical slug was not as effective in oil displacement as the preequilibrated middle-phase slug. The injection of the microemulsion slug resulted in much better performance. Doubling the treatment slug size appeared to favor (larger incremental increase) the straight chemical slug experiments slightly more than when using middle-phase slugs. The final oil saturations of the latter type slugs were still lower than the straight chemical slug experiments. Additional experiments will be needed to confirm this observation.

Methods are described to determine polymer flow characteristics through porous media and determine minimum mobility requirements for chemical flooding applications. Several polyacrylamide polymers were studied. They differed in the amount of anionic character in the polymer chain. Lower anionic character provides less sensitivity to increased salt concentration in makeup waters. The polymers tested, however, were sensitive to the ionic strength of the solution and would not provide good mobility control for either high or low viscosity oil in either high or low permeability Berea sandstone core. If solution ionic strength was reduced, however, polymer viscosity increased and favorable mobility could be achieved. Xanthan biopolymer is much less sensitive to solution ionic strength, and its flow behavior through porous media was different than polyacrylamide. Biopolymer results from this study agreed with previous studies reported in the literature.

A CT-monitored coreflood designed with poor mobility control indicated relatively even chemical sweep, but poor overall reduction in oil saturation. This contrasted with a previous coreflood with poor mobility control where the oil saturation at the core outlet was much greater than at the core inlet, and chemicals appeared to channel through oil that had initially been mobilized by an alkaline-surfactant chemical formulation. CT-imaging should provide additional insight into problems of oil mobilization as a function of both mobility and core properties.

A review was conducted of the input parameters for the UTCHEM simulator for use in simulating laboratory and field oil recovery applications. Plans include the use of the simulator to compare oil saturations with those determined in the CT-imaging coreflood experiments. Present computing capability at NIPER will result in very long computation times to simulate the oil saturation distribution information, however.

1.0 INTRODUCTION

For many U.S. domestic oil reservoirs, chemical flooding Improved Oil Recovery (IOR) may be the only viable means of extending their productive lives. Chemical flooding has the capability of being a flexible EOR method which can recover more residual crude oil than other available methods. Sensitivity to changes in reservoir conditions, loss of effectiveness caused by chemical depletion, dilution, and separation, and cost make chemical IOR a complex process to apply, however. Mixed surfactant systems are adaptable to different reservoir conditions of salinity, temperature, and oil type and can be designed to achieve improved tolerance to adverse and/or variable reservoir conditions encountered by the injected fluids as compared to the types of surfactant systems studied extensively in the past. Broad based studies, including evaluating different chemical systems and optimizating application parameters, must be conducted for efficient and economic application at current and projected oil prices.

A multifaceted research effort involves evaluation of improved chemical flooding systems for field applications including Class 1 reservoirs. Areas of investigation described in this report include:

- Evaluation of mixed surfactant system phase behavior, solubilization parameters, and interfacial tension (IFT) at targeted temperature and salinity conditions

- Determination of oil-displacement potential and optimal injection strategy of selected chemical systems using conventional and CT-imaging methods to determine oil saturations

- Evaluation of mobility control requirements for candidate chemical systems

- Determination of the feasibility of using numerical simulators to compare simulated results from conventional and CT-aided core flood experiments and applications such as evaluating scaling criteria for experimental design for field applications of chemical IOR systems

The research work for FY 1994 continues to focus on the use of mixed surfactant systems. The phase behavior and oil displacement experiments were conducted on several mixed anionic-nonionic systems. These experiments were conducted to evaluate possible improved phase behavior and overall oil recovery potential of these mixed systems over a broad range of conditions. Different experimental parameters were evaluated to determine their corresponding effect on overall solution behavior. These included: temperature, salinity, hydrocarbon chain length, the presence of polymer in solution, and proportion of anionic and nonionic component in the system. These phase behavior studies were conducted to determine the presence of different phase transition behavior, depending on the proportions of the chemical components in the surfactant system. Efforts to optimize the chemical system for oil displacement potential were undertaken. Several coreflooding experiments were conducted to determine the effectiveness of the chemical system for oil recovery. These oil recovery experiments were conducted on a select chemical formulation to evaluate the effect on oil recovery potentialof the several variables, including: (1) effective brine permeability (2) slug formulation (3) slug content (4) slug size (5) initial oil saturation and (6) injection strategy. Both conventional and CT-

monitored coreflooding experiments were conducted. The CT-monitored experiment lend excellent support to the results obtained from the conventional experiments. CT-aided monitoring has become a valuable tool in evaluating displacement performance, and future displacement experiments need to be fully complemented with the routine use of these types of tools.

Design of chemical floods involving polymers for mobility control requires an understanding of polymer flow characteristics and rheology in porous medium. Previous oil recovery studies at NIPER and elsewhere have stressed the importance of adequate mobility control to keep oil that has been mobilized by a low interfacial tension chemical system moving in the direction of the producers. A number of factors affect polymer characteristics in the reservoir. These factors include the size, chemical composition, and concentration of the polymer, interaction of the polymer with other chemicals and minerals in the rock, rate of polymer degradation, rate of movement through the rock, and the type of rock structure in the reservoir, i.e. pore and pore throat sizes. Measurement of bulk rheological properties give only one aspect of the viscosity behavior of polymers. Evaluation of flow properties through rock provide additional important information for mobility design for both laboratory and field scale experiments.

During FY 1994, polymer flow experiments were conducted using several polyacrylamide polymers and one Xanthan polymer in Berea sandstone core with permeabilities in the range of 200 to 700 mD. Mobility control design requirements were reviewed. The polymer flow data were analyzed to provide general information for mobility control design for present and future laboratory experiments. One coreflood was conducted to evaluate mobility control design criteria for laboratory studies. This experiment also included computer-aided tomography (CT) monitoring of oil saturation distribution during various stages of oil production.

Finally, the ability to simulate coreflood results and oil saturation distribution results from CT imaging can provide a method to improve interpretation and provide input for evaluation of chemical processes for field applications. DOE has supported the development of a complex chemical flood simulator, UTCHEM, at the University of Texas. To gain familiarity with the capabilities of the UTCHEM simulator and to identify experimentally obtainable parameters to simulate the results of laboratory coreflood experiments, the input data file of UTCHEM (version 5.03) was reviewed. Future efforts will be incorporated into the research program to utilize the capabilities of this simulator.

This reports summarizes the results of the studies conducted. This work is part of a DOE sponsored research project, Development of Improved Chemical Methods (Task 2.1).

2.0 EXPERIMENTAL PROCEDURES

2.1 Phase Behavior

Phase behavior studies were conducted on selected chemical systems to screen for specific range of application. The effects of several experimental factors, such as: salinity, oil chain length, proportion of different combinations of anionic and nonionic surfactants, and the presence of mobility control polymer, on the phase behavior of the overall chemical/hydrocarbon systems were evaluated. The studies included the conventional salinity and alkane scans to determine optimal conditions and solubilization parameters, interfacial tension measurements, phase inversion temperature determination, and compatibility screening.

Details of the actual chemical systems studied for phase behavior and oil recovery experiments are given in the Results and Discussion section.

2.2 Salinity and Alkane Scans

Conventional salinity and alkane scans were conducted on select combinations of anionic and nonionic surfactants to determine optimal conditions for their application. From these studies, optimal salinity and alkane range were determined and used for further evaluation. Solubilization parameter is an important factor determined from these studies. The parameter is an indicator of the degree of interfacial activity and the balance of the oil and water affinity of the overall chemical system. These scans were typically conducted using solutions that were made up at a fixed water/oil ratio of 1:1, unless otherwise specified. These solutions were prepared in 10-mL glass pipets that were sealed and equilibrated in approved safety ovens at the desired temperature. The relative volumes of the different phases were read and recorded at set time intervals until constant readings were obtained. The solubilization parameters of the oil and the brine in the microemulsion phase were then calculated from stable phase volume readings. Specific details regarding the solubilization parameter calculations were discussed in an earlier report (Lorenz and Brock 1987).

2.3 Phase Inversion Temperature (PIT) Measurements

The determination of the phase inversion temperature (PIT) was used as a means of identifying the relative proximity of optimal conditions for the anionic-nonionic systems studied. This method was particularly applicable for chemical systems that exhibit significant changes in solution electrical conductivity during phase transition. The PIT measurements were conducted using a computer-controlled apparatus designed and constructed at NIPER (Llave and Olsen 1988). The PIT was determined as the temperature at which a water-in-oil emulsion changed into an oil-in-water emulsion or vice versa. This phase transition can be detected by monitoring the electrical conductivity of a well-stirred mixture as a function of the solution temperature.

2.4 Interfacial Tension (IFT) Measurements

The interfacial tension (IFT) of the different chemical systems tested was measured using a Model 300 Spinning Drop Interfacial Tensiometer, manufactured at University of Texas at Austin. These measurements were conducted using different equilibrated chemical systems at selected temperature conditions. These measurements were taken after sufficient equilibration time had been allowed at the temperature desired. Multiple measurements were taken until stable and reproducible values were obtained. Other parameters needed in the calculation of the IFT, such as densities and refractive indices, were measured using a Mettler/Paar DMA 45 Calculating Digital Density Meter and a Bausch & Lomb Refractometer. Details of these experimental and calculation procedures have been reported earlier (Llave *et al.* 1990).

2.5 Coreflooding Experiments

Coreflooding experiments were conducted to evaluate the oil displacement potential of several chemical systems. A series of these experiments was conducted to determine the effect of injection strategy, slug size, chemical slug formulation, permeability, and mobility control on overall oil displacement capacity of these systems. The experiments were conducted in Berea sandstone core plugs (3.8 cm in diameter and about 14 cm in length) of different brine permeabilities. The general procedures of conducting these experiments have been described in earlier reports (Llave *et al.* 1992). These procedures pertain to general fluid saturation steps, fluid pore volume, and core permeability determination. The injection strategy (oil displacement strategy) employed in each of the test conducted was systematically varied and was designed to identify the effects of different parameters on overall displacement efficiency. Some of these experiments were conducted with the aid of NIPER CT-imaging capability. The use of the CT-scanning capability provided a means to monitor the progression of the experiment during several stages of the run. The procedures to incorporate CT-monitoring with laboratory coreflooding experiments have been descibed previously (Gall 1992).

2.6 Computer-Aided Tomography Imaging Techniques

CT equipment, general operating procedures, and image processing techniques at NIPER have been developed and described previously (Tomutsa *et al.* 1990; Gall 1992). CT imaging is used to determine oil saturation distributions within the core during various stages of a chemical core flooding experiment. Formation and shape of the oil bank can be observed during surfactant injection, and non-uniform oil saturation distributions caused by core heterogeneities or inefficient fluid mobility properties can be visualized.

2.7 Polymer Studies

2.7.1 Materials

The flow characteristics of several commercial polymers were studied to determine mobility control characteristics for a few selected conditions. Polyacrylamide polymers included Alcoflood 935 and 1135 from Allied Chemicals and MO3000H-SF from Mitsubishi Kasei Corp. These products were solids presumed to be 100% active. A Xanthan biopolymer, 4800C, from Pfizer was an emulsion containing 13% to 16% active polymer. Polymer precipitation using isopropanol indicated that the

sample contained 14% biopolymer. An alkaline-surfactant-polymer flood was conducted as part of the mobility control investigations. The surfactant used for this test was Stepan's Petrostep B-100. The sample contained 48.3% active surfactant. All solutions were prepared by active weight unless otherwise noted.

2.7.2 Polymer Preparation

Polyacrylamide polymers were prepared in brines of interest by slowly sprinkling dried polymer into a fluid vortex produced by a magnetic stirrer. Polymer was either prepared with a desired concentration, or a 5000 ppm solution was prepared and diluted to the desired concentration. Preparation using these techniques minimize shear degradation of polyacrylamide polymers.

Xanthan gum was prepared by slowly adding concentrated polymer emulsion to a rapidly stirrer brine solution in a blender. The solution was stirred for approximately 1 minute at high speed. Brine was added to dilute the solution to the desired concentration. The solution was then stirred for 2 to 3 minutes.

2.7.3 Viscosity Measurements

Most polymer solution viscosities were measured using either a Brookfield Viscometer or a Contraves Low-shear-rate Viscometer. Since polymer solutions are non-Newtonian fluids, apparent viscosities were measured at several shear rates. A summary of apparent viscosity measurements as a function of shear rate for the polymers used in this study is given in the appendix.

2.7.4 Polymer Flow in Porous Media

Cylindrical core plugs approximately 14 cm long by 3.8 cm in diameter were cut from large blocks of Berea sandstone. Several different permeability ranges for the Berea sandstone were selected to determine polymer flow characteristics in porous medium. In general, the two permeability ranges of Berea sandstone used for the tests were labelled "700 mD" and "260 mD" from average air permeability measurements of the blocks. Liquid permeabilities were usually slightly lower than the air permeability values. However, for ease in comparison these general permeability labels are used throughout the text.

The core plugs were saturated with brine and loaded in a Hassler coreholder similar to that used in the oil recovery experiments. This apparatus has been described in previous reports. Brine permeability was then determined. Polymer solution at the highest level of polymer concentration (1500 ppm) was then pumped through the core until the pressure drop across the core stabilized. Differential pressures were then determined for different flow rates of polymer through the core. Typical flow rates varied from 0.0143 to 2.85 mL/min. (Darcy velocities of 0.06 to 12 ft/D). The measurements were then repeated for 1000 and 500 ppm polymer. Data analysis is described in the Results and Discussion section.

3.0 RESULTS AND DISCUSSION

3.1 Surfactant Phase Behavior Studies

Phase behavior studies were conducted on selected series of ethoxylated nonionic surfactants in combination with a primary anionic surfactant system. The objective of these studies was to evaluate and identify combinations of these anionic-nonionic surfactant mixtures that may exhibit improved phase behavior at selected conditions. The primary anionic surfactant system used in this study was the TRS 10-410/IBA system. This surfactant system has been fairly well-evaluated (Glinsmann 1978; Boneau and Campitt 1977). Prior tests with this system exhibited favorable solution behavior over a broad range of conditions in the presence of ethoxylated secondary surfactants. The present work was conducted to further evaluate the candidate chemical system over a select range of conditions, including the systematic evaluation of its oil recovery potential, and to evaluate the effect of the presence of mobility control polymers on solution behavior. Particular emphasis was made in determining effective solution behavior with different component proportions while maintaining a fixed nonionic surfactant component's hydrophilic-lipophilic balance (HLB) values. For this study, several experimental methods were employed in determining optimum conditions for the surfactant systems, including conventional salinity and alkane scans, the PIT determination, and IFT measurements.

Experimental evaluation of selected mixed surfactant systems included screening of several systems under different conditions. The phase behavior studies included evaluation of these mixtures for dependence on salinity and the type of hydrocarbon phase present. The primary system studied was an anionic-nonionic system of TRS 10-410/IBA + DM-530. The TRS 10-410/IBA component was a mixture of petroleum sulfonate surfactant with isobutyl alcohol (IBA), used as a base surfactant system. The DM-530 was an ethoxylated dialkyl phenol surfactant. Earlier work conducted with this chemical system narrowed down a range of salinities where it can be used. (Llave *et al.* 1993) This work was conducted to determine the effect of the proportion of the anionic-nonionic components of the mixture on optimal conditions.

The results of the phase behavior studies on the TRS 10-410/IBA + DM-530 system are presented in Figures 1 to 5. These experiments were conducted in the presence of n-decane as the oil phase with the proportion of anionic-nonionic component in the chemical systems varied. These mixtures were formulated over a broad range of chemical proportions from all nonionic component to all anionic component. As mentioned earlier, the purpose of the study was to quantify the effect of the proportion of the anionic-nonionic components of the mixture on optimal conditions.

Figure 1 shows a plot of the solution conductivity as a function of temperature at a fixed component proportion of 1:1. This plot corresponds to results of earlier studies under these conditions. (Llave *et al.* 1993) This Figure shows a typical plot of phase transition from a highly conducting water-external microemulsion to a poorly conducting oil-external microemulsion. This plot shows fairly significant transition behavior indicated by the magnitude (10^{-1} to 10^{-6} mhos) of the conductivity deviation at the phase inversion temperature. Figures 2 through 5 show plots of the solution conductivity as a function of temperature at different component proportions. As a comparison, figure 6 shows a plot of the transition behavior when the system was formulated with all nonionic

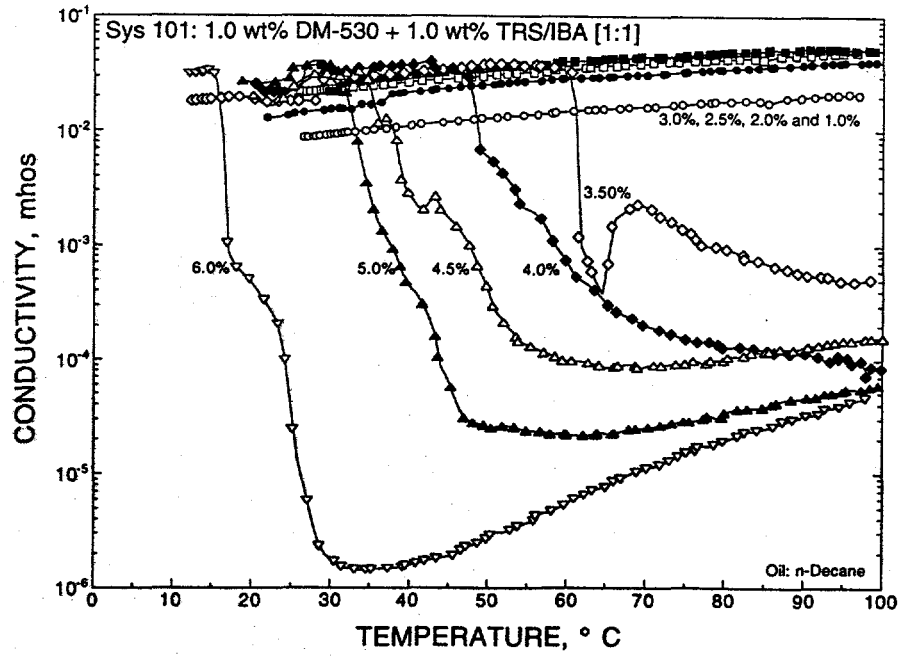

Figure 1 **Phase inversion temperature (PIT) for 1.0 wt% DM-530 + 1.0 wt% TRS/IBA [1:1] with n-decane.**

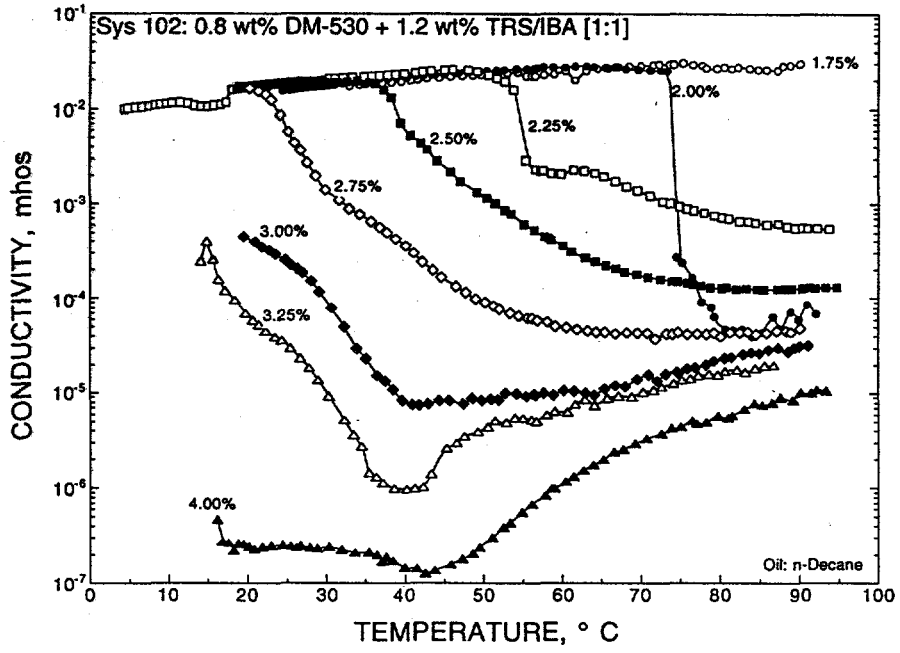

Figure 2 **Phase inversion temperature (PIT) for 0.8 wt% DM-530 + 1.2 wt% TRS/IBA [1:1] with n-decane.**

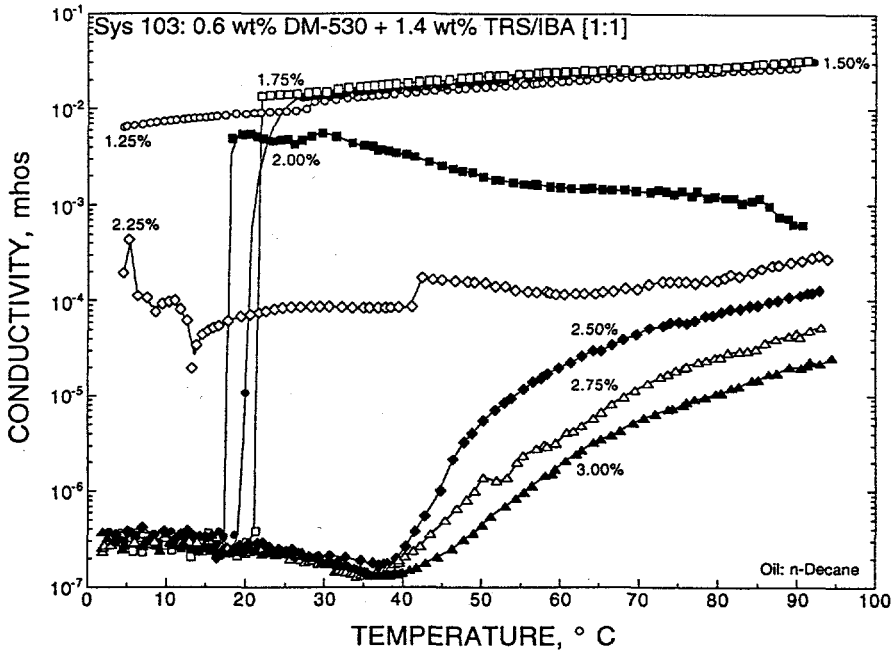

Figure 3 **Phase inversion temperature (PIT) for 0.6 wt% DM-530 + 1.4 wt% TRS/IBA [1:1] with n-decane.**

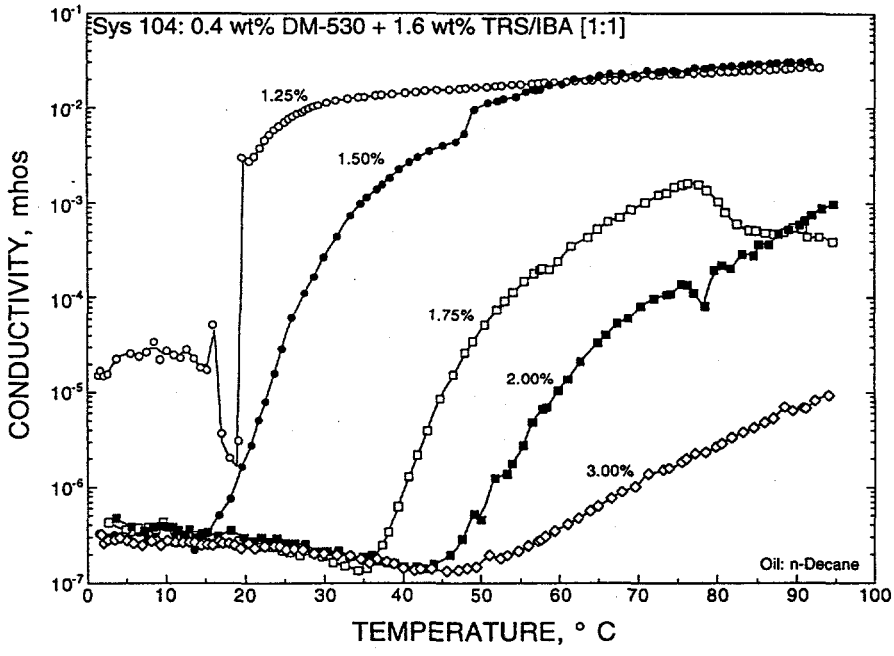

Figure 4 **Phase inversion temperature (PIT) for 0.4 wt% DM-530 + 1.6 wt% TRS/IBA [1:1] with n-decane.**

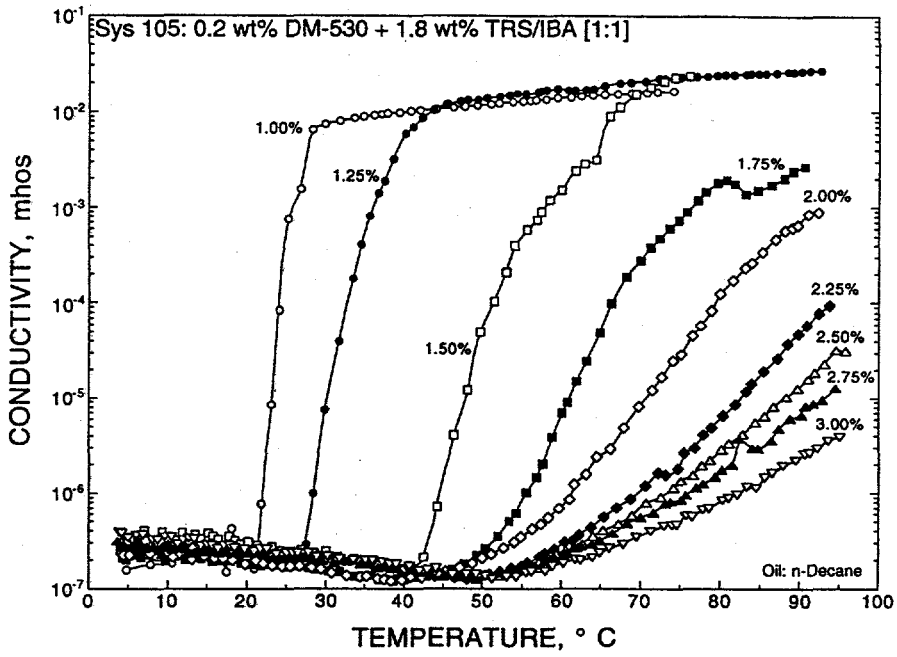

Figure 5 **Phase inversion temperature (PIT) for 0.2 wt% DM-530 + 1.8 wt% TRS/IBA [1:1] with n-decane.**

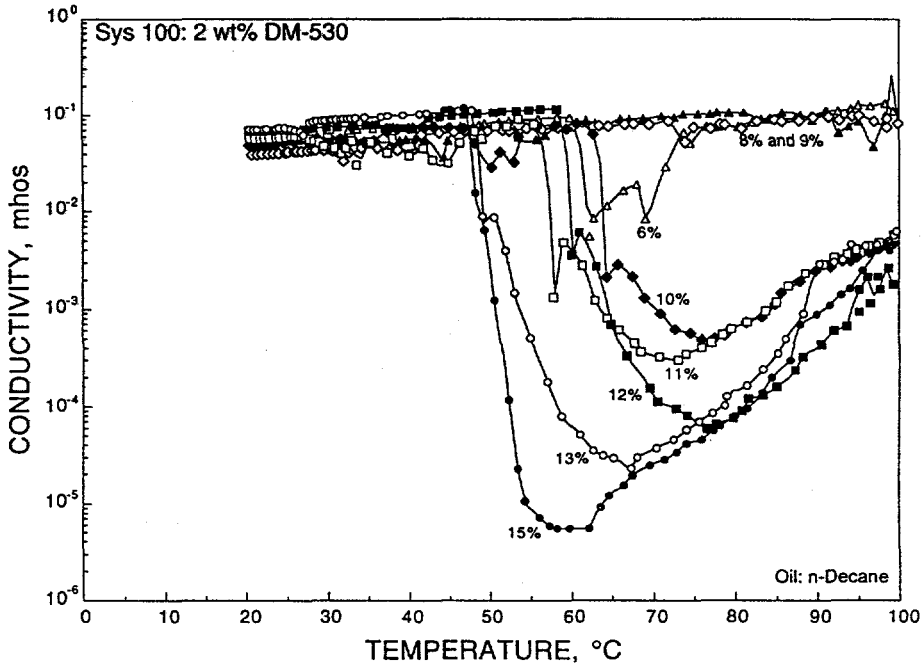

Figure 6 **Phase inversion temperature (PIT) for 2.0 wt% DM-530 with n-decane.**

component. This behavior was very similar to the behavior exhibited in Figures 1 and 2, nonionic-component dominated. The results of these measurements indicated a significant transition in terms of the overall solution behavior of these mixed systems, as a function of the anionic-nonionic component proportion in the formulation. The results showed that at relatively low nonionic-components present (Figs. 4 and 5), the dominant behavior was that of the anionic surfactant. As the nonionic-component proportion increased (Figs. 1 to 3), the phase transition behavior was dominated by the nonionic component. The results of earlier tests with the anionic component alone did not exhibit sharp phase inversion behavior, overall solution remained low (10^{-6} mhos) over the temperature range tested (Llave *et al.* 1993). The results presented in Figure 1 for measurements conducted with the (1:1) mixture indicated a definitive transition from highly conducting (water-external microemulsion) to poorly conducting (oil-external microemulsion) (Llave *et al.* 1993). Measurements using intermediate proportions of the anionic-nonionic mixtures indicated a transition in behavior with temperature. As shown in Figure 3, two different behaviors were monitored over the range of salinity tested: (1) highly conducting water-external to nonconducting oil-external, and (2) nonconducting oil-external to highly conducting water external microemulsion phases.

These measurements can be used to determine the relative proximity of optimal regions. The first type of transition corresponded to more conventional transition behavior, attributed to nonionic-dominant surfactant systems. The latter type was attributed by an earlier researcher to a condition of attaining a lower critical micelle splitting temperature (MST) (Akstinat 1981). This temperature determined the condition beyond which the mixed micelles formed from anionic-nonionic mixtures separate into water- and oil-soluble surfactants (Akstinat 1981). Temperature has a different effect on the oil/water affinity of these mixed systems. Nonionic surfactants were more lipophilic at elevated temperatures; while anionics exhibited the opposite effect. Experiments were conducted to map out this region. As shown in Figure 3, the transition from one dominant behavior to another was determined at the component proportion tested. Determining these transition ranges provided more insight on how the behavior of these surfactant mixtures was affected as the component proportions of the chemical slug may change as it propagated through the rock matrix.

Specific alkane and salinity scans were conducted on the TRS/IBA + DM-530 [1:1] system to identify optimal conditions where corresponding coreflooding experiments can be performed. The salinity level for these scans was arbitrarily set at about 3 wt% NaCl. This salinity level was based on the results of earlier screening tests conducted. Details will be discussed in a later section.

The alkane scan was conducted at room and at 40 °C with different alkanes, n-heptane to n-hexadecane, including iododecane, tagging agent used for CT-aided experiments. Figures 7 and 8 shows plots of the solubilization parameter determined from the scans as a function of the alkane used. Distinct middle phase behavior was determined for the scans using n-heptane to n-decane, at the two temperatures tested. Relatively high solubilization values were obtained for both cases. For the purpose of conducting room temperature coreflood experiments, n-heptane was selected for the oil phase. Additional salinity scans were then conducted with this oil to determine the extent of the middle phase behavior in this oil.

Figure 9 shows a plot of the salinity vs. the surfactant concentration for the chemical system tested. This plot is similar to a salinity requirement diagram original proposed by Nelson (Nelson 1982). Also shown are the upper and lower limits of the middle-phase region, as well as the estimated

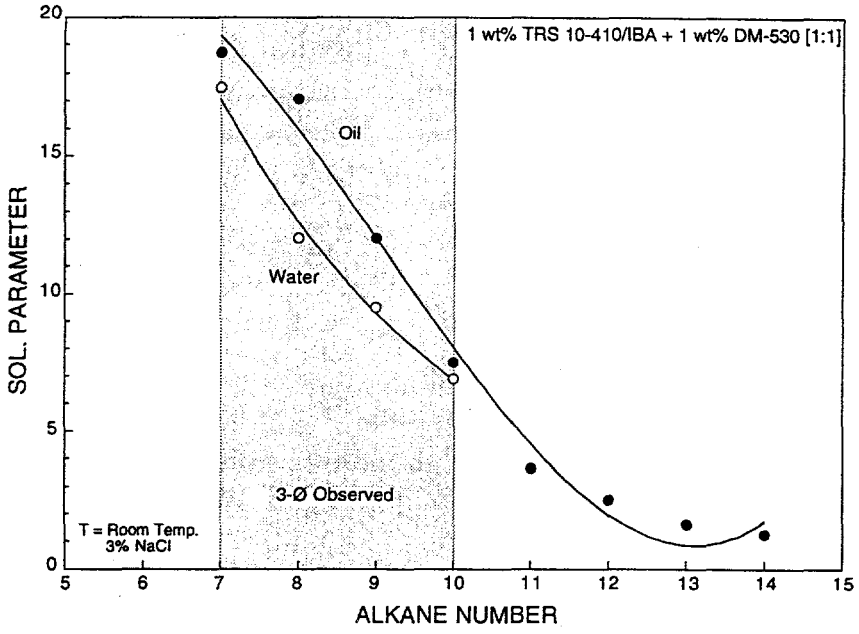

Figure 7 Alkane scan for TRS/IBA + DM-530 system at ambient temperature.

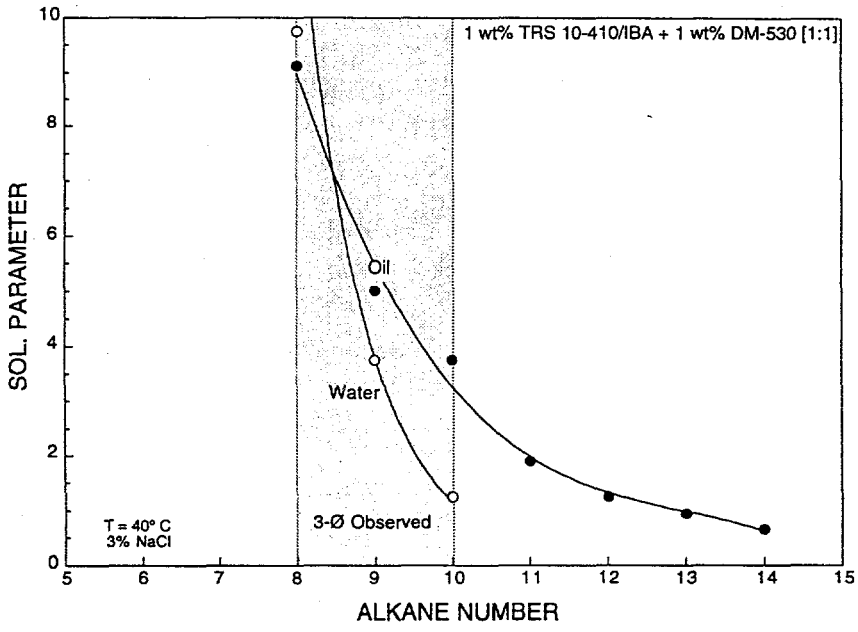

Figure 8 Alkane scan for TRS/IBA + DM-530 system at 40 °C.

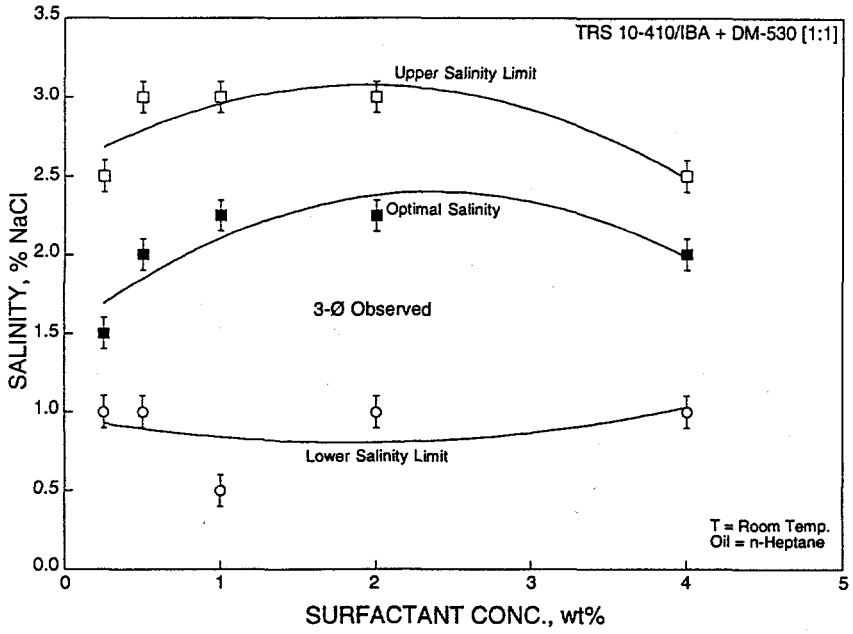

Figure 9 **Middle phase behavior limits for TRS/IBA + DM-530 system.**

optimal salinity. These limits are not to be considered as definitive values. Instead, they should be considered as the approximate range of limits, ± 0.5% based on the span of salinity values tested. These limits provided guidelines for the coreflooding experiments conducted.

Earlier PIT studies were conducted with the TRS/IBA + DM-530 system with n-heptane. Results are shown in Figure 10. From these results, the salinity of 3 wt% NaCl was selected as the level at ambient temperature where the coreflooding experiments were conducted. As mentioned earlier, this salinity was also determined in the conventional alkane and salinity scans conducted with this system.

PIT and salinity scans were also conducted in the presence of Xanthan gum biopolymer. These experiments were designed to determine any interaction effects in the presence of the polymer on overall solution behavior. Different loadings of biopolymer were formulated with the TRS/IBA + DM-530 system and tested with the n-heptane at the salinity and temperature desired. The results of the PIT measurements are presented in Figures 11 and 12. These two Figures show plots of the solution conductivity vs. temperature for the systems formulated with 500 and 1000 ppm polymer loadings, respectively. For both cases tested, the solution behavior observed was relatively similar to that exhibited by the chemical system alone, without polymer added (Fig. 10). Figure 13 shows a comparison plot of the solution conductivity vs. temperature monitored for these tests. The behavior observed showed only a slight difference/shift in the presence of the polymer. The results of the salinity scans also supported the results from the PIT determination. Based on these observations, no

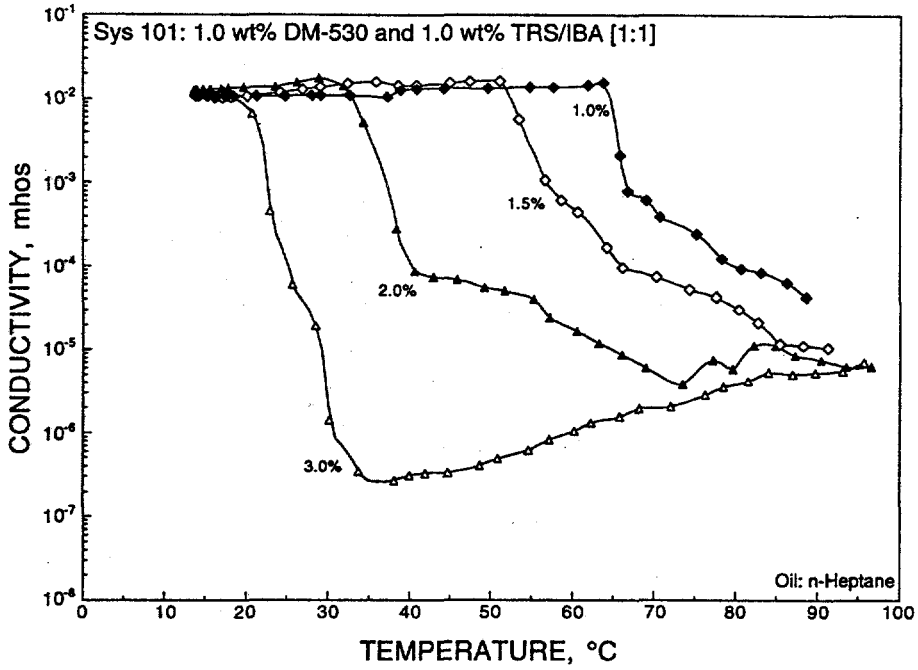

Figure 10 **Phase inversion temperature (PIT) for 1.0 wt% DM-530 + 1.0 wt% TRS/IBA [1:1] with n-heptane.**

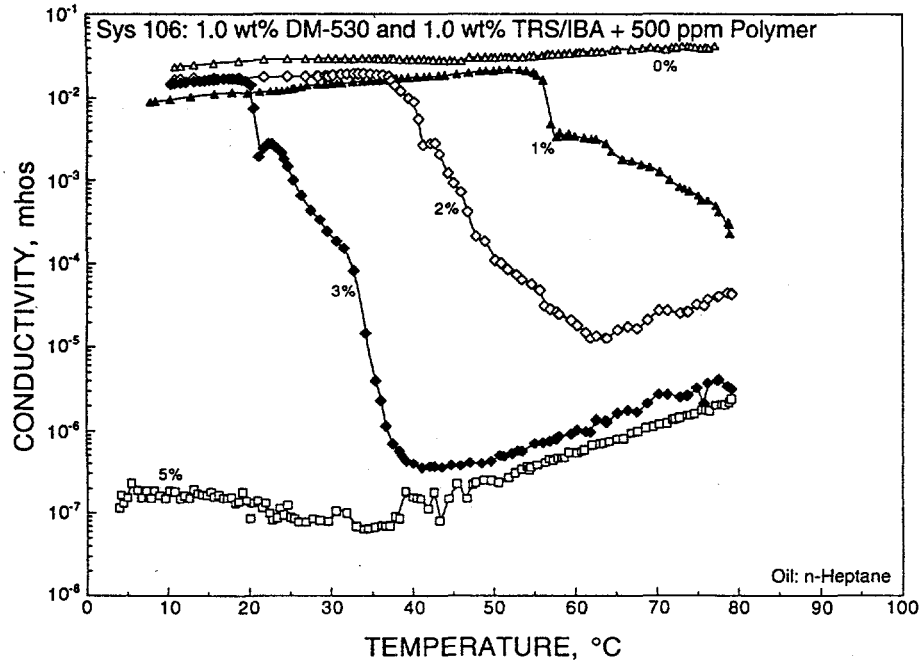

Figure 11 **Phase inversion temperature (PIT) for 1.0 wt% DM-530 + 1.0 wt% TRS/IBA with n-heptane and 500 ppm polymer.**

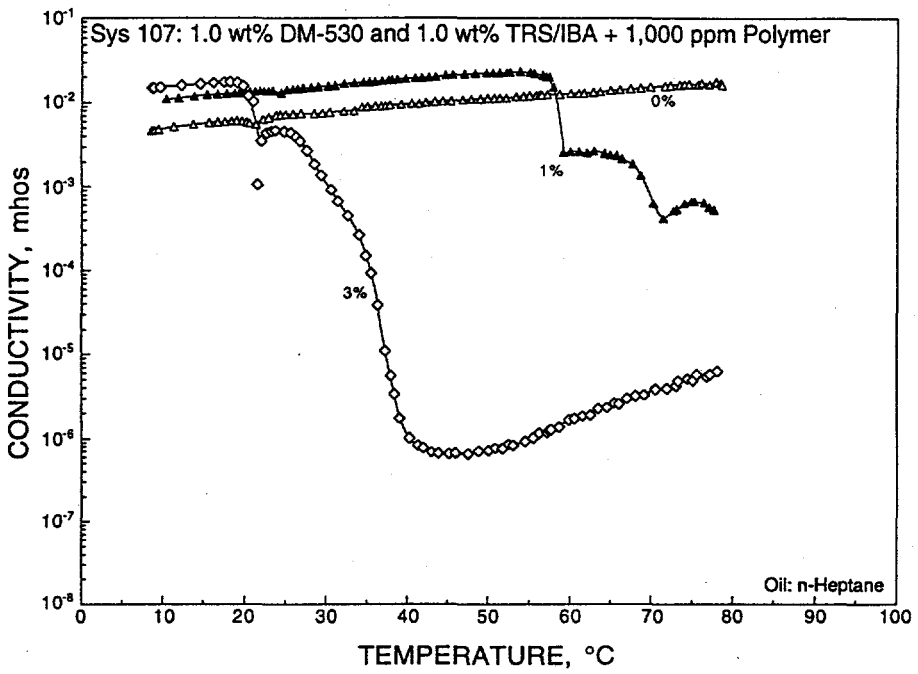

Figure 12 **Phase inversion temperature (PIT) for 1.0 wt% DM-530 + 1.0 wt% TRS/IBA with n-heptane and 1000 ppm polymer.**

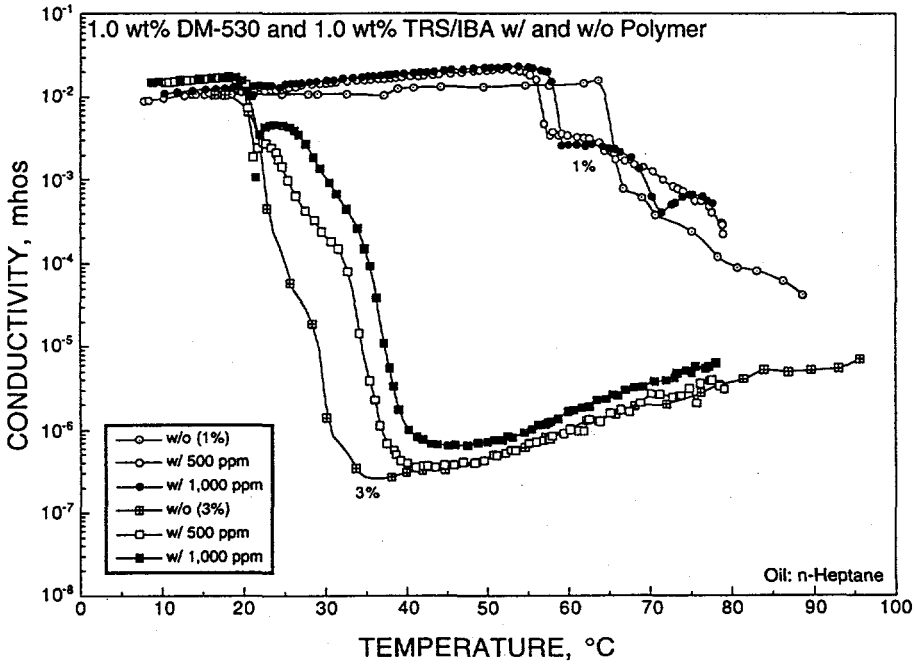

Figure 13 **Effect of polymer loading on phase behavior of DM-530 + TRS/IBA system with n-heptane.**

significant shift in solution behavior during the coreflooding tests would be expected for the range of polymer concentrations tested.

3.2 Coreflooding Experiments

Coreflooding displacement experiments were conducted to evaluate the oil recovery potential of a select chemical system. The chemical system used for the study was the TRS 10-410/IBA + DM-530 [1:1]. The selection of the alkane, salinity conditions, and experimental parameters used in the study was based on the results of the phase behavior studies discussed earlier. These experiments were mainly conducted with n-heptane, with and without iododecane present as a tagging agent for the CT-monitored experiment. This involved a systematic study to evaluate different experimental parameters and their effect on oil recovery. The oil displacement capacity of the selected chemical system was also evaluated based on the slug being injected as a straight chemical slug or a microemulsion slug.

The results of the study are presented in figures 14 through 26. Table 1 shows a detailed listing of the experiments conducted and a summary of the results. These experiments were conducted to evaluate the effect of the following variables: (1) effective brine permeability, (2) slug formulation, (3) slug content, (4) slug size, (5) initial oil saturation, and (6) injection strategy.

Figure 14 shows a plot of the oil saturation and recovery efficiency vs. the brine permeability for the experiments involving the injection of 3-Ø slug in an fully oil saturated core. The injection sequence in these experiments involved: (1) brine saturation of the dry core; (2) brine displacement by oil to initial oil saturation (S_{oi}); (3) middle phase (3-Ø) slug injection; (4) polymer injection for mobility control (1.0 PV total), and (5) follow-up brine as drive fluid. The results shown in figure 14 indicate a definite trend in the relation of oil recovery (oil saturation reduction) vs. permeability. The results show that at relatively low permeabilities (< 200 mD), the final oil saturations after the flood were much higher (25%-28% S_{ocf}) than those obtained in cores of higher brine permeabilities (< 20% S_{ocf}), when subjected to similar displacement conditions. The degree of reduction in oil saturation in low permeability cores was considerably lower than in high permeability core. This result was similar to those obtained by others for the range of permeabilities tested. (French 1994) The lower permeabilities range represented a significant challenge for designing a chemical system that can effectively displace/sweep residual oil. Poor sweep was often attributed to the lackluster performance of most promising chemical systems.

These results were compared to similar displacement experiments conducted earlier using an alkaline-enhanced surfactant-polymer (ASP) system. Figure 15 shows a plot of the final oil saturation vs. brine permeability for the sets of experiments compared. As mentioned earlier, the relationship between oil saturation reduction and brine permeability was evident. One interesting observation from this figure was the parallel trends of these plots. The results from experiments conducted with the straight chemical slug and the 3-Ø slug parallel those results from the earlier ASP experiments. The results showed that the experiments conducted using the straight chemical system had much higher final oil saturation (3%-5% more) at comparable brine permeability values. The straight chemical slug was not as effective in displacing the oil as the 3-Ø slug did. On the other hand, the results of the experiments using the ASP slug showed much lower final oil saturations (5%-6% less) at comparable brine permeability values. The difference in saturation between the two optimized systems can be

Table 1. - Summary of Coreflooding Experiments

Test No.	Waterflood	Perm md	Slug PV %	Oil in Slug %	Oil in Core	S_{oi} %	S_{owf} %	S_{ocf} %	$\%R_{eff}$ %	Injection Sequence
1	yes	690	24.61	55.56	Heptane	70.27	38.16	22.22	41.76	W.F. + 3-Ø C.F. + P.F. + W.F.
2	yes	592	26.91	50.00	Heptane	70.14	41.01	22.73	44.59	W.F. + 3-Ø C.F. + P.F. + W.F.
3	yes	552	25.27	0.00	Heptane	67.20	41.40	27.29	34.09	W.F. + (no 3-Ø) C.F. + P.F. + W.F.
4	yes	569	50.27	48.87	Heptane	72.38	32.14	16.08	49.97	W.F. + 3-Ø C.F. + P.F. + W.F.
5	yes	363	48.80	59.89	Heptane	67.41	38.26	24.37	35.38	W.F. + 3-Ø C.F. + P.F. + W.F.
6	yes	729	26.32	48.41	Heptane	68.73	40.42	14.74	63.54	W.F. + 3-Ø C.F. + P.F. + W.F.
7	yes	762	50.50	0.00	Heptane	70.69	44.25	17.67	60.06	W.F. + (no 3-Ø) C.F. + P.F. + W.F.
8	yes	743	24.99	73.86	Heptane	70.22	41.35	30.01	27.43	W.F. + 3-Ø C.F. + P.F. + W.F.
9	yes	625	25.12	32.50	80:20	69.71	42.33	21.68	48.77	W.F. + 3-Ø C.F. + P.F. + W.F.
10	no	772	28.30	43.00	80:20	67.74	67.74	14.66	78.36	3-Ø C.F. + P.F. + W.F.
11	no	617	25.31	43.00	80:20	68.86	68.86	20.30	70.52	3-Ø C.F. + P.F. + W.F.
12	no	124	24.90	45.00	80:20	65.67	65.67	26.46	59.72	3-Ø C.F. + P.F. + W.F.
13	no	937	25.67	38.70	80:20	65.81	65.81	16.49	74.95	3-Ø C.F. + P.F. + W.F.
14	yes	929	29.94	26.00	80:20	69.49	38.98	25.16	35.46	W.F. + 3-Ø C.F. + P.F. + W.F.
15	yes	887	31.17	31.00	80:20	70.84	41.47	17.91	56.83	W.F. + 3-Ø C.F. + P.F. + W.F.
16	yes	130	24.72	31.25	80:20	68.78	37.24	31.97	14.15	W.F. + 3-Ø C.F. + P.F. + W.F.
17	no	565	25.01	31.25	80:20	64.05	64.05	22.87	64.29	3-Ø C.F. + P.F. + W.F.
18	no	215	25.77	23.40	80:20	76.39	76.39	27.40	64.13	3-Ø C.F. + P.F. + W.F.
20	no	110	25.03	33.30	80:20	74.69	74.69	37.60	49.65	3-Ø C.F. + P.F. + W.F.
21	no	739	28.97	42.86	80:20	67.58	67.58	16.33	75.84	3-Ø C.F. + P.F. + W.F.

Note: W.F. - waterflood; 3-Ø C.F. - middle phase chemical flood; and P.F. - polymer flood

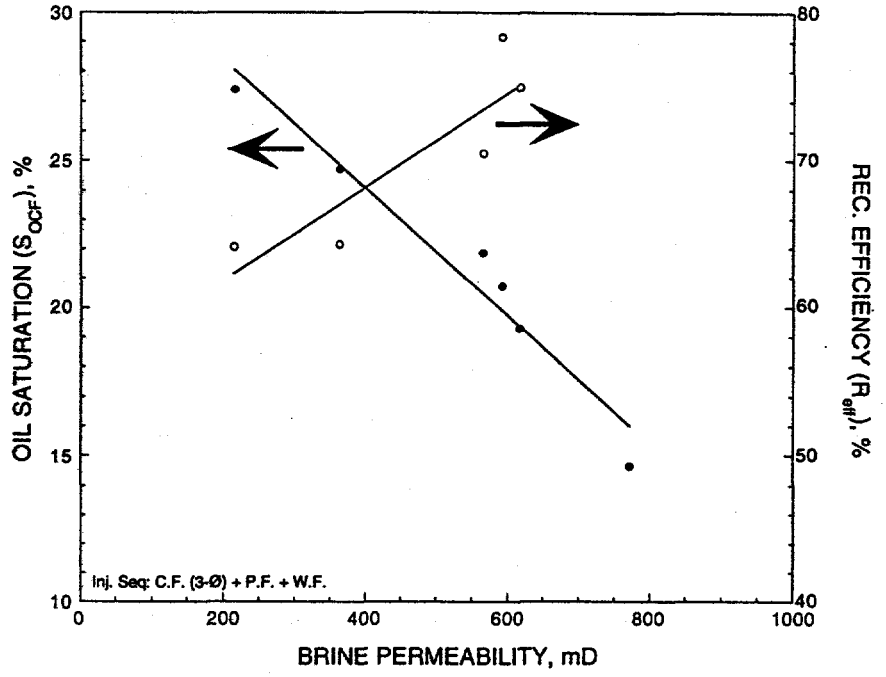

Figure 14 **Effect of brine permeability on oil saturation reduction and recovery efficiency of an optimized chemical system.**

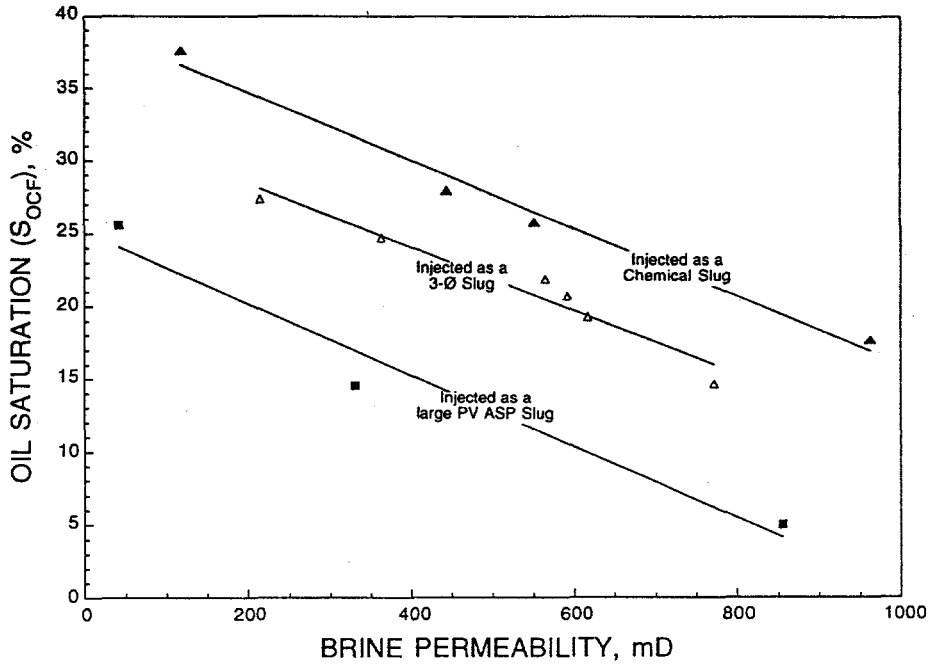

Figure 15 Comparison of oil saturation (S_{ocf}) vs. brine permeability. Experiments using (a) straight chemical slug , (b) 3-Ø slug, and (c) large pore volume ASP slug.

directly attributed to the size of chemical slug injected, 0.25 PV (with about 50% oil and 50% brine/surfactant) for the 3-Ø slug as opposed to about 0.75 PV (total of 1.5 PV chemical treatment including preflush) for the low concentration ASP slug. The amount of total chemical in the 3-Ø slug experiments and the large pore volume ASP slug experiments were comparable, while the straight chemical slug experiments had about twice the amount of total chemical.

Comparisons made with results from experiments with the a small pore volume (0.45 PV) ASP slug resulted in much higher final oil saturations, which closely parallel the results of the chemical slug and the 3-Ø slug experiments. The total amount of chemical in the two ASP experiments were different. The treatment slug sizes were different but the concentration levels remained the same. The results from the comparison indicated almost similar degree of reduction in oil saturation for the small pore volume ASP slug experiments and the 3-Ø slug experiments. Overall, these results support the earlier trends identified, in terms of the relationship between the degree of oil saturation reduction and the effective brine permeability of the core. This reemphasized the need to properly account for the effective permeability of the core in displacement experiments in order to maximize oil recovery. Detailed discussion of these ASP results were presented elsewhere (French 1994). Comparable oil recovery experiments with different slug sizes will be discussed in a later section.

Figures 16 and 17 show plots of the oil cut and the oil recovery versus pore volume injected in three of the 3-Ø slug experiments conducted. The injection sequence used in these experiments was similar to the sequence earlier discussed. Figure 17 shows the oil cut during the progress of the experiments. The results showed the difference in drive fluid breakthrough in these experiments. The breakthrough time (in terms of pore volume injected) increased with increasing effective brine permeability. A breakthrough time of about 0.4 PV injected was indicated for the experiment conducted with the 110 mD core, while the high permeability core (770 mD) had a breakthrough time of about 0.6 PV injected. The delayed breakthrough time appeared to be an indication of more effective sweep (oil bank formation) in the high permeability core compared to the low permeability core. CT-monitored coreflooding experiments supported this indication of much better sweep with the higher permeability cores. Results of earlier oil displacement studies also showed much better oil displacement in the higher permeability cores. Details of the CT-monitored experiments are discussed in a later section.

Figure 17 shows a more dramatic comparison of the effect of permeability on oil recovery. This plot shows similar displacement trends throughout each of the experiments (prior to breakthrough). At the breakthrough point, the oil production almost ceased completely (with some additional production from the high permeability core), also shown in figure 16. The level of oil recovery (after breakthrough), tapered off at a much higher level for the high permeability core than for the low permeability core. An effective oil bank was indicated in the high permeability core experiments, which resulted in an effective sweep of the core (83% recovery of OOIP, about 78% recovery efficiency).

A comparison was made with the type of injection strategy employed in these experiments. The first set of experiments involved displacing the oil saturated core with the 3-Ø chemical slug, as discussed earlier. The second set of experiments involved displacing the oil saturated core with brine to residual oil saturation (S_{ow}), prior to chemical slug injection. Figure 18 shows a comparison of the results from the two sets of experiments. Almost similar trends in oil saturation reduction as a function of core permeability was indicated. There was a slight difference indicated at the higher end of the

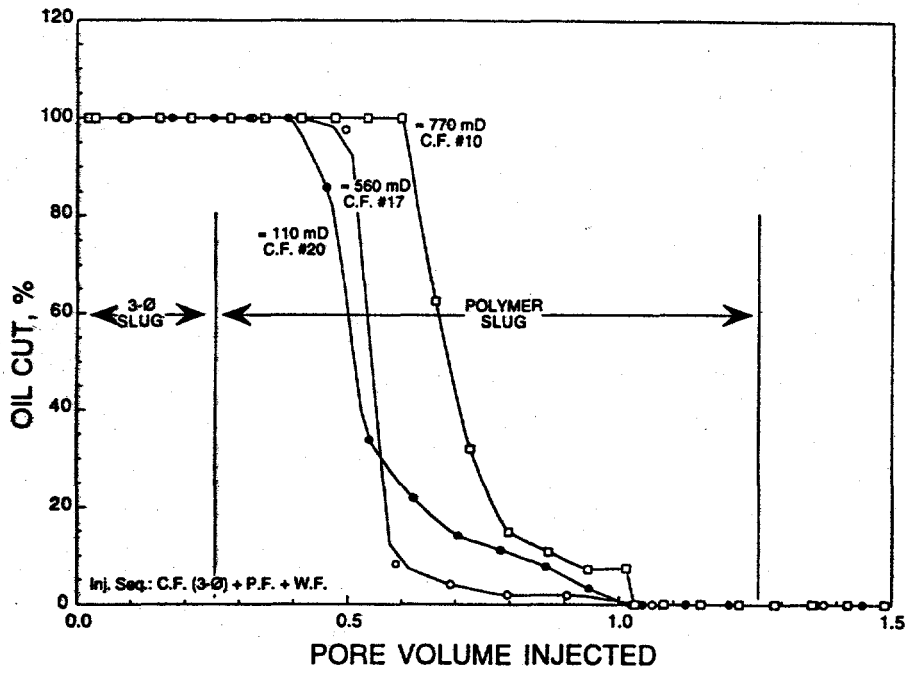

Figure 16 **Oil cut vs. pore volume injected in different permeability cores. Permeability ranges: (a) 770 mD, (b) 560 mD, and (c) 110 mD.**

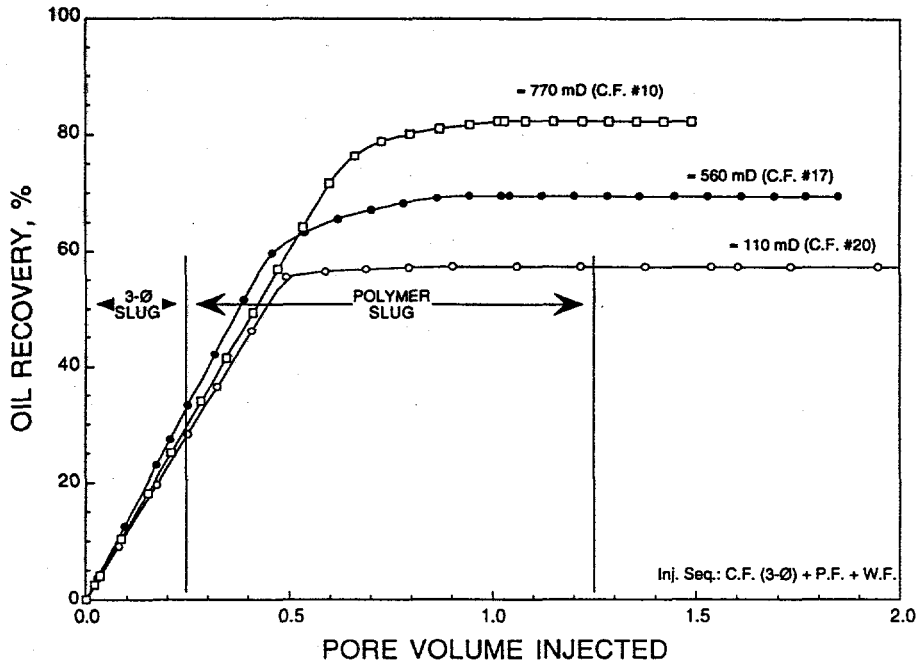

Figure 17 **Oil recovery vs. pore volume injected in different permeability cores. Permeability ranges: (a) 770 mD, (b) 560 mD, and (c) 110 mD.**

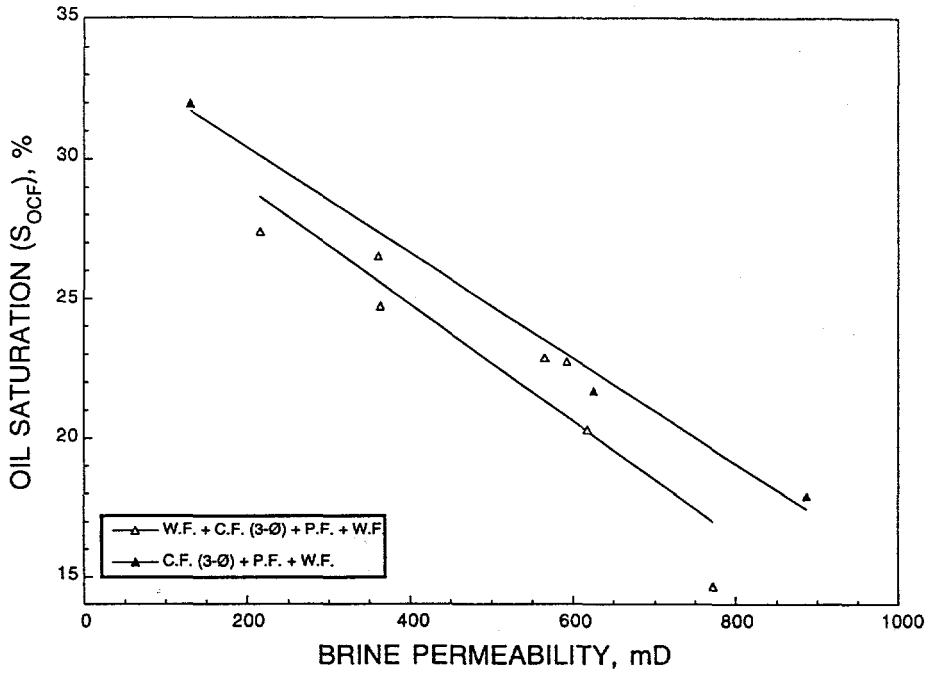

Figure 18 **Final oil saturation (S_{ocf}) vs. permeability for chemical floods started at initial oil saturation and at residual oil saturation after waterflood.**

permeability range tested. At relative low permeabilities (< 200 mD) the difference results was getting smaller, while the difference in degree of oil saturation reduction increased at the higher permeability values (circa 800 mD).

The results indicated that at low permeability levels, the resulting oil saturation did not differ much with the type of injection strategy employed (whether brine flooded or not, prior to chemical injection). The results did indicate that at high permeability levels, the displaceable amount of oil (initial oil saturation before chemical slug injection) can make a difference. With higher oil saturations to begin with (series without waterflood), the effective formation of an oil bank was helpful in ultimately reducing the oil saturation in the high permeability cores to a lower value (about 2%-3% lower). Overall though, the core permeability had a significant impact of the effectiveness of the chemical slug in displacing oil.

The proportion of the oil/brine/surfactant in the 3-Ø slug also affected the effective oil displacement. Experiments were conducted to compare 3-Ø slugs with difference proportions of oil in the slug (whether over, under, or at optimal conditions). Figures 19 through 21 show plots of the oil saturation and oil cut vs. pore volume injected from three sample experiments conducted with different slug formulations. Common to all three experiments was the injection sequence (chemical injection after waterflood) and other experimental parameters (particularly the core permeability), except the 3-Ø slug formulation. These figures corresponded to experiments conducted with increasing proportion of oil in the 3-Ø slug. The results presented in these figures show that the chemical proportion in the injected slug can significantly affect the effectiveness of the system. At near optimal conditions, (≈ 50% brine/surfactant) the system was much effective in reducing oil saturation levels compared to the system with higher oil proportions (above optimal). As much as 13% oil saturation difference was

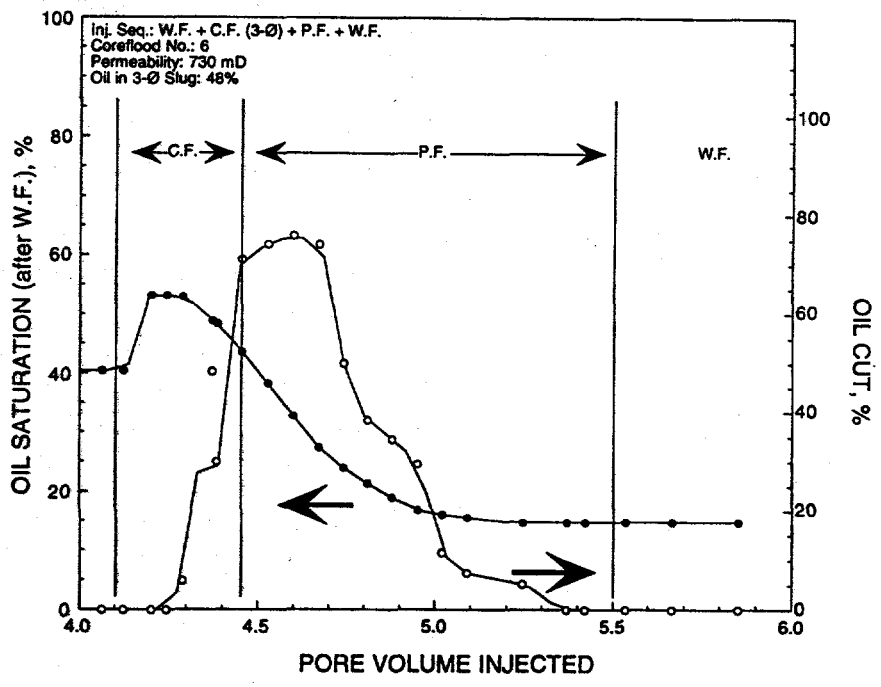

Figure 19 Oil saturation (S_{ocf}) and oil cut vs. pore volume injected for coreflood no. 6.

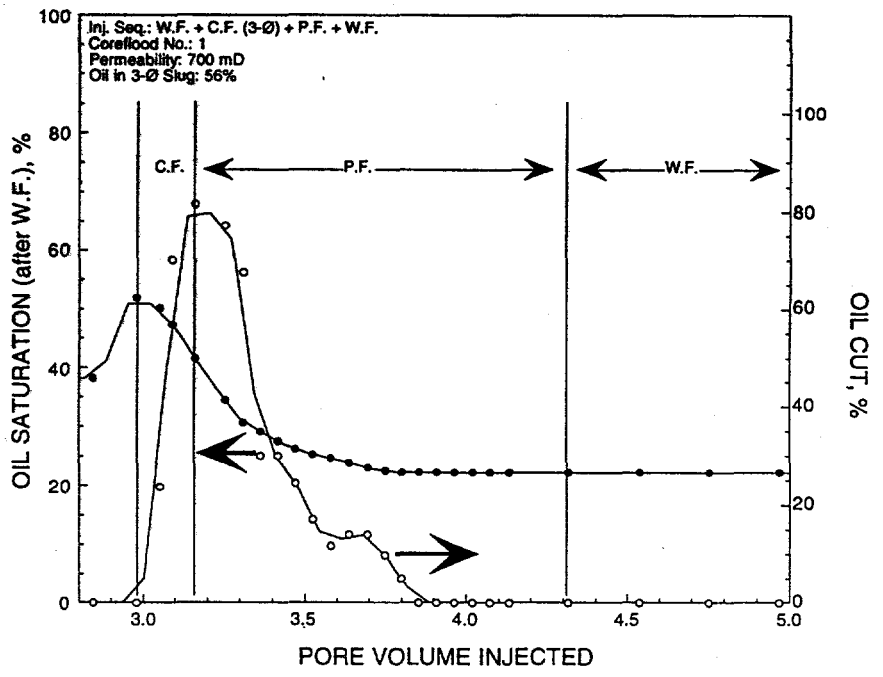

Figure 20 Oil saturation (S_{ocf}) and oil cut vs. pore volume injected for coreflood no. 1.

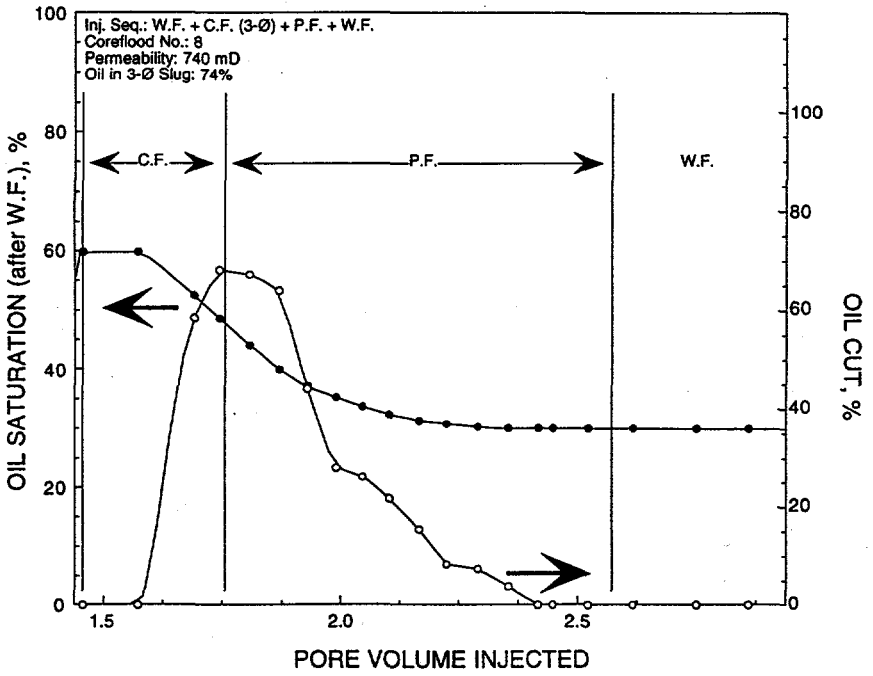

Figure 21 **Oil saturation (S_{ocf}) and oil cut vs. pore volume injected for coreflood no. 8.**

indicated in these experiments. Displacement experiments conducted at suboptimal conditions indicated comparable ineffective chemical system performance. The effectiveness of the system in terms of oil recovery potential, followed a similar trend:

Optimal >Under Optimal >>Above Optimal

Operating at conditions relatively close to the optimal conditions appeared to be mandated by the chemical system tested.

As mentioned earlier, experiments were conducted to determine an optimal slug size for application. The results of preliminary experiments support a known contention that bigger (meaning larger slug size) is better, as expected (up to a certain point). Figures 22 through 25 show plots of oil saturation vs. pore volume injected for several experiments. Figures 22 and 23 show a comparison of experiment nos. 2 (0.25 PV slug) and 4 (0.5 PV slug). As expected, the performance of the larger slug injected was significantly better than the small slug experiment. Much broader distribution of oil cut was observed with the latter experiment. The final oil saturation difference between the two experiments was about 5%, after 5.0 PV total fluid injected.

Figures 24 and 25 show a comparison of experiment nos. 3 and 7. These experiments were conducted using straight chemical slugs (not as a preequilibrate 3-Ø). These results, as expected, also indicated that the larger slug test (experiment no. 7: two separate chemical slug cycles) was better than the smaller slug test (experiment no. 3). The final oil saturation difference between the experiments was about 9%.

A direct comparison of the results of the experiments conducted with a 3-Ø slug and the straight chemical slug showed significant difference in effectiveness. As shown earlier, (Fig. 15), the

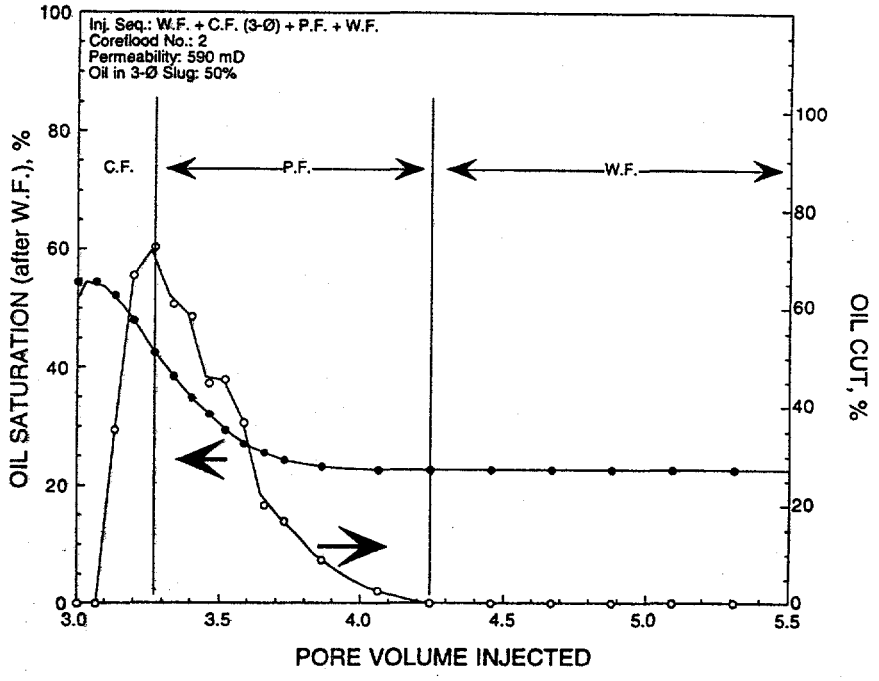

Figure 22 **Oil saturation (S_{ocf}) and oil cut vs. pore volume injected for coreflood no. 2.**

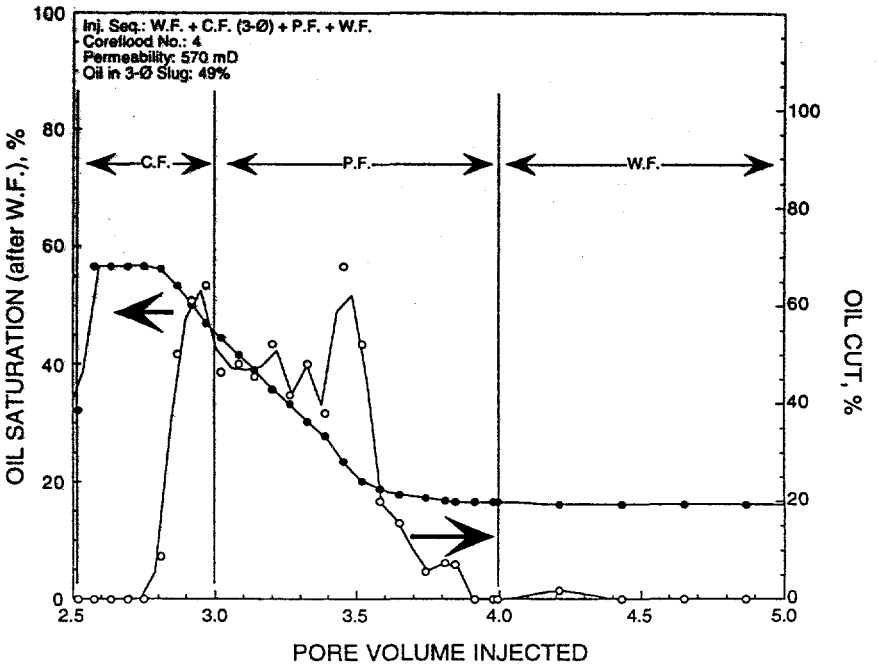

Figure 23 Oil saturation (S_{ocf}) and oil cut vs. pore volume injected for coreflood no. 4.

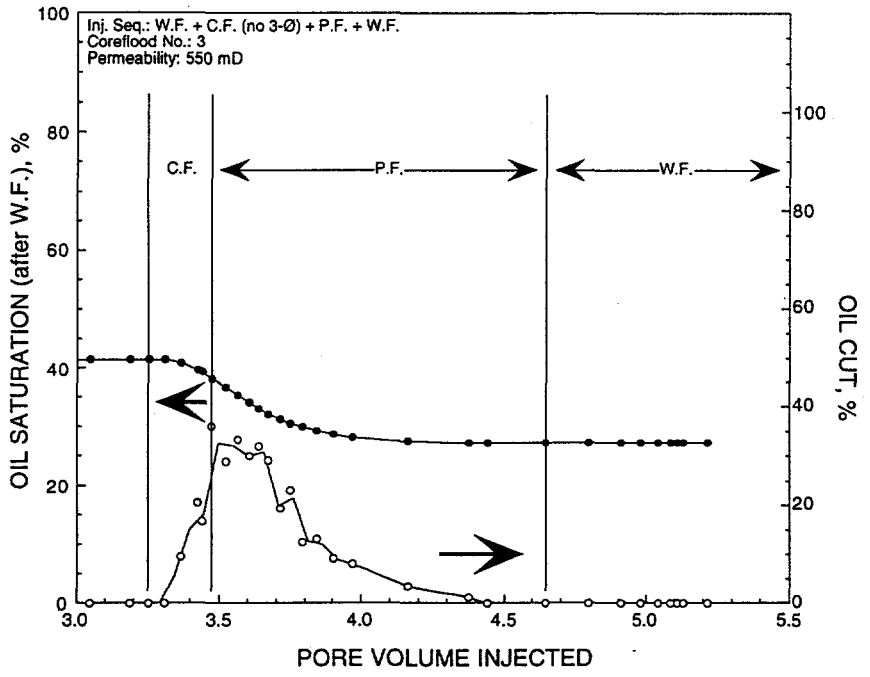

Figure 24 Oil saturation (S_{ocf}) and oil cut vs. pore volume injected for coreflood no. 3.

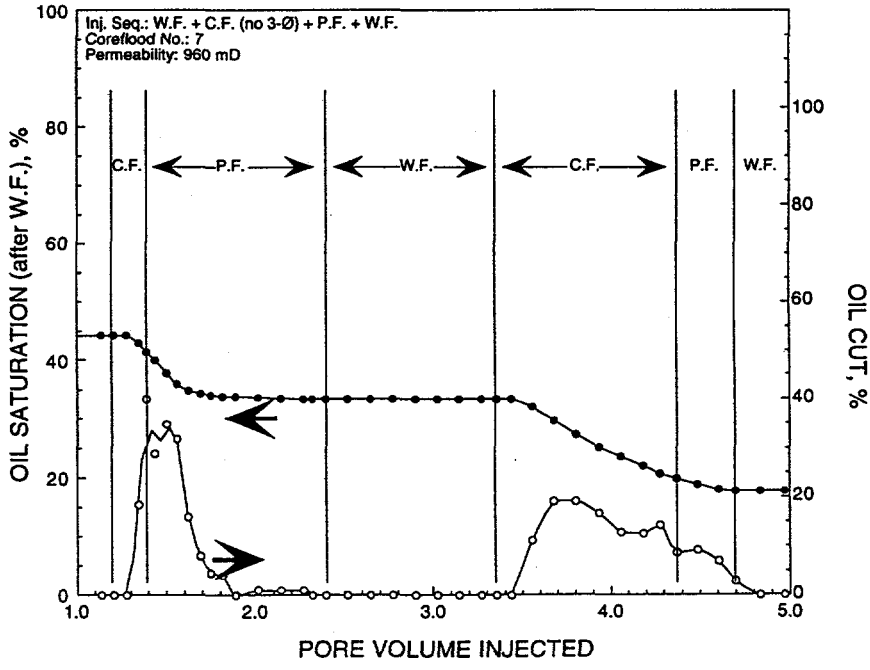

Figure 25 Oil saturation (S_{ocf}) and oil cut vs. pore volume injected for coreflood no. 7.

resulting saturations from the straight chemical slug experiments were much higher compared to saturations from the 3-Ø slug experiments, at comparable brine permeability. Although both sets of experiments were formulated (brine salinity, component concentration, and experimental conditions) to be optimal, the straight chemical slug formulation was not as effective in oil displacement as the preequilibrated 3-Ø slug was. The injection of the microemulsion slug resulted in much better performance, which is similar to results from 3-Ø (microemulsion phase) injection obtained by others. These results also indicated that an increase in slug size favored the straight chemical slug experiments slightly more than the experiments with the 3-Ø slugs. The larger straight chemical slugs (which corresponded with more active chemical component) appeared to be favored more over the 3-Ø chemical slugs. Additional experiments will be needed to confirm this observation.

Coreflooding experiments were also conducted with the aid of NIPER's CT-imaging capability. These CT-monitored experiments were conducted to facilitate the evaluation of the effectiveness of the chemical system in mobilizing and recovering oil. Figure 26 shows plots of the progress of one of the experiments during different stages of the run (Figs. 26a through 26d).

This experiment was similar to experiment no. 10. The injection sequence in these experiments involved: (1) brine saturation of the dry core, (2) brine displacement by oil to initial oil saturation (S_{oi}), (3) 3-Ø slug injection, (4) polymer injection for mobility control (1.0 PV total), and (5) follow-up brine as drive fluid. CT-scan images were generated during different stages of the experiment. Figure 26a shows the fully oil saturated core, with an average initial oil saturation of 67.6% (by material balance). Fairly uniform oil saturation was obtained from the experiment, with some slightly lower (5% to 10%) saturation values detected in the later three quarters of the length of the core. Figure 26b shows the scan taken immediately after the untagged chemical system was injected. The figure shows fairly good frontal sweep of the core, almost piston-like, indicative of good oil recovery in the areas contacted. One thing to note about the experiment was that there was oil present in the slug injected. The 0.25 PV chemical slug injected was a 3-Ø slug containing approximately 43% oil (n-heptane). The image may show almost zero saturation in areas contacted but some untagged oil remained (was reintroduced) with the injection of the 3-Ø slug. Figure 26c shows the scan taken immediately after 0.6 PV slug of the polymer was injected. Fairly good sweep can be seen through the sections of the core that was contacted. Some degree of fingering of the front can be observed at this stage. Figure 26d shows the image taken after 3.0 PV of untagged brine was injected as drive fluid. The images showed excellent sweep of about three quarters of the length of the core with some override/bypass indicated in the tail end. As mentioned earlier, although the image may indicate almost zero oil saturation in majority of the sections of the core, the slug injected contained some untagged oil and may have higher saturation in some spots contacted. The final oil saturation of the core was about 16%, for a recovery efficiency close to 76%. About 80% of the oil (both original saturation and in the slug) was recovery. The results are comparable to those of previous test under similar conditions (experiment no. 10).

The results from the CT-monitored experiment lend excellent support to the observations made with regards to the effect of permeability on oil recovery potential. The experiments conducted in the high permeability cores showed very good frontal sweep, indicative of favorable oil displacement. Experiments conducted in low permeability cores showed the opposite, in terms of significant fluid bypass indicated, representative of the amount of oil (greater than 26% oil saturation) remaining the core.

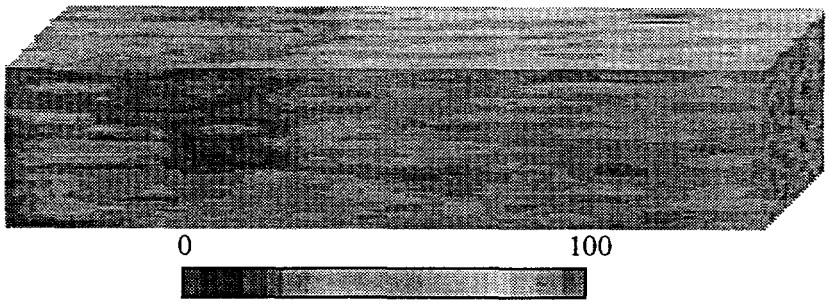

(a)

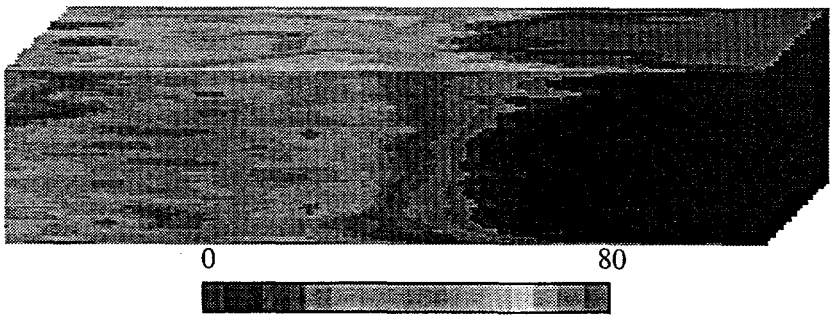

(b)

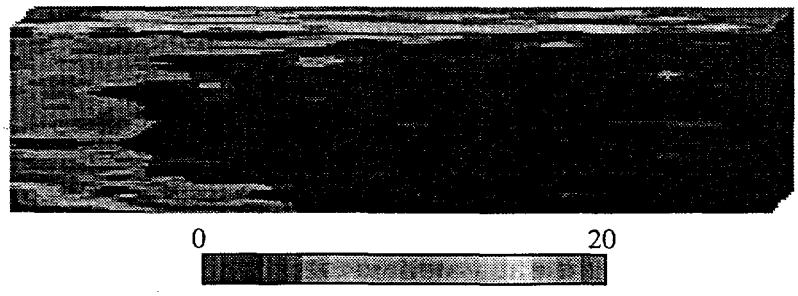

(c)

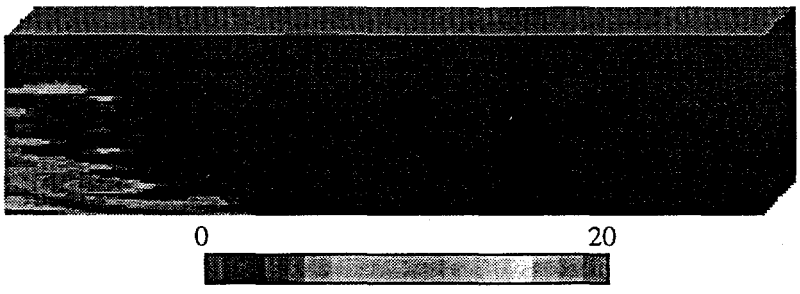

(d)

Figure 26 CT-monitored flow profile of experiment: (a) oil saturated core, (b) 0.25 PV untagged 3-Ø chemical slug injected, (c) 0.6 PV untagged polymer slug injected, and (d) 3.0 PV untagged brine injected, end of experiment. Fluid injection is from the right.

3.3 Mobility Control Studies

During FY 1994, flow characteristics of several polymers were studied to provide information to design adequate mobility control for coreflooding experiments that are conducted in laboratories at NIPER. These studies were not intended to measure mobility characteristics of these polymers under all possible conditions. Instead, they were designed to develop quality laboratory operating procedures, test mobility design criteria, provide some flow data for several types of polymers, and provide information to design CT-monitored corefloods to examine the effects of mobility control on oil movement in porous media. The following sections summarize flow studies using polyacrylamide polymers with different degrees of anionic character and one sample of Xanthan biopolymer. Calculation of relative mobility for two permeability ranges of Berea sandstone cores are demonstrated. One CT-monitored chemical coreflood has been completed to initiate the study of the effect of mobility control effectiveness on oil movement in porous media.

Table 2 lists chemical conditions of the tests described in this section.

TABLE 2 Chemical Formulations Used in the Mobility Control Studies

TEST #	Brine, wt.%	Perm, mD	ϕ, %	[Polymer], ppm	Chemical type
PF-1	NaCl - 3.28 $CaCl_2$ - 0.755 $MgCl_2$ -0.099	144	20.6	500	Polyacrylamide - Alcoflood 935
PF-2	NaCl - 5.90 $CaCl_2$ - 1.36 $MgCl_2$ -0.06	336	23.6	1500 1000 500	Polyacrylamide - Alcoflood 935
PF-3	NaCl - 5.87 $CaCl_2$ - 1.35 $MgCl_2$ -0.06	725	24.3	1500 1000 500	Polyacrylamide - Alcoflood 935
PF-4	3.0% KCl	439	25.4	1507 1017 510	Xanthan biopolymer Flocon 4800 C
PF-5	3.0% KCl	173	20.0	1504 1000 407	Polyacrylamide - Alcoflood 1135
PF-6	3.0% KCl	540	23.7	1519 1000 523	Polyacrylamide - Alcoflood 1135
PF-7	3.0% KCl	695	23.3	1506 1072 523	Polyacrylamide - Alcoflood 1135
SP-1	1.8% NaCl	662	22.5	1500	Polyacrylamide - MO3000H-SF 0.2% B-100,[a] 1.6% Na_2CO_3

[a]Alkyl aryl sulfonate

3.3.1 Polyacrylamide Polymers

Previous studies at NIPER have emphasized the development of mixed surfactant systems to extend the application of surfactant-based Improved Oil Recovery techniques to intermediate to high salinity reservoirs (Llave *et al.* 1991; 1992; 1993). Solution properties of polyacrylamide polymers traditionally are very sensitive to ionic strength of the solution. High salinity reservoirs were not amenable to flooding applications using polyacrylamide polymers because viscosity of solutions of this polymer type were typically very low under these conditions.

Polymer manufacturers have recognized these important limitations and have attempted to develop products with improved solution characteristics for higher salinity applications. Reduction in ionic character of the polymer chain has been used to increase polymer stability for reservoirs with high brine and temperature levels. Products with different average molecular weights can then be selected for applications in different permeability reservoirs.

3.3.1.1 Polymer Stability Studies

The first polymer selected for study (Alcoflood 935) was a medium molecular weight polyacrylamide of low ionic character for use in higher salinity brine. The manufacturer describes polymer properties in 720, 35,000 and 155,000 ppm TDS to illustrate viscosity behavior at different salinity levels. Stability of this polymer was tested at 23 and 50 °C by measuring viscosities as a function of time for solutions with different polymer and salinity concentrations. The brine contained NaCl, $CaCl_2$, and $MgCl_2$ in a ratio of 5.9/1.3/0.1, by weight. Polymer concentrations ranged from 500 to 2000 ppm and the total dissolved salt (TDS) concentration ranged from 4.2 to 16.8 wt%. Oxygen was excluded from solution, and the aging was conducted under a nitrogen atmosphere. Figure 27 shows the change in viscosity after aging for one month. Little change in viscosity was observed for samples held at ambient temperature. Some viscosity loss was observed, however, for samples aged at 50 °C. In general, the percentage viscosity loss increased with an increase in polymer concentration and brine concentration.

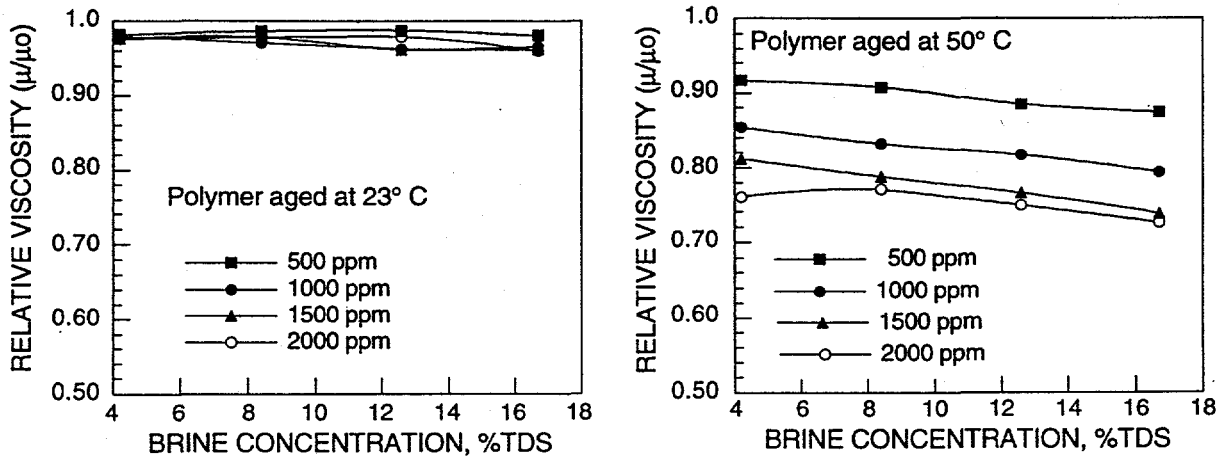

Figure 27 **Relative change in viscosity for different polymer and salinity concentrations after aging for one month at (a) 23 and (b) 50 °C.**

After four months at elevated temperature, all polymer solutions at 50 °C contained white precipitate. At 23 °C, however, viscosities for all polymer and salt concentrations remained within 96% of the initial values. Degradation was significantly less at ambient temperature than that observed at 50 °C. The presence of divalent ions appeared to be detrimental to this polymer at elevated temperatures. Thermal degradation would cause problems in field applications where long term viscosity stability is important to maintain adequate mobility control to maximize oil production.

Laboratory studies using this polymer were conducted at ambient temperature in order to minimize degradation problems.

3.3.1.2 Flow Through Berea Sandstone Core

Flow tests in several types of Berea sandstone cores were conducted to determine relative mobility characteristics of two polyacrylamide polymers. In addition to Alcoflood 935, Alcoflood 1135 was used in this study. Alcoflood 1135 has a higher anionic character than Alcoflood 935 and will produce higher viscosity at low salinities. It is not as stable as 935 at high salinities and temperature, however.

Using the core procedures outlined in the Experimental Section, differential pressure measurements were made for a number of fluid flow rates through the core. Plots were made of the pressure gradient, $\Delta P/L$, as a function of the fluid Darcy velocity, q/A.

Figures 28 and 29 show examples of pressure versus flow results for the two polymers at several different concentration levels. Both tests were conducted in high permeability (700-mD) Berea sandstone core. The cores for these tests were very similar. Therefore, the differences in pressure gradient behavior were mainly caused by the difference in viscosity of the two polymer solutions. Figure 30 shows a comparison of the flow behavior of the 1500 ppm polymer for the two tests taking into account the relative viscosity difference of the two polymer solutions. The pressure response was very similar for these polymers. In a later section, comparison of flow data for polyacrylamide and polysaccharide polymers demonstrates very different flow behavior in porous media for polymers of different molecular structure.

As concentration was reduced, measured pressure differentials also declined. At each flow rate, however, the decline was not as great as the decline in solution viscosity. The initial polymer through the core may have changed core pore properties by adsorption or blocking of smaller pores that can affect the flow of subsequent solutions of lower concentration. In the reservoir, this may allow gradual reduction of polymer concentration for the mobility buffer without loss of effective mobility control and improve economics of chemical injection.

Finally, figure 31 shows a comparison of flow characteristics of 1500 ppm Alcoflood 1135 in different permeability Berea sandstone core. The salinities of these polymer solutions are also different. The curves, however, are approximately parallel to each other. Greater pressure drop in the lower permeability core is caused by pore structure differences between the two cores. This emphasizes the importance of determining flow behavior in rock appropriate to the application.

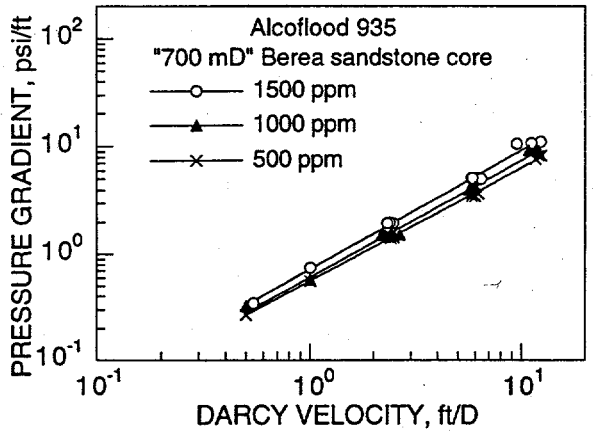

Figure 28 Flow characteristics of Alcoflood 935 in high permeability Berea sandstone core

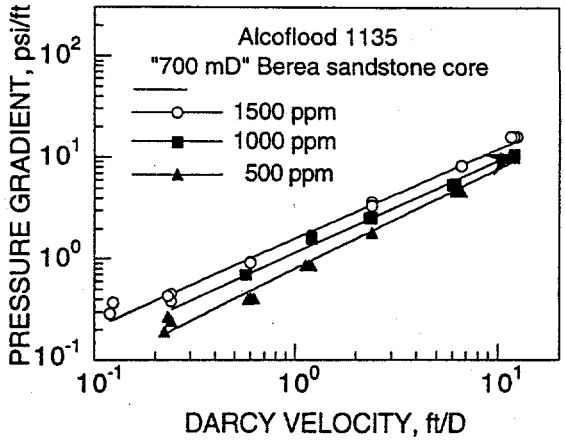

Figure 29 Flow characteristics of Alcoflood 1135 in high permeability Berea sandstone core

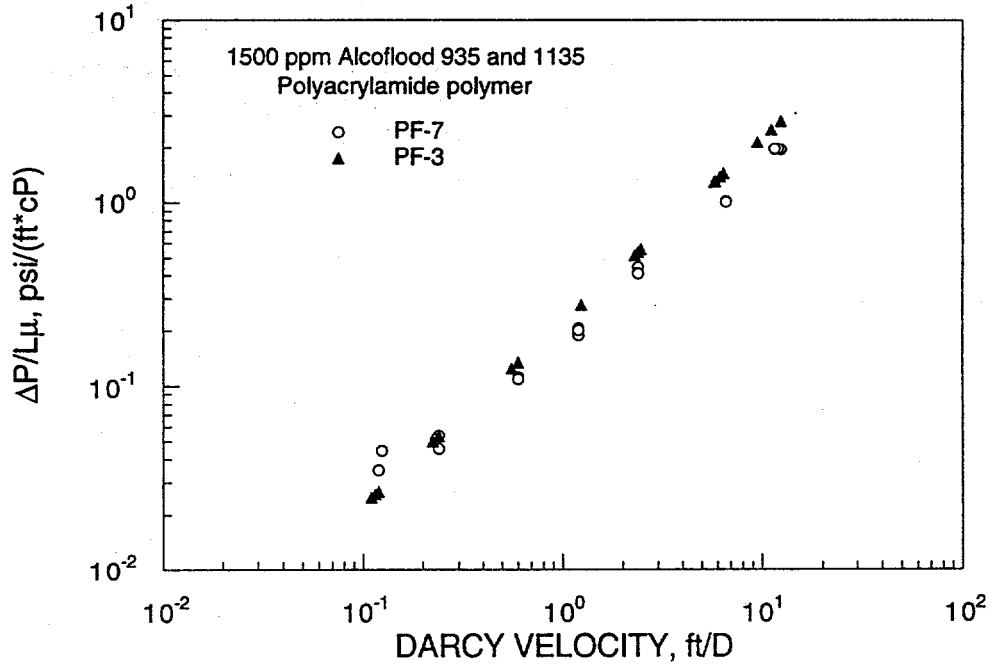

Figure 30 Comparison of flow behavior of two polyacrylamide polymers in similar Berea sandstone core.

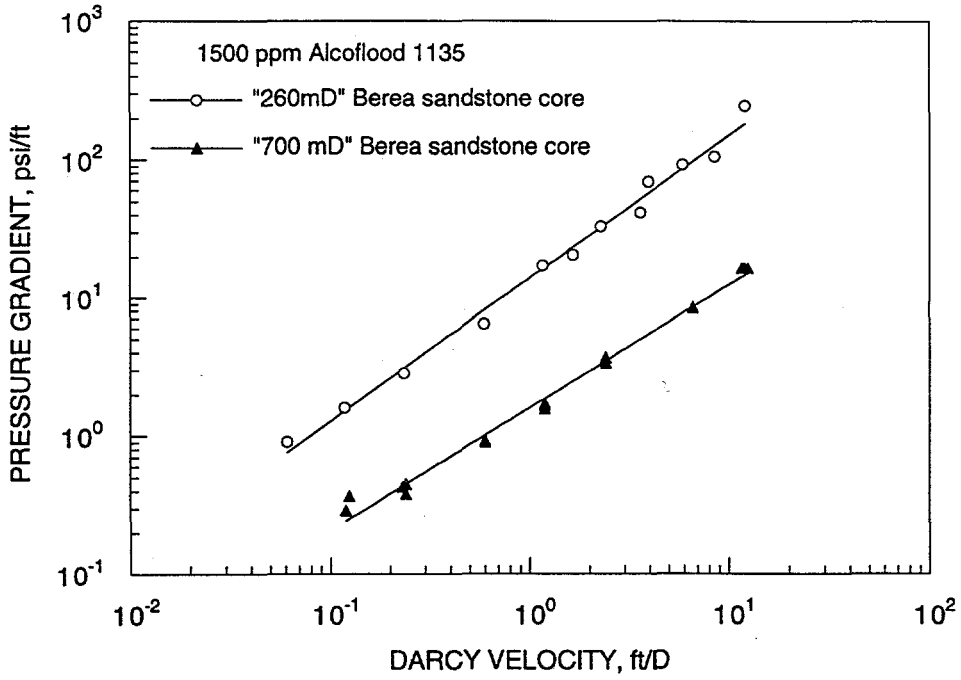

Figure 31 **Flow characteristics of Alcoflood 1135 in different permeability core.**

3.3.2 Flow Characteristics of Xanthan Biopolymer

Similar flow studies were conducted using a Xanthan biopolymer. Figure 32 shows the pressure/flow relationship in Berea sandstone core for several concentration of the biopolymer, Flocon 4800C. The flow properties of this polymer has been studied previously in sandpacks of several different permeabilities including one permeability approximately the same as that of the Berea sandstone used in this study (Hejri *et al.* 1991). Figure 33 shows a comparison of flow properties for polymers of comparable concentrations. Agreement between these two curves measured by different research groups is excellent. Willhite and Uhl (1989) measured Xanthan biopolymer flow properties in consolidated Berea sandstone with a wide range of permeabilities. Correlations using the power law parameters describing polymer solution viscosity and core properties of porosity and permeability to polymer have been developed by these researchers. The flow data obtained in this study appear to be in reasonable agreement with the previous studies.

The pressure response to changes in flow rate were very different for the biopolymer than for the polyacrylamide polymer. Figure 34 shows the difference in slope of the log-log plot of pressure gradient versus flow rate. Differences in polymer shape, inter- and intra-molecular interactions, and response to deformation can contribute to differences in flow response of these polymers.

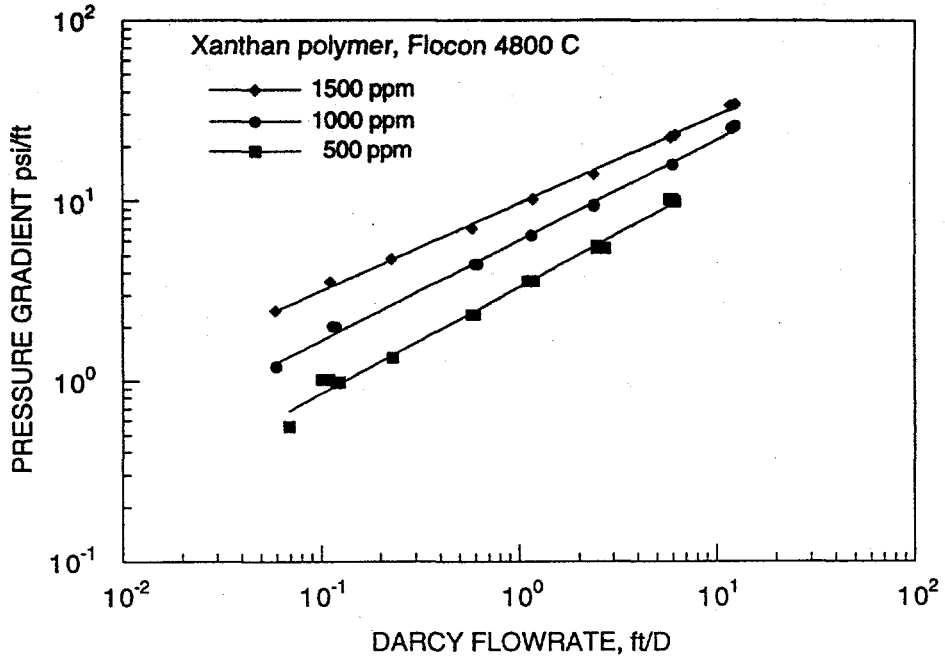

Figure 32 Flow characteristics of Flocon 4800C in high permeability Berea sandstone core.

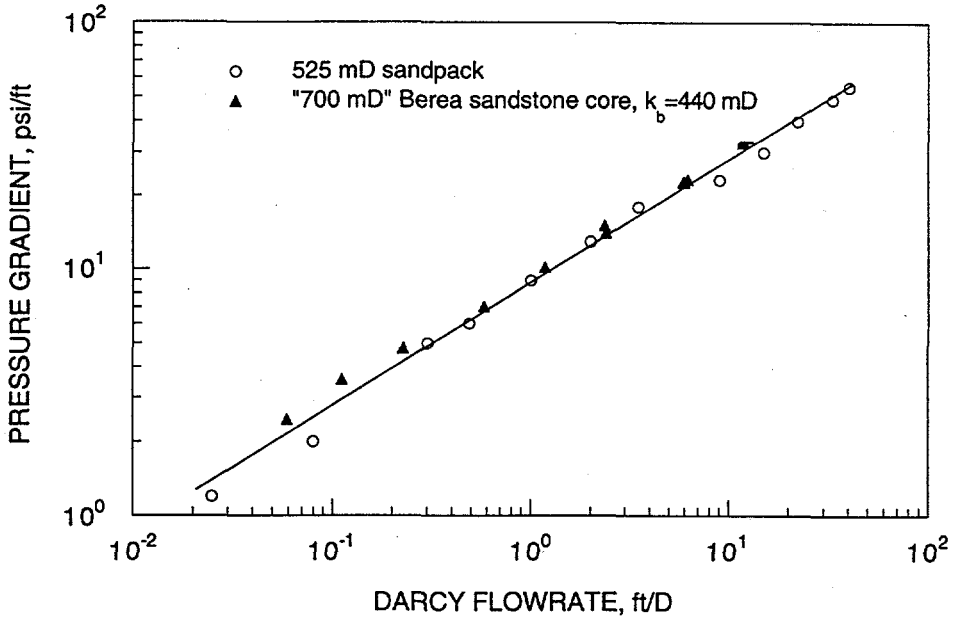

Figure 33 **Comparison of Xanthan biopolymer flow characteristics in porous media with similar permeability.**

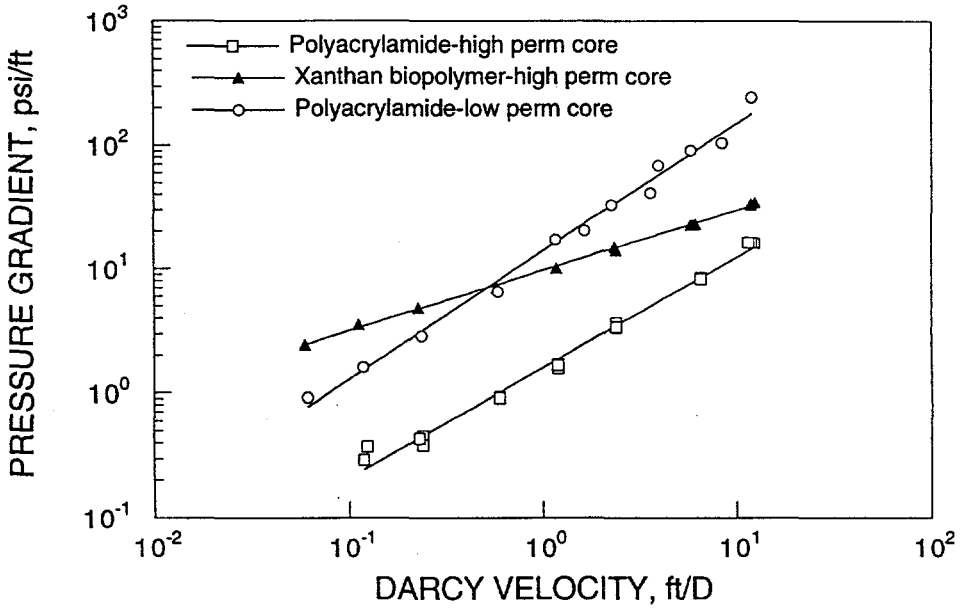

Figure 34 **Differences in flow characteristics of polyacrylamide polymer and Xanthan biopolymer. Slope of the power fit curve for Xanthan biopolymer is approximately 50% of that for the polyacrylamide polymers.**

3.3.3 Relative Permeability Curves and Mobility Control Design

3.3.3.1 Calculation Methods

Adequate mobility control during miscible oil recovery processes such as tertiary oil recovery using surfactants has been described and discussed in the literature. Methods to design adequate mobility control for micellar solutions were given by Goherty *et al.* (1970) They discussed the use of relative-permeability curves to determine design mobility requirements and methods to select representative relative-permeability curves from field core data. Trushenski *et al.* (1974) and Chang *et al.* (1978) described determination of mobility control requirements for surfactant/polymer corefloods from laboratory pressure measurements. The following discussion summarizes the discussions found in these papers to determine design criteria for adequate mobility control and methods to determine the required data for systems of interest and provides definition of appropriate terms used to discuss mobility control requirements.

Relative mobility of a fluid (λ) is defined as the relative permeability of that fluid divided by its apparent viscosity in the porous medium (k_r/μ). In two-phase flow, the total relative mobility (λ_t) is the sum of oil and water relative mobilities.

$$\lambda_t = \lambda_{rw} + \lambda_{ro} \tag{1}$$

Successful miscible flooding results in the formation of a stable oil bank in front of the miscible zone. Since both oil and water are displaced in a miscible flood, the combined flow of water and oil in the bank establishes the mobility requirements for the displacing fluids. Flow in the bank is governed by the principles of fractional flow for immiscible systems (Buckley and Leverett, 1942). Total flow within the water-oil bank, neglecting capillary pressure, is given by:

$$q_t = \frac{k_e A \, \Delta P}{\mu_e L} = kA \left(\frac{k_{rw}}{\mu_w} + \frac{k_{ro}}{\mu_o} \right) \frac{\Delta P}{L} \tag{2}$$

where:

q_t = total fluid flow, cm^3/sec

A = area, cm^2

$\Delta P/L$ = pressure gradient, atm./cm

k_e = effective permeability, Darcy

k = base permeability for relative permeability measurements (k_w at 100% water saturation)

μ_e = effective viscosity, cP

$_w$ and $_o$ refer to water and oil respectively

Total relative mobility for a rock type is calculated as a function of fluid saturation using viscosities of the water and oil of interest and the relative permeability curves for that rock. As an example, figure 35 shows relative permeability curves for high permeability Berea sandstone core used in a number of polymer flow experiments described in this report. For convenience, this core is referred to as 700-mD core from average air permeability measurements. (Liquid permeabilities for this core type are lower than 700 mD.) Figure 36 shows λ_t as a function of water saturation for three different viscosity oils for the 700-mD core. The minimum mobility requirement or design mobility is shown by the minimum in the curve. The actual mobility of an oil bank mobilized by the chemical system may be

equal to or higher than the minimum mobility, but the bank cannot have a mobility less than the minimum. Mobility buffers, therefore should have a mobility value less than or equal to the design mobility over the range of expected fluid velocities to be found in the reservoir.

In the reservoir, flow rates of injected fluids are high around the wellbore and decline as fluids flow in a radial pattern toward producers. The flow properties of mobility-control chemicals (polymers) are dependent on shear rate experienced by the fluids. Therefore, their mobility characteristics will depend on flow rate through porous media. In the laboratory, these properties are measured by pumping mobility solutions through core of interest and measuring pressure differentials as a function of fluid flow rate. This mode of measurement will take into account pore structure of the porous media and its effect on fluid movement as well as non-Newtonian behavior (affect of shear rate) of the polymer.

The relative mobility of the buffer solution is calculated from the flow measurement data using equation 3. The mobility is then compared with the design mobility to determine if the chemical formulation exhibits adequate mobility control characteristics for the experimental conditions under study.

$$\lambda_t = \frac{k_e}{k\,\mu_e} = \frac{q\ L}{kA\ \Delta P} \qquad (3)$$

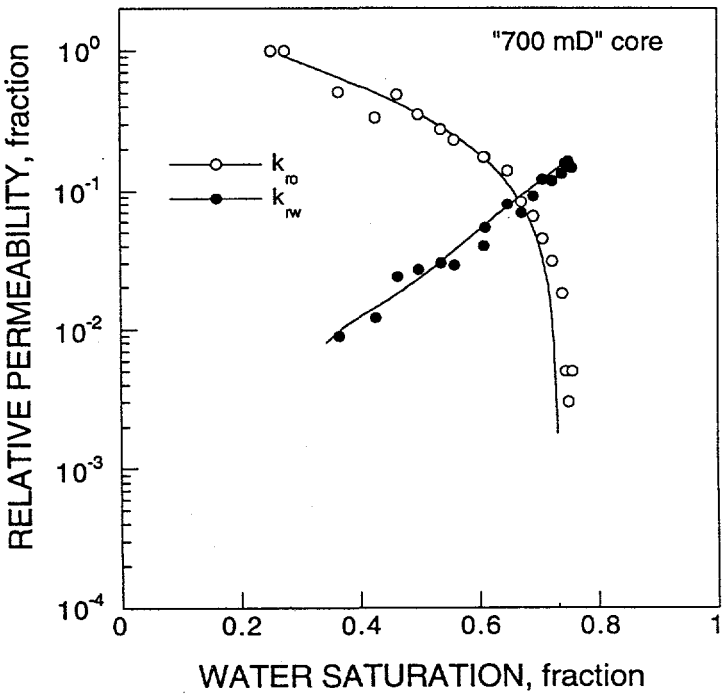

Figure 35 **Oil and water relative permeability curves for high permeability Berea sandstone core.**

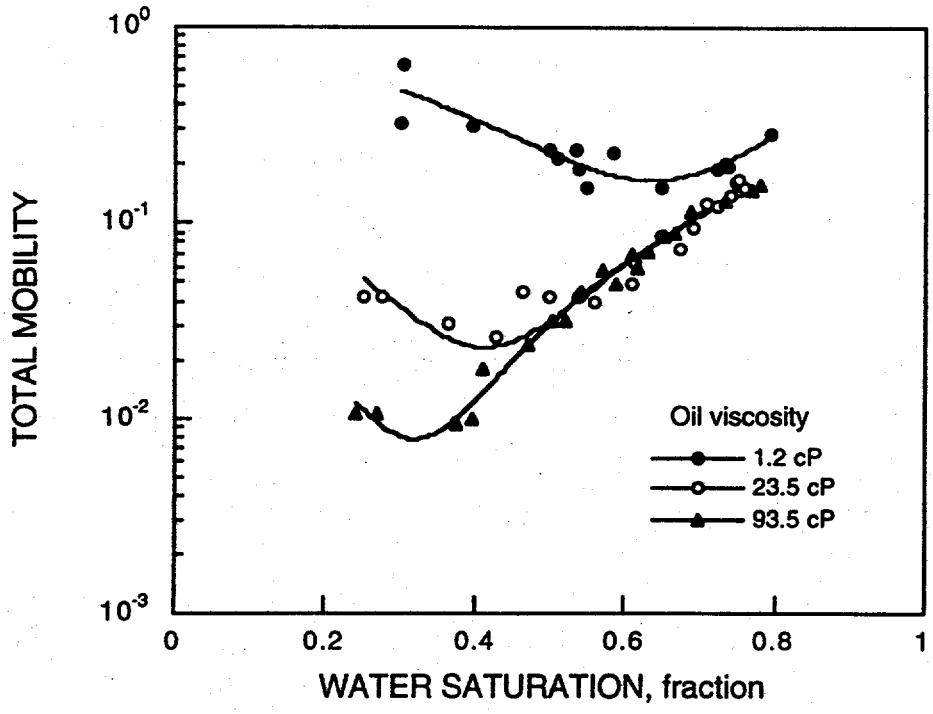

Figure 36 **Total mobility in high permeability Berea sandstone core as a function of oil viscosity**

3.3.3.2 Mobility Calculations for Polymers Used in this Study

In addition to 700-mD Berea core, studies were also conducted in 260-mD Berea sandstone core. The relative permeability curves for this core type is represented in figure 37.

Design mobility calculation for the two types of Berea sandstone core using the relative permeability data shown in figures 35 and 37 are compared in figures 38 and 39 for two different viscosity oils. As expected mobility requirements increased as oil viscosity increased and as core permeability decreased. The minimum values of these curves are used as the design mobility for comparison purposes when plotting mobility data for the polymers in this study.

The mobility values calculated using equation 3 for the polyacrylamide polymer, Alcoflood 1135 (in 3% KCl brine) for flow tests in 260-mD and 700-mD Berea sandstone core are plotted as a function of fluid frontal velocity through the core. (The frontal velocity is the Darcy velocity divided by core porosity.) These relationships are shown in figures 40 and 41, respectively.

The 1000 and 1500 ppm Alcoflood 1135 polymer in 3% KCl would provide adequate mobility control for low viscosity oils in high permeability rock over most flow regimes found in the reservoir where typical flows around the wellbore may be as much as 10 ft/D and deeper in the reservoir around 1 ft/D. The mobility values, however, line above the value for design mobility for higher viscosity oil in the high permeability core. In addition, none of the polymer solutions tested would provide adequate mobility control for either low or high viscosity oil in the 260-mD Berea sandstone core.

Figure 42 shows that Alcoflood 935 prepared in a higher ionic strength brine containing relatively high concentrations of divalent ions does not provide adequate mobility characteristics for

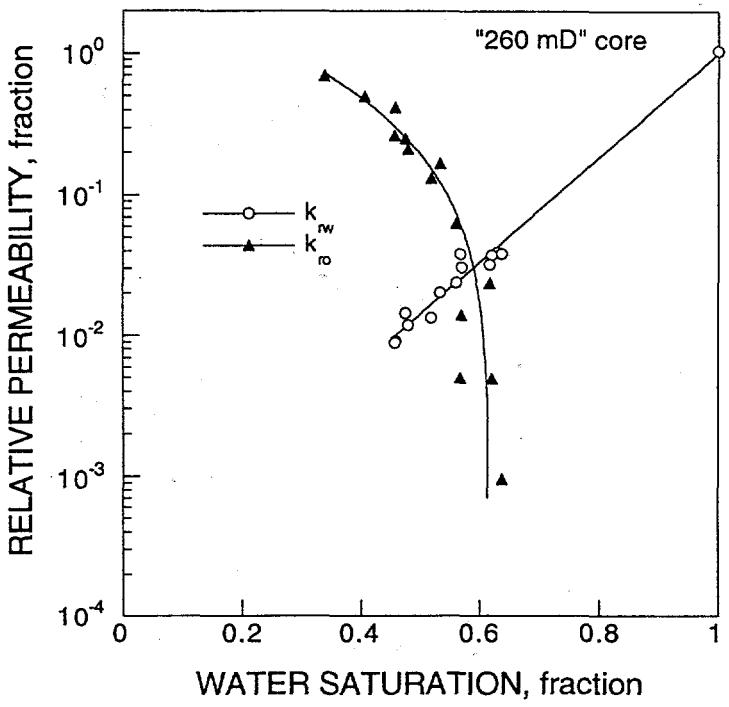

Figure 37 Oil and water relative permeability as a function of aqueous phase saturation for 260-mD Berea sandstone core.

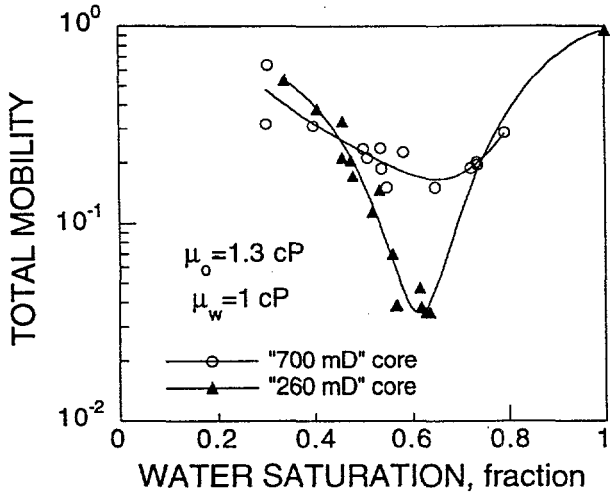

Figure 38 Comparison of total mobility for 1.3 cP oil as a function of core permeability.

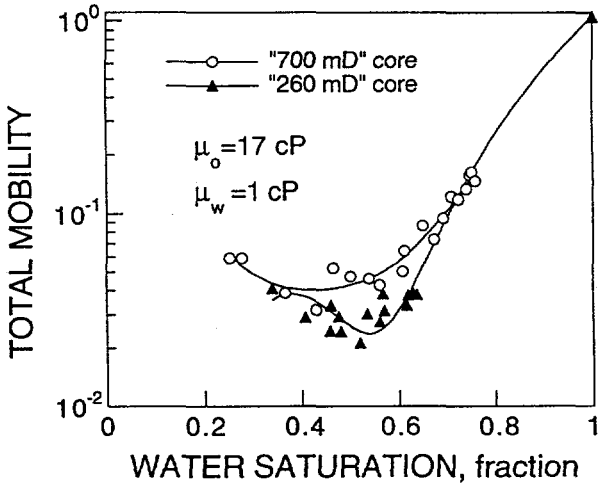

Figure 39 Comparison of total mobility for 17 cP oil as function of core permeability.

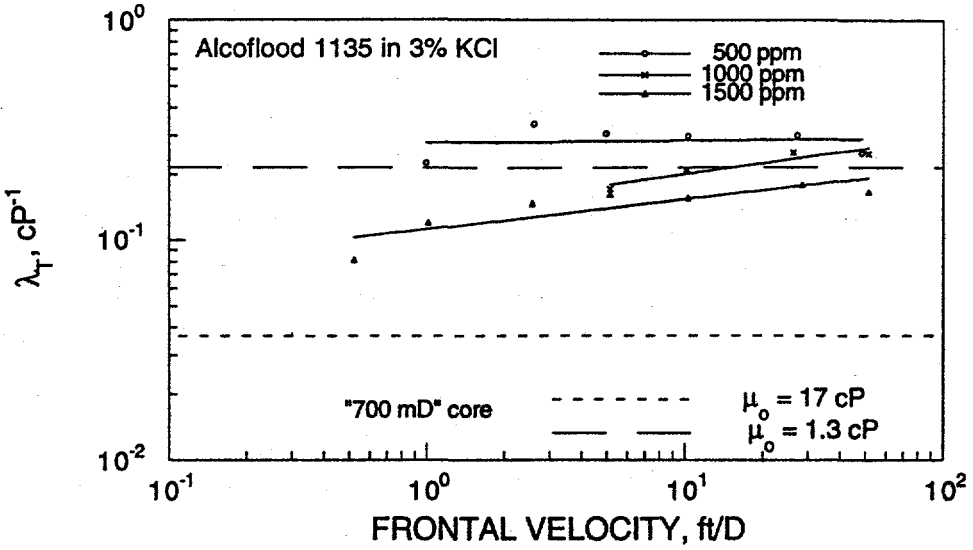

Figure 40 **Polymer mobility in 700-mD Berea sandstone core as a function of fluid frontal velocity.**

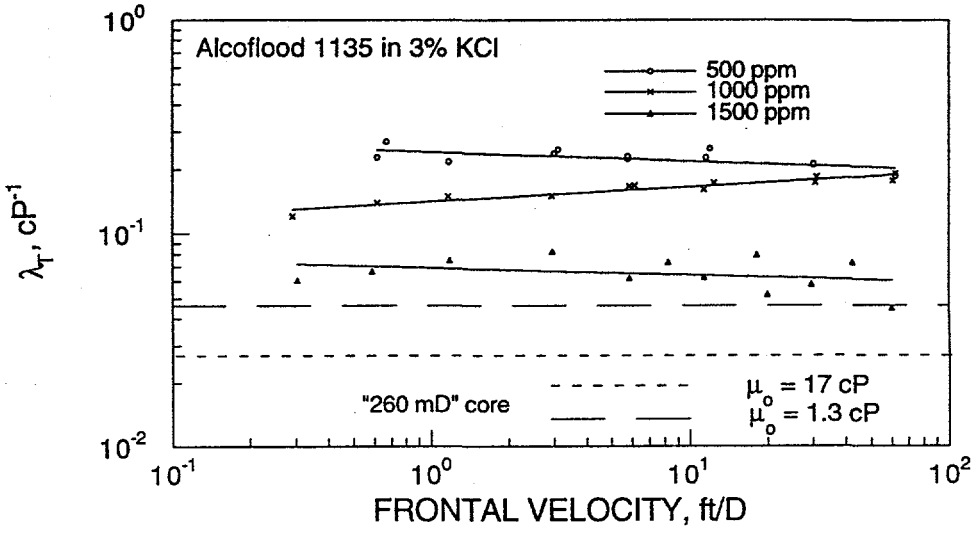

Figure 41 **Polymer mobility in 260-mD Berea sandstone core as a function of fluid frontal velocity.**

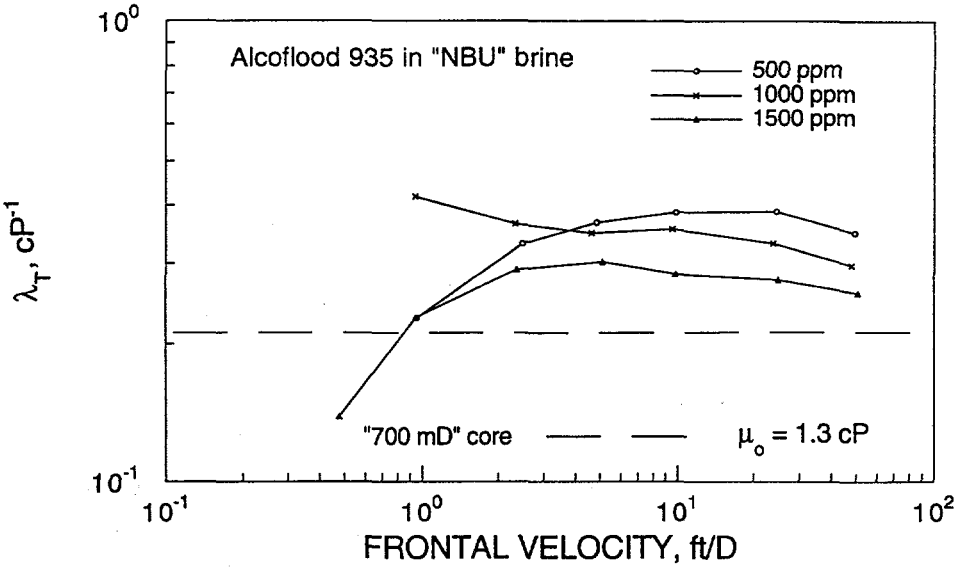

Figure 42 **Mobility characteristics of Alcoflood 935 polymer in high permeability Berea sandstone core.**

low or high viscosity oil even in the high permeability Berea sandstone. It is well known that polyacrylamide polymer solution properties such as viscosity are sensitive to ionic strength. Polyacrylamide polymers are typically prepared in the freshest water available. Polymer properties at lower ionic strength must be evaluated to determine suitability for application in a specific reservoir situation. In the reservoir, however, dilution with reservoir brine may result in degradation of solution properties and accompanying loss of mobility control.

It is possible to obtain adequate mobility control in cores of this type by preparing polyacrylamide polymer in solutions of lower ionic strength. Flow characteristics of another polyacrylamide product were determined in connection with a different project being conducted at NIPER. One example is shown in figure 43 to illustrate the change in mobility characteristics of this polymer prepared in fresh water containing some divalent ions (TDS = 700) and in fresh water with added alkaline agents for use in alkaline-surfactant-polymer applications. In 260-mD Berea sandstone core, more than adequate mobility characteristics are obtained for an oil with viscosity of approximately 19 cP using 1000 ppm polymer prepared in fresh water. The alkaline agents, however, reduce polymer viscosity, and mobility values rise to the level or exceed the design mobility for this oil and core combination.

The other type of polymer tested during this project was a polysaccharide, Xanthan biopolymer Flocon 4800 C, prepared in 3% KCl. Polysaccharide polymers have some advantages over polyacrylamide polymer since their viscosities are less sensitive to changes in solution ionic strength. They are, however, more susceptible to microbial degradation, which causes some concern for long term injection in the field.

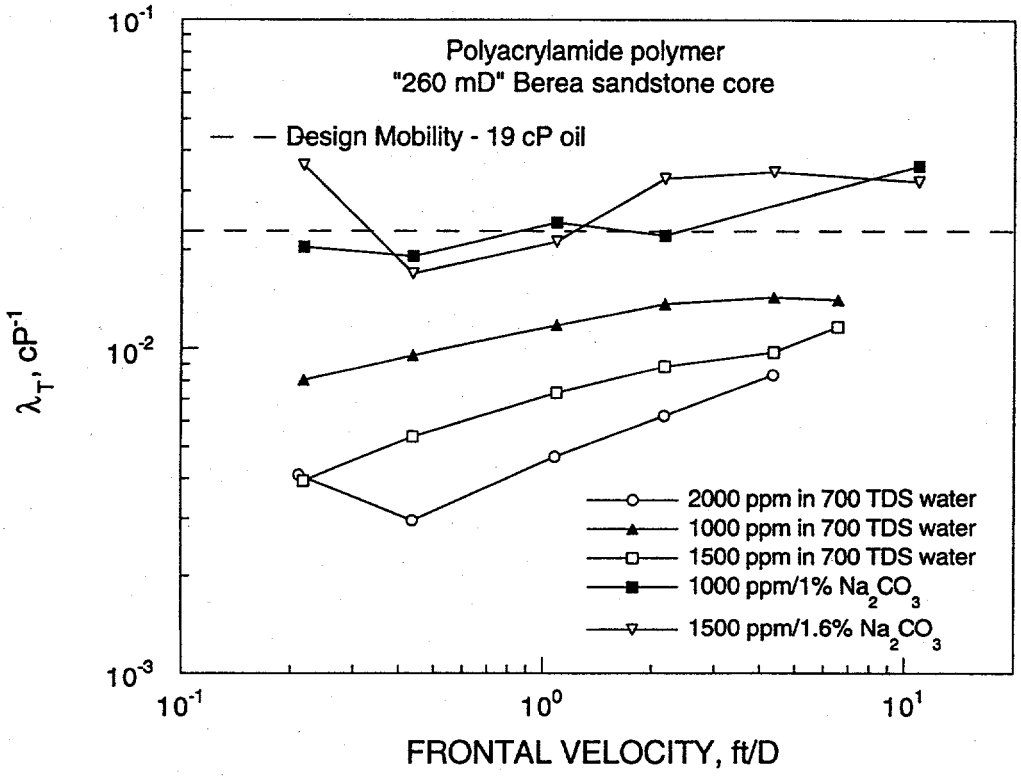

Figure 43 **Mobility characteristics of polyacrylamide polymer MO3000H-SF prepared in low ionic strength water and in sodium carbonate solutions.**

Figure 44 shows the mobility curves for the Xanthan biopolymer. For the same ionic strength level, The Flocon 4800 has better mobility characteristics for low viscosity oil than the Alcoflood 1135, as shown in figure 40. Solutions of higher concentration, however, would be required to provide adequate mobility control for 17 cP oil. Higher concentrations, however, imply greater cost and possibly greater injection problems. The balance between cost and guaranteed effectiveness most often is decided in the direction of cost when planning field projects.

3.3.3.3 Summary of Mobility Study

In summary, mobility control for chemical flooding can be evaluated using the following procedures:

- Determine relative permeability for the rock of interest.
- Calculate design mobility using the viscosities of oil and brine of interest from equation 1.
- Determine pressure differentials as a function of fluid velocity for rock that is completely saturated with the solution of interest. Mobility characteristics will be a function of polymer type, solution ionic strength, flow paths in the porous media, and fluid velocity.
- Calculate solution mobility using equation 3 and compare with the design mobility.

The polyacrylamide polymers studied during this project were adversely affected by solution ionic strength. This included two polyacrylamide polymers that differed by the anionic character of

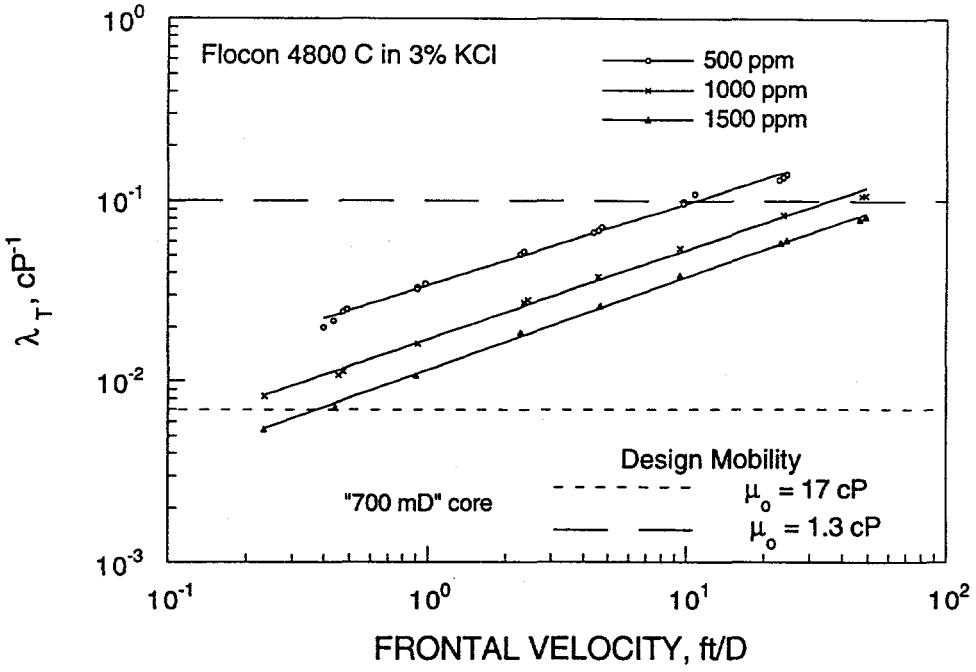

Figure 44 **Mobility characteristics of Xanthan biopolymer in high permeability Berea sandstone core as a function of fluid frontal velocity.**

the polymer. The polymer of lower anionic was designed for use in higher salinity brines. In this work, however, the testing conditions were too harsh, and good mobility control would not be achieved even for high permeability rock and low viscosity oil. This product may perform well at lower salinities, but these conditions were not tested. A second polyacrylamide polymer prepared in a lower salinity brine performed slightly better but was still unsuitable for use with high viscosity oil. Polyacrylamide polymers prepared in relatively fresh water should provide adequate mobility control for oil viscosities up to or even greater 19 cP.

Xanthan biopolymer is less salt sensitive. At the same salinity and concentration, the Xanthan biopolymer provided greater mobility control characteristics than the polyacrylamide polymer. At low salinity, however, this comparison may not apply. The flow results obtained in this study in consolidated core compared well with results from studies in the literature of flow through sandpacks of similar or higher permeability. Correlations reported in the literature study should be useful for predicting Xanthan mobility characteristics in high permeability consolidated core.

3.3.4 CT-Monitored Coreflood for Initial Mobility/Oil Recovery Study

One oil recovery experiment, SP-1, was performed in connection with the polymer mobility control study to evaluate the use of CT-imaging to monitor oil movement and recovery as a function of polymer mobility characteristics. A description of the results of this experiment will be provided in this report. Further studies, however, will be required to obtain comparative information for recovery experiments with different mobility requirements.

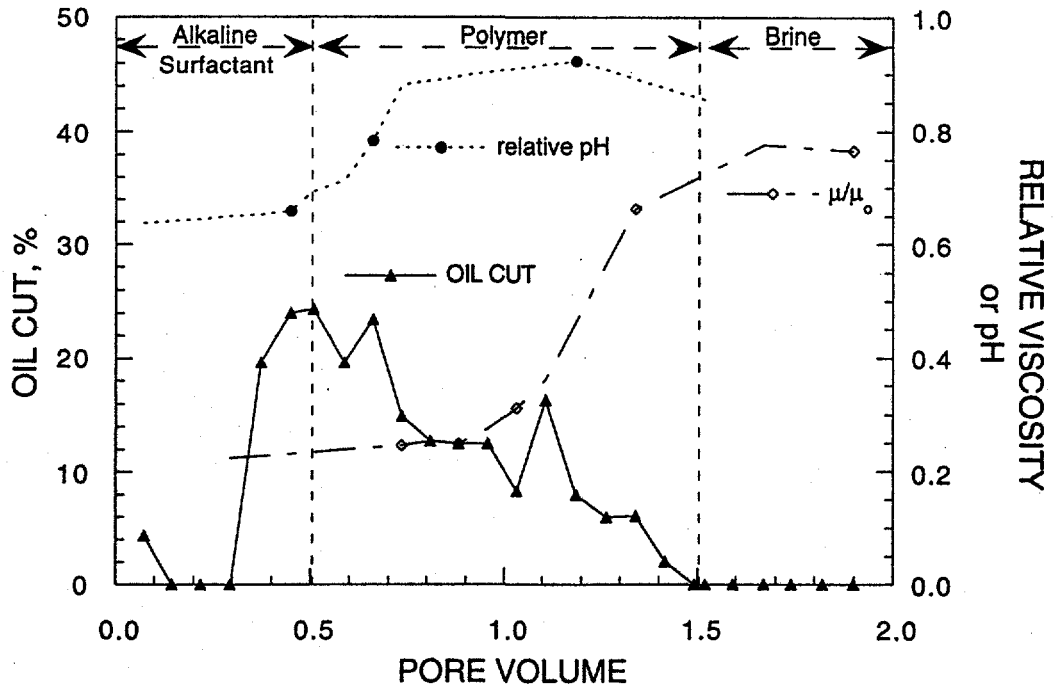

Figure 45 **Oil production for a chemical flood using an alkaline-surfactant-polymer system in high permeability Berea sandstone core. The polymer was designed with poor mobility control characteristics. Also shown are pH and relative viscosity values for the produced fluids.**

The oil recovery test was conducted in high permeability Berea sandstone core using a high viscosity oil. The oil was prepared from 55 cP stock tank oil that was diluted with iododecane (tagging agent for CT-imaging) and n-hexane. The ratio of components was 80/15/5 % by volume. The viscosity of the diluted oil was 17 cP. An alkaline surfactant system was used in the chemical flood that was 0.2% B-100 and 1.6% Na_2CO_3. The IFT that was measured between oil and chemical system was very low, 0.002 mN/m. The polymer used in the test was 1500 ppm polyacrylamide in 1.6% Na_2CO_3 that was aged to reduce solution viscosity. The viscosity of this polymer was much lower than that of the polyacrylamide polymer in 1.6% Na_2CO_3, shown in figure 17. It closely matches the viscosity measured for the Alcoflood 935 in brine. Figure 16 shows that mobility control would not even be adequate for low viscosity oils. It was expected, therefore, that this polymer would not provide adequate mobility control to most effectively produce oil in this flood.

The chemicals were injected after waterflooding the core. Figure 45 shows oil production as a function of fluid through the core. The average oil saturation in the core was reduced from 34.2% after the waterflood to 18.3% after the chemical flood for a recovery efficiency of 46% of the residual oil saturation. While this amount of oil recovery is not insignificant, higher recovery efficiencies are expected and have been achieved in previous laboratory studies. Saturations as low as 5% have been achieved in high permeability Berea core using high viscosity oil, low IFT surfactant systems, and high viscosity polymers (Gall 1992; Llave *et al.* 1993; French and Josephson 1991).

PH measurements indicated that the alkaline solution broke through after approximately 0.6 to 0.7 PV after before all the oil had been produced. The polymer, as indicated by an increase in fluid viscosity, also broke through approximately 0.6 to 0.7 PV after the start of polymer injection. Solution viscosity, however, did not reach the level of that of the injected polymer.

CT images of the core at various stages of the coreflood experiment are shown in figure 46. No major porosity variations such as laminations or barriers are seen in the porosity image of this core. There does appear to be a slight increase in porosity from the core inlet to outlet, however. Oil saturation after the oil flood was slightly higher at the core inlet. After the waterflood, the oil saturation was slightly higher at the core outlet. Average oil saturation after the waterflood was 34%. The chemical flood image shows that an oil bank was produced ahead of the chemical slug. The highest oil saturation was approximately 60%.

After polymer injection, the oil saturation distribution was fairly uniform throughout the core. In a previous coreflood experiment (CT-CF 3) using inadequate polymer concentration to obtain good mobility control, the oil saturation distribution at the end of the polymer flood was much less homogeneous from core inlet to outlet (Gall 1992). The average final oil saturation after complete injection of the chemical system the oil saturation was slightly higher than for SP-1, 22%, but was much lower at the core face and higher at the core outlet than the comparative saturations of SP-1. For comparison, the CT-CF 3 image in shown in figure 47. The differences may be attributed to an even greater mobility control contrast between oil and polymer since the oil used in CT-CF 3 had more than twice the viscosity as the oil used in this study (38 versus 17 cP). Since other differences including type of polymer and surfactant formulation exist between the two tests, further, more systematic investigations are necessary to determine the reasons for these differences in residual oil saturation distributions.

In summary, one coreflood was conducted with polymer having poor mobility control characteristics. Final average oil saturation after completion of the test was 18.3 %. Oil saturation was fairly uniform throughout the core in contrast to a previous test where the oil saturation at the core inlet was much lower than at the core outlet. Additional studies will be required to more systematically compare oil recoveries as a function of mobility control characteristics of the chemical systems, however.

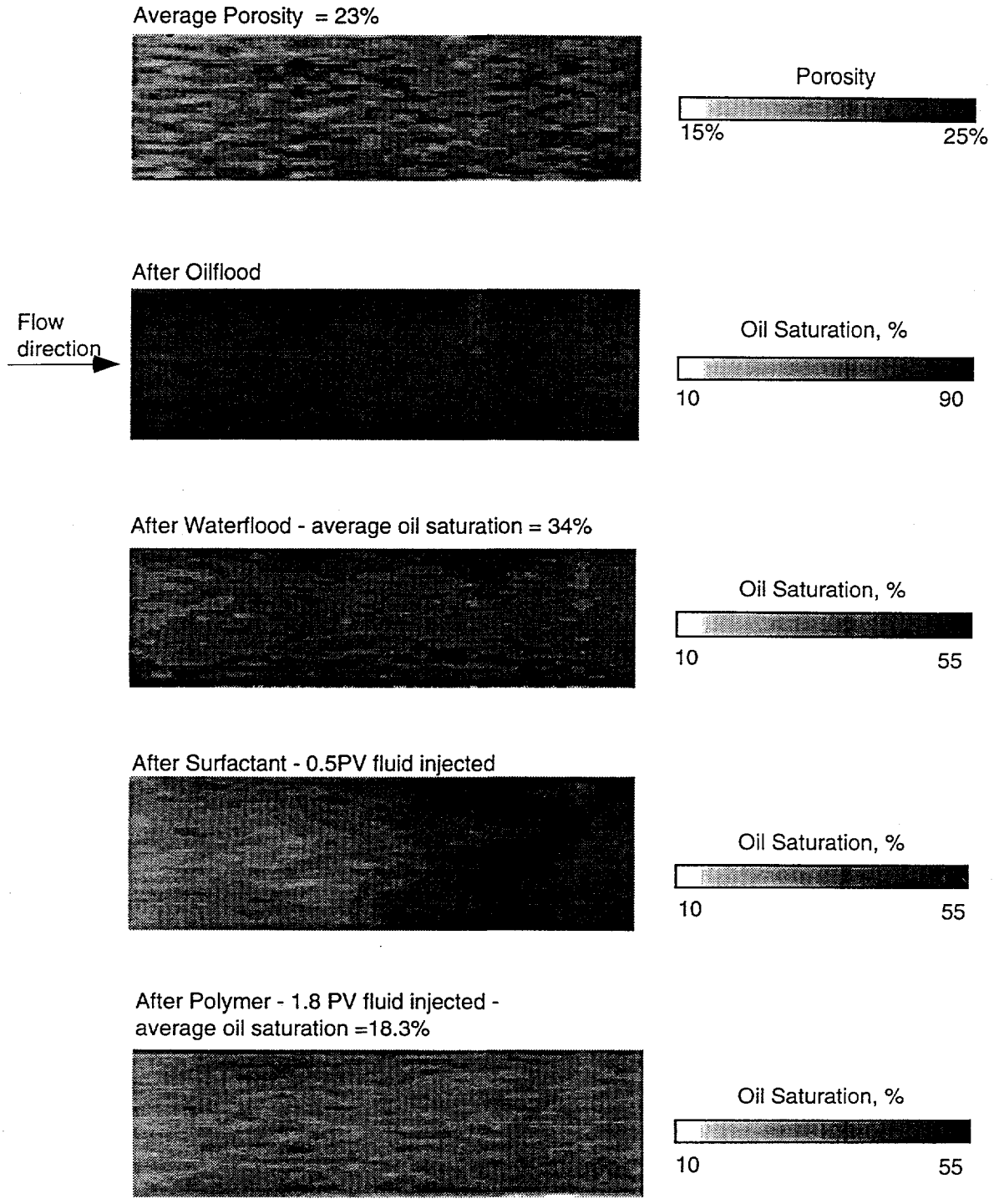

Figure 46 **CT images of porosity and oil saturation distributions after various stages of a coreflood experiment in high permeability Berea sandstone core. The chemical system is 0.2% B-100/1.6% Na_2CO_3/1500 ppm aged polyacrylamide polymer in 1.6% Na_2CO_3 with 17 cP oil.**

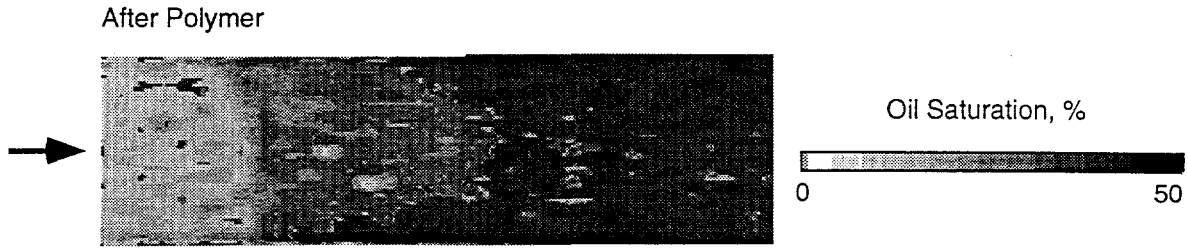

Figure 47 **Oil saturation distribution of a 38 cP oil after polymer injection of an alkaline-surfactant-polymer chemical system with poor mobility control characteristics. The experiment is described in reference 2.**

3.4 Simulation of Corefloods with UTCHEM Simulator

Capability to simulate coreflood results and oil saturation distribution results from CT imaging will provide a method to improve interpretation and provide input for evaluation of chemical processes for field applications. DOE has supported the development of a complex chemical flood simulator, UTCHEM, at the University of Texas. To gain familiarity with the capabilities of the UTCHEM simulator and to identify experimentally obtainable parameters that in the task of comparing the results of laboratory coreflood experiments, the input data file of the UTCHEM simulator (version 5.03) (User's Guide 1991) was reviewed. A trip to the University of Texas at Austin was also made to consult with Professor Gary Pope, two staff members, and three graduate students.

UTCHEM is a three-dimensional chemical flooding simulator (User's Guide 1991). Its solution scheme solves for pressure implicitly and for concentrations explicitly. Phase saturations and concentrations are solved based on equilibrium or equations of state. Basically, the input data file is divided into five sections, title and reservoir description data, output option data, reservoir properties, physical property data, and recurrent injection/production data set. Although the simulator has the capability to simulate permeability modification using gelled polymers, the input data file section that is related to the polymer gel treatment has not been reviewed.

In the first section, options on the type of run (first run or restart run), time-step size control (constant or automatic), numerical dispersion control method, coordinate system (cartesian or radial), chemical EOR method, and grid size (fixed or variable) can be selected. Up to two alcohols and three tracers can be simulated. There are four options on alkaline flooding. The maximum number of components that must be set depends on whether gel reactions or alkaline options are used or not. The units for water, oil, surfactant and alcohol are volume fraction. For polymer and tracers, the units used are weight %. The units for calcium and chloride are milliequivalents/mL.

The second input section consists of output options. Pore volume or day interval output option is available. Concentration profile of each component in each phase, phase pressure profile, phase saturation profile, profile of tracer phase concentrations, profile of capacitance properties, profile of gel properties and profile of properties related to the alkaline option can be selected to be printed out. In addition, options of printing surfactant, polymer, calcium, gel chromium, hydrogen and sodium adsorption data, phase viscosities, relative permeabilities, phase capillary numbers, interfacial tensions, and permeability reduction factors are also available.

The third input section consists of reservoir properties, including rock compressibility, porosity, permeability, initial pressure, depth to the top layer, initial water saturation, and initial anion and divalent cation concentrations of brine. Except for the rock compressibility and brine concentration, different values of reservoir properties can be specified for each grid block.

The fourth section of the input data file consists of physical property data. These data include phase behavior, IFT, capillary desaturation, relative permeability, compositional phase viscosity, polymer properties, phase specific weights, capillary pressure, molecular diffusivities of components in each phase, longitudinal and transverse dispersivities of each phase, surfactant adsorption, cation exchange, tracer properties, gel properties, and properties related to alkaline flooding.

In UTCHEM, all phase behavior parameters are defined as a function of an effective salinity (Hirasaki 1992) , CSE, which is calculated according to the equation (Satoh 1984):

$$CSE = \frac{C51}{(1 - \beta_6 f_6^s)(1 + \beta_7 f_7^s + \beta_8 f_8^s)} \tag{4}$$

where C51: meq Cl^-/ml water,

f_6^s: fraction of divalent cations associated with surfactant (meq/meq)

f_7^s: volume fraction of alcohol 1 in surfactant pseudocomponent

f_8^s: volume fraction of alcohol 2 in surfactant pseudocomponent

and β_6, β_7, and β_8 are the slope parameters for calcium, alcohol 1, and alcohol 2 dilution effects. The parameters, β_6, β_7, and β_8, can be determined from the effects of f_6^s, f_7^s, and f_8^s on the optimum C51 concentration. (Lchne 1991)

The phase behavior is modeled by the Hand equation. (Pope and Nelson 1978)

$$\frac{C_{33}}{C_{23}} = A\left(\frac{C_{33}}{C_{13}}\right)^B \tag{5}$$

where C_{i3} is the volume fraction of component i in the surfactant pseudocomponent phase. C_{13}, C_{23}, and C_{33} denote the composition along the binodal curve. The Hand parameter A describes the height of the binodal curve and B gives the shape of the binodal curve. The parameter A is related to the maximum height of the binodal curve C_{3MAX} as follows:

$$A = \left(\frac{2C_{3MAX}}{1 - C_{3MAX}}\right)^2 \tag{6}$$

For symmetrical binodal curves, B = -1. This is the only option UTCHEM version 5.03 has. In the latest version UTCHEM-D-5.31, unsymmetrical binodal curve is available. In UTCHEM, required input data are the intercepts of the maximum height of the binodal curve at zero fraction of alcohol 1 (component 7) and the slopes for maximum height of the binodal curve vs. fraction of alcohol 1 associated with the surfactant pseudocomponent at zero salinity, optimal salinity and twice optimal salinity. Similar input data are also required for alcohol 2 (component 8) if two alcohols are used. These parameters can be obtained by matching the volume fraction diagrams corresponding to at least three different total chemical concentrations.

Two alcohol partition models are available in the simulator. Hirasaki's model (Hirasaki 1982) assumes a constant alcohol partition coefficient between oil and water and a constant alcohol partition coefficient between surfactant and water. Prouvost's model (Prouvost *et al.* 1985) requires a self-association constant of monomeric alcohol in oleic pseudophase, *K*, and the ratio of molar volume of monomeric alcohol to equivalent molar volume of surfactant, in addition to the partition coefficients between aqueous and oleic pseudophases, k_w, and between interfacial and oleic pseudophases, k_m. *K*, k_w, and k_m can be determined experimentally.

To determine the interfacial tension parameters for water-microemulsion interface and for oil-microemulsion phase, data on IFT as a function of V_w/V_s (V_w = volume of water in microemulsion phase, V_s = volume of surfactant in microemulsion phase) and as a function of V_o/V_s (V_o = volume of oil in microemulsion phase) are required. (Healy, et al. 1976) The surfactant volume does not include the

alcohol cosolvent. All data were measured by varying only salinity. The parameters can then be obtained by matching the experimental data with the model equation used in the simulator (Healy *et al.* 1976). Phase viscosity parameters can be obtained by matching the model equation with experimentally determined microemulsion viscosity as a function of salinity (Camilleri *et al.* 1987). Microemulsion phase viscosity approaches the water viscosity in Type II(-) phase environment and oil viscosity in Type II(+) phase environment. The phase viscosity correlation used in the UTCHEM simulator depends only indirectly on alcohol via the phase behavior.

Required polymer properties include the polymer solution viscosity as a function of polymer concentration, salinity and shear rate, polymer adsorption, residual resistance factor, and inaccessible pore volume to polymer. Inaccessible pore volume to surfactant and surfactant adsorption are also required. Both polymer adsorption and surfactant adsorption were modeled by Langmuir-type isotherms.

For alkaline flooding, four options are available (Bhuyan *et al.* 1989). Option 1 is mainly for the simulation of alkaline or softened water preflush before a micellar/polymer flood. Alkaline agents that can be used are restricted to sodium carbonate and sodium hydroxide. Sodium, hydrogen, magnesium and carbonate components are included in this option. Option 2 has the ability to account for acidic crude oil and in situ generation of the surfactant species. This option can be used to simulate alkaline, alkaline/polymer or alkaline/surfactant/polymer floods where the crude oil has acidic components capable of producing surface active anions and where clay and silica dissolution/precipitation can be neglected. Option 3 is similar to option 1 except that aluminum and silicon are considered. Alkaline agent that can be used include different sodium silicates in addition to sodium carbonate and sodium hydroxide. Option 4 can handle the same types of reaction chemistry as those in option 3 except that this option has the ability to account for acidic crud oils and in-situ generated surfactant species. The alkaline agents that can be used are similar to those used in option 3.

The input data file must be created using the EQBATCH program. Required experimental data include the pH value above which surfactant adsorption is constant and the critical pH above which surfactant adsorption is pH independent if surfactant adsorption is pH dependent. If the crude oil has acidic component capable of producing surface active anions, lower and upper optimum salinity limits for generated surfactant are also required.

Required initial chemical species concentrations include the concentrations of nonreacting anions, total calcium concentration in aqueous phase, concentration of acid in oil, solid species concentrations, concentrations of adsorbed cations, water concentration in aqueous phase and oil concentration in oleic phase.

Other required input information includes the total numbers of fluid species, solid species, sorbed species, surfactant associated cations, independent fluid species, insoluble exchangers, and elements comprising the solid species. Position numbers corresponding to each element in the element array, and names of elements, fluid species, solid species, adsorbed cations on rock surface, and adsorbed cations on micelles must be specified. In addition, stoichiometric coefficients and charge of each fluid species, each adsorbed species and each surfactant associated cation are required. Equilibrium constants, exchange equilibrium constants, solubility products, cation exchange capacity, dissociation constant and equivalent weight of petroleum acid are also required.

The last section consists of the recurrent injection/production well data. Number of wells, well location, direction of each well, rate or pressure constrained injection or production well, and minimum and maximum flowing bottom hole pressure and flow rate for each well are specified in this section. Chemical species concentrations in the injection fluid, flowing bottom hole pressure if pressure constraint is selected, total production rate if rate constraint is selected, cumulative injection time, output files print control, time step size, and tolerance for concentration change are also specified in this section.

3.4.1 Simulation Run

After the input data file was reviewed, a simulation run for a surfactant/polymer flood was conducted on NIPER's Micro VAX computer (VMS V5.4) using a sample input data file that came with the UTCHEM simulator. The reservoir model having dimensions 250 x 250 x10 ft was represented by 11 x 11 x 2 (242) grid blocks. The injection rate used was 112.3 ft^3/day. Using the NIPER's Micro VAX computer (VMS V5.4), it took about 49 minutes to run 1000 time steps. To simulate CT-imaging corefloods in FY 1995, rectangular cores of 4 x 4 x 25 cm will be used. Each core will be represented by 8 x 25 x 64 (12,800) grid blocks. Based on this reservoir model (12,800 grid blocks), the estimated CPU time for running 1000 time steps on the NIPER's Micro VAX computer will be about 43 hours. Since simulation runs will be conducted frequently, a computer such as a Work Station that will give at least 100 times faster than the current computer is desirable. The minimum required RAM is 65 megabytes.

3.4.2 Summary

This review revealed that required data for running the UTCHEM simulator for chemical flooding (surfactant/polymer or alkaline/surfactant/polymer flooding) include:

- phase behavior of the chemical including the volume fraction diagrams corresponding to at least three different total chemical (alcohol + surfactant) concentrations
- lower and upper salinity limits for type III phase region and optimal salinity as a function of volume fraction of alcohol associated with surfactant pseudocomponent and as a function of fraction of divalent cations associated with surfactant pseudocomponent
- alcohol partition coefficients between oil and water and between surfactant and water
- IFT of the water-microemulsion interface and that of oil-microemulsion interface as a function of solubilization ratios
- IFT of the water-oil interface
- phase viscosity data including that of the microemulsion viscosity as a function of salinity
- polymer solution viscosity as a function of polymer concentration, shear rate and salinit

- polymer adsorption, residual resistance factor and inaccessible pore volume

- surfactant adsorption and inaccessible pore volume to surfactant

For alkaline/surfactant/polymer flooding, the pH value above which surfactant adsorption is constant and the critical pH above which surfactant adsorption is pH independent must be determined if surfactant adsorption is pH dependent. If the crude oil has an acidic component capable of producing surface active anions, lower and upper optimum salinity limits for generated surfactant must also be determined.

A work station that will give at least 100 times faster than the Micro VAX/VMS^{TM} computer is desirable. The minimum required RAM is 65 megabytes.

4.0 Summary and Conclusions

Selected surfactant systems containing a series of ethoxylated nonionic surfactants in combination with an anionic surfactant system have been studied to evaluate phase behavior as well as oil recovery potential under different conditions.

One of the studies conducted involved the evaluation of the effect of anionic-nonionic surfactant proportion on overall phase behavior. Two distinct transition behaviors were observed, depending on the dominant surfactant in the overall system. The first type of transition corresponds to more conventional transition behaviors attributed to nonionic-dominant surfactant systems. The latter type was attributed by an earlier research to a condition of attaining a lower critical micelle splitting temperature, which determined the condition beyond which the mixed micelles formed from anionic-nonionic mixtures separate into water- and oil-soluble surfactants. Temperature has an opposite effect on the oil/water affinity of anionic and nonionic surfactants. At elevated temperatures, nonionic surfactants are more lipophilic (higher oil affinity), while the opposite has been exhibited by anionic surfactants. This difference in behavior can contribute to the presence of a distinct transition region at the right surfactant component ratios. Experiments were conducted to map out the transition region from one type to another. For the chemical systems tested, the formulation containing 0.6 wt% DM-530 and 1.4 wt% TRS 10-410/IBA exhibited the transition from nonionic-surfactant dominant behavior to anionic-surfactant dominant behavior. Systems formulated with more anionic surfactant in proportion exhibited no sharp solution conductivity changes while those systems formulated with more nonionic surfactant in the system exhibited very sharp solution conductivity changes. Both types of transition can be used to identify the relative proximity of optimal areas. Determining these transition ranges provided more insight on how the behavior of these surfactant mixtures was affected as the component proportions of the chemical slug may change as it propagates through the rock matrix.

Efforts to optimize the chemical system for oil displacement potential were undertaken. Salinity and alkane scans were conducted to determine the degree of oil and brine solubilization in the chemical system tested. From these results, a distinct middle phase behavior was determined for the scans using n-heptane to n-decane, at the two temperatures tested. Relatively high solubilization values were obtained for both cases. For the purpose of conducting ambient temperature coreflood experiments, n-heptane was selected for the oil phase. The results of the salinity scans helped identify the upper and lower limits of the middle phase behavior for this chemical system in the oil used.

Similar phase behavior studies with systems formulated with some polymer in solution were conducted. The results indicated that the overall solution behavior showed only a slight difference/shift in the presence of the polymer. The results of the salinity scans also supported the results from the PIT determination. Based on these observations, no significant shift in solution behavior attributed to the presence of the polymer was expected during the coreflooding for the range of polymer concentrations tested.

Oil recovery experiments were also conducted on a select chemical formulation. These experiments were conducted to evaluate the effect of the following variables on oil recovery potential: (1) effective brine permeability, (2) slug formulation, (3) slug content, (4) slug size, (5) initial oil saturation, and (6) injection strategy.

A comparison was made of the results of the experiments conducted in different brine permeability cores. The results showed that the experiments conducted in low permeability cores (< 100 mD) yielded resulting oil saturations that were much higher (25%-28% S_{ocf}) than those obtained in cores of higher brine permeabilities (< 20% S_{ocf}), under comparable displacement conditions. The degree of reduction in oil saturation in low permeability cores was considerably lower than in high permeability cores. The results were similar to those obtained by others for the range of permeabilities tested. Comparison with results of earlier experiments conducted using alkaline-enhanced surfactant polymer systems indicated similar degree of oil saturation reductions. The trend in oil saturation reduction vs. permeability observed in the chemical slug and the middle-phase slug experiments almost parallel those of the large pore volume ASP experiments. The results of the comparison did show that the ASP (large pore volume used) experiments had much lower oil saturations (about 5%-6% less) than the saturations from the middle-phase slug experiments, using comparable brine permeability cores. On the other hand, the results from the small pore volume ASP experiments yielded much higher oil saturations (slightly higher than the straight chemical slug experiments). Two factors need to be considered in this case, one the effect of the brine permeability and the other the effect of slug size. The effective brine permeability had a more significant effect on oil recovery potential than the slug size (up to a reasonable, economic limit). Increasing the slug size of the chemical treatment was only one of the means to overcome the limiting effects of low permeability on oil recovery. These lower permeabilities ranges represented a significant challenge for designing chemical system that can effectively displace/sweep residual oil. The lackluster performance of most promising chemical systems was often attributed to poor sweep under reservoir conditions.

A comparison was made with the type of injection strategy employed in these experiments. The first set of experiments involved displacing the oil-saturated core with the middle-phase chemical slug. The second set of experiments involved displacing the oil saturated core with brine to residual oil saturation (S_{ow}), prior to chemical slug injection. Comparable trends in oil saturation reduction as a function of core permeability was indicated. There was a slight difference indicated at the higher end of the permeability range tested. At relatively low permeabilities (< 100 mD) the results for the two sets of experiments were almost similar, while the difference in degree of oil saturation reduction increased at the higher permeability values (circa 800 mD). These results indicated that the resulting oil saturation was not as sensitive to the type of injection strategy employed (no significant difference in final oil saturation whether the core was brine flooded or not, prior to chemical injection). On the other hand, the type of injection strategy employed indicated some difference in resulting oil saturations in high permeability cores. These results indicated that at high permeability levels, the displaceable amount of oil (initial oil saturation before chemical slug injection) can make some difference in final oil saturations levels achieved. Conditions where the high permeability cores contained higher oil saturations to begin with (series without waterflood), were favorable for the formation of a moveable oil bank. The formation of an effective oil bank was very helpful in ultimately reducing the oil saturation in these high permeability cores to lower values (about 2%-3% lower). Overall, the core's permeability still had a significant impact of the effectiveness of the chemical slug in displacing oil.

The proportion of the oil/brine/surfactant in the middle-phase slug also affected the effective oil displacement. Experiments were conducted to compare middle-phase slugs with difference proportions of oil in the slug (whether over, under, or at optimal conditions). The results of the study showed that the chemical proportion in the injected slug had a significantly affect the effectiveness of the system. At near optimal conditions (≈ 50% brine/surfactant), the system was much more effective in

reducing oil saturation levels compared to the system with higher oil proportions (above optimal). As much as 13% oil saturation difference was indicated in these experiments. Displacement experiments conducted at suboptimal conditions indicated comparable ineffective chemical system performance. In order to maximize oil recovery potential of these chemical systems, selective conditions of the following order need to be adhered to:

Optimal >Under Optimal >>Above Optimal

A direct comparison of the results of the experiments conducted with a middle-phase slug and the straight chemical slug showed significant difference in effectiveness. The results indicated that the final oil saturations from the straight chemical slug experiments were much higher compared to saturations from the middle-phase slug experiments, at comparable brine permeability. Although both sets of experiments were formulated (brine salinity, component concentration, and experimental conditions) to be optimal, the straight chemical slug formulation was not as effective in oil displacement as the preequilibrated middle-phase slug was. The injection of the microemulsion slug resulted in much better performance. These results also indicated that doubling the treatment slug size favored the straight chemical slug experiments slightly more than the experiments with the middle-phase slugs. The larger straight chemical slugs (which corresponded with more active chemical component) appeared to be favored more over the middle-phase chemical slugs. Additional experiments will be needed to confirm this observation.

The results from the CT-monitored experiment lend excellent support to the observations made with regards to the effect of permeability on oil recovery potential. The experiments conducted in high permeability cores showed very good frontal sweep, indicative of favorable oil displacement. The experiments conducted in low permeability cores exhibited the opposite, in terms of significant fluid bypass indicated, representative of the amount of oil (greater than 25% oil saturation) remaining the core. CT-aided monitoring has emerged as a valuable tool in evaluating the treatment effectiveness of these chemical systems. Future displacement experiments need to be fully complemented with the routine use of these types of tools.

Results from the mobility control study indicated that the following procedures should be used to evaluate mobility control for chemical flooding applications.

- Determine relative permeability for the rock of interest.
- Calculate design mobility using the viscosities of oil and brine of interest from equation 1.
- Determine pressure differentials as a function of fluid velocity for rock that is completely saturated with the solution of interest. Mobility characteristics will be a function of polymer type, solution ionic strength, flow paths in the porous media, and fluid velocity.
- Calculate solution mobility using equation 3 and compare with the design mobility.

The polyacrylamide polymers studied during this project were adversely affected by solution ionic strength. This included two polyacrylamide polymers that differed by the anionic character of the polymer. The polymer of lower anionic was designed for use in higher salinity brines. In this work, however, the testing conditions were too harsh, and good mobility control would not be achieved even for high permeability rock and low viscosity oil. This product may perform well at lower salinities, but these conditions were not tested. A second polyacrylamide polymer prepared in a lower salinity brine performed slightly better but was still unsuitable for use with high viscosity oil. Polyacrylamide

polymers prepared in relatively fresh water should provide adequate mobility control for oil viscosities up to or even greater than 19 cP.

Xanthan biopolymer is less salt sensitive. At the same salinity and concentration, the Xanthan biopolymer provided greater mobility control characteristics than the polyacrylamide polymer. At low salinity, however, this comparison may not apply. The flow results obtained in this study in consolidated core compared well with results from studies in the literature of flow through sandpacks of similar or higher permeability. Correlations reported in the literature study should be useful for predicting Xanthan mobility characteristics in high permeability consolidated core.

One coreflood was conducted on a polymer with poor mobility control characterisitcs. Final average oil saturation after completion of the test was 18.3%. Oil saturation was fairly uniform throughout the core, in contrast to a previous test, where the oil saturation at the core inlet was much lower than at the core outlet. Additional studies will be required to more systematically compare oil recoveries as a function of mobility control characteristics of the chemical systems, however.

The parameters required to utilize the UTCHEM simulator for chemical flooding (surfactant/polymer or alkaline/surfactant/polymer flooding) were reviewed. To use this program to help simulate results of CT-monitored laboratory coreflooding experiments. a work station that will give at least 100 times faster than the Micro VAX/VMS^{TM} computer is desirable. The minimum required RAM is 65 megabytes.

5.0 REFERENCES

Akstinat, M. H. *Surfactants for Enhanced Oil Recovery Processes in High Salinity Systems - Product Selection and Evaluation.* Enhanced Oil Recovery. Elsevier Science Publishers, NY 1981, pp. 43-62.

Bhuyan, D. *Development of An Alkaline/Surfactant/Polymer Compositional Reservoir Simulator.* Ph.D. Dissertation, University of Texas at Austin, December 1989.

Boneau, V. K. and R. L. Clampitt. *A Surfactant System for the Oil-Wet Sandstone of the North Burbank Unit. J. P. T., May 1977,* pp. 501-506.

Buckley, S. E. and M. C Leverett. *Mechanism of Fluid Displacemenit in Sands.* Trans. of AIME, Vol.146 1942, pp. 107-116.

Camilleri, d., A. Fil, G. A. Pope, B. A., Rouse, and K. Sepehrnoori, *Improvements in Physical-property Models Used in Micellar/Polymer Flooding, SPERE* (November 1987) pp. 433- 440.

Chang H. L., H. M. Rikabi, W. H. Pusch. *Determination of Oil/Water Bank Mobility in Micellar-Polymer Flooding.* J. Pet. Tech., July 1978, pp. 1055-1060.

French, T. R. and C. Josephson. *Alkaline Flooding Injection Strategy.* Department of Energy Report No. NIPER-563, September 1991.

French, T. Evaluation of a Site in Hepler (KS) Oil Field for a Surfactant-Enhanced Alkaline Chemical Flooding Project and Supporting Research. NIPER/BDM-0073, September 1994.

Gall, Bonnie L. *CT Imaging of Enhanced Oil Recovery Experiments.* Department of Energy Report No. NIPER-611, December 1992.

Glinsmann, G. R. Aqueous Surfactant Systems for In Situ Multiphase Microemulsion Formation. U.S. Patent No. 4,125,156. November 14 1978.

Goherty, W. B., H. P. Meabon, and H. W. Milton, Jr. *Mobility Control Design for Miscible-Type Waterfloods Using Micellar Solutions.* J. Pet. Tech., Feb. 1970, pp. 141-147.

Healy, R. N., R. L. Reed, and D. G. Stenimark, *Multiphase Microemulsion Systems. SPEJ.* (June 1976) 16 pp. 147- 160.

Hejri, S., G. P. Willhite, and D. W. Green. *Development of Correlations to Predict Biopolymer Mobility in Porous Media.* SPE Res. Eng., Feb. 1991, pp. 91-98.

Hirasaki, G. J. *Interpretation of the Change in Optimal Salinity with Overall Surfactant Concentration, SPEJ.* (Dec. 1982) 22 pp. 971-982.

Lchne, A. *Phase Behavior modeling in Surfactant Flooding.* DOE Report RF--5/91, May 1991. NTIS Order No. DE93-752942.

Llave, F. M. and D. K. Olsen. *Development of an Automated System for Phase Inversion Temperature Measurements.* Department of Energy Report No. NIPER-318, June 1988.

Llave, F. M., B. L. Gall, and L. A. Noll. *Mixed Surfactant Systems for Enhanced Oil Recovery.* Department of Energy Report No. NIPER-497, December 1990.

Llave, F. M., B. L. Gall, T. R. French, L. A. Noll, and S. A. Munden. *Phase Behavior and Oil Recovery Investigations Using Mixed and Alkaline-Enhanced Surfactant Systems.* Department of Energy Report No. NIPER-567, March 1992.

Llave, F. M., T. R. French, and P. Lorenz. *Evaluation of Mixed Surfactants for Improved Chemical Flooding.* U. S. Dept. of Energy Report - NIPER-631, November 1992.

Llave, F. M. B. L. Gall, P. Lorenz, I. M. Cook, and L.J. Scott. *Screening of Mixed Surfactant Systems: Phase behavior Studies and CT Imaging of Surfactant-Enhanced Oil Recovery Experiments.* U. S. Dept. of Energy Report - NIPER-710, September 1993

Lorenz, P. B. and S. Brock. *Surfactant and Cosurfactant Properties of Mixed and Polysulfonated Surfactant by Phase Volume Measurements.* Department of Energy Report No. NIPER-256, October 1987.

Nelson, R. *The Salinity Requirement Diagram -- A Useful Tool in Chemical Flooding Research and Development.* SPEJ, April 1982. pp. 259-270.

Pope, G. A. and R. C. Nelson. *A Chemical Flooding Compositional Simulator. SPEJ.*, (October 1978) 18 pp. 339-354.

Prouvost, L., G. A. Pope, and B. Rouse, *Microemulsion Phase Behavior: A Thermodynamic Modeling of the Phase Partitioning of Amphiphilic Species. SPEJ.* (October 1985) 25 pp. 693-703.

Satoh, T, *Treatment of Phase Behavior and Associated Properties used in a Micellar/Polymer Flood Simulator.* Master's Thesis, University of Texas at Austin, August 1984.

Tomutsa, L. D., D. Doughty, S. Mahmood, A. Brinkmeyer, and M. Madden. *Imaging Techniques Applied to the Study of Fluids in Porous Media.* Dept. of Energy Report No. NIPER-485, August 1990.

Trushenski, S. P., D. L. Dauben, and D. R. Parrish. *Micellar Flooding – Fluid Propagation, Interaction, and Mobility.* Soc. Pet. Eng. J., Dec. 1974, pp. 633-642.

User's Guide for UTCHEM-V-5.01- *A Three-Dimensional Chemical Flood Simulator, Enhanced Oil and Gas Recovery Research Program, Center for Petroleum and Geosystems Engineering,* The University of Texas at Austin, April 1991.

Willhite, G. P. and J. T. Uhl. *Correlation of the Mobility of Biopolymer With Polymer Concentration and Rock Properties in Berea Sandstone.* in Water Soluble Polymers fir Petrolerum Recovery, Ga. A. Stahl and D. N. Schlutz, eds., Plenum Press, New York City 1988, pp. 101-119.

APPENDIX

Figures A-1 to A-12 show apparent viscosities as a function of shear rate for Alcoflood 935 polyacrylamide polymer solutions. The figures are grouped to allow comparison for each polymer concentration for the initial viscosities and for the viscosities after aging at 23 ° and 50 °C. The polymer solutions were prepared with polymer concentrations ranging from 500 to 2000 ppm in brines of different ionic strength. Table A1 shows the composition of the brines. The weight percent designation for each brine signifies an approximate equivalent sodium chloride solution without added divalent ion. The TDS for each solution is approximately 75% of the weight percent designation. The 10% brine is representative of the simulated North Burbank Unit brine that has been used in a number of studies performed at NIPER. The North Burbank Unit, Osage County, Oklahoma produces from the Bartlesville Formation, a Class 1 reservoir. Viscosities were measured for initial solutions and for solutions aged at 23 ° and 50 °C for one month. Solutions were observed for at least four months. Results are reported in the text. Solution viscosities were not greatly affected by aging at ambient temperature but were considerably reduced after aging at 50 °C. In addition, a white precipitate was observed for all samples aged at 50 °C. These observations would cause concern for use long term of this product at moderate temperature and high salinity reservoirs.

TABLE A-1 Brine Composition Used in Polymer Stability Tests

Compound	20% concentration, wt%	18% concentration, wt%	15% concentration, wt%	10% concentration, wt%	5% concentration, wt%
NaCl	13.30	11.97	9.98	6.65	3.33
$CaCl_2$	3.06	2.75	2.30	1.53	0.77
$MgCl_2$	0.40	0.36	0.30	0.20	0.10

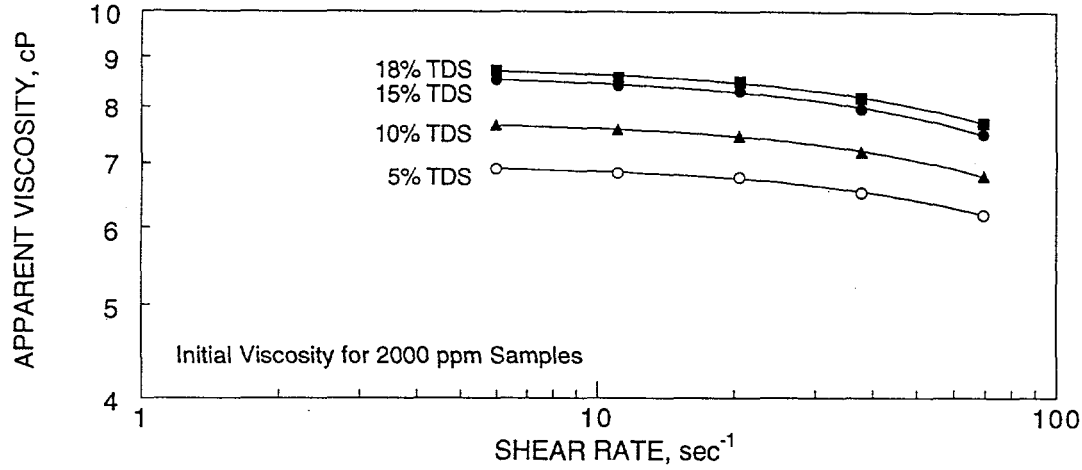

FIGURE A-1 **Initial viscosity of 2000 ppm polyacrylamide polymer, Alcoflood 935, in different salinity brines.**

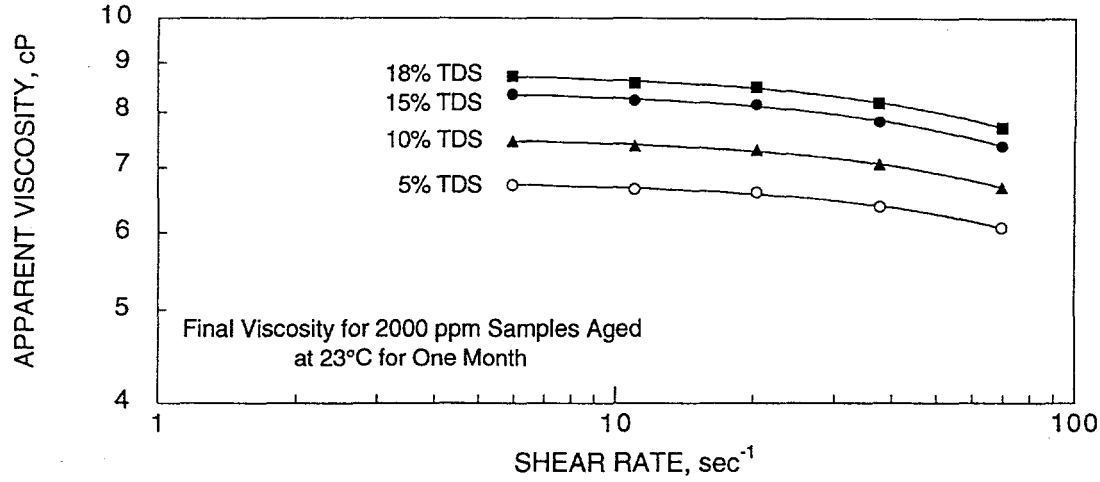

FIGURE A-2 **Apparent viscosity of 2000 ppm polyacrylamide polymer, Alcoflood 935, in different salinity brines after aging at ambient temperature.**

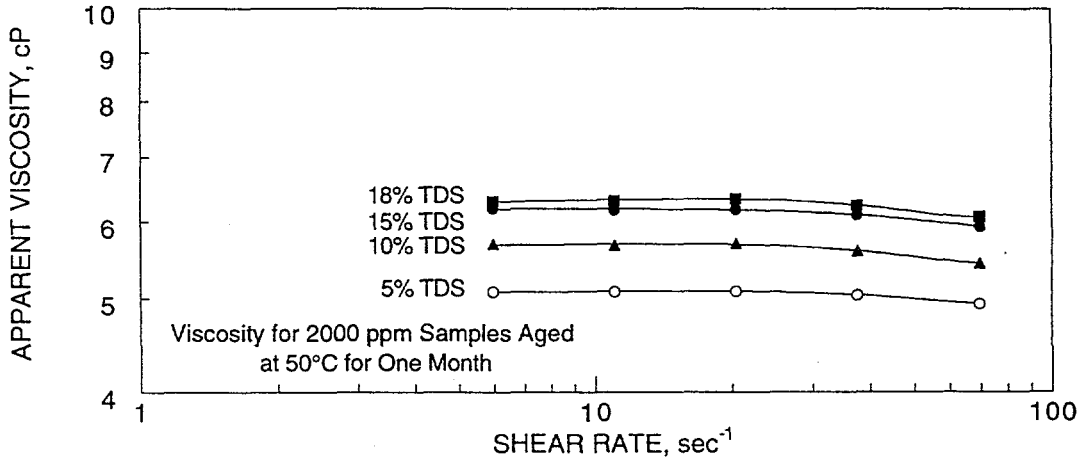

FIGURE A-3 **Apparent viscosity of 2000 ppm polyacrylamide polymer, Alcoflood 935, in different salinity brines after aging at 50 °C.**

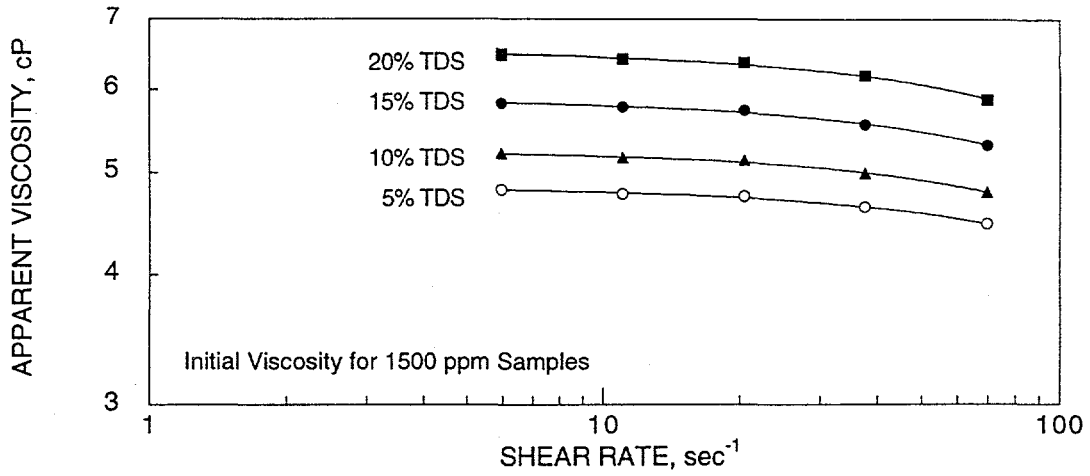

FIGURE A-4 **Initial viscosity of 1500 ppm polyacrylamide polymer, Alcoflood 935, in different salinity brines.**

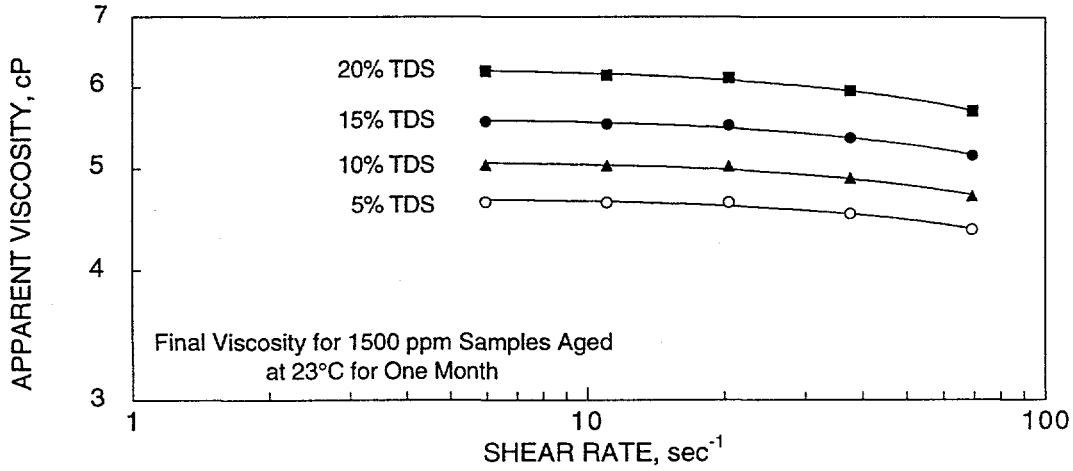

FIGURE A-5 **Apparent viscosity of 1500 ppm polyacrylamide polymer, Alcoflood 935, in different salinity brines after aging at ambient temperature.**

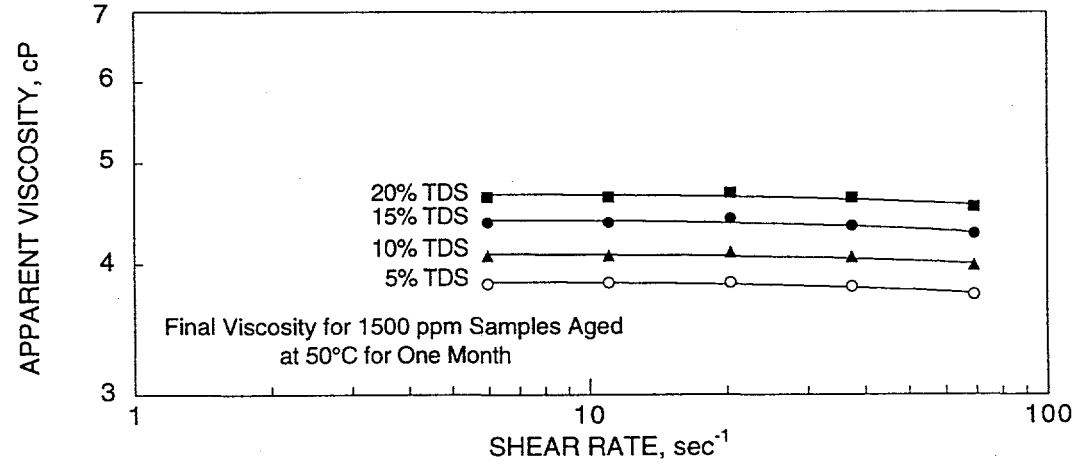

FIGURE A-6 **Apparent viscosity of 1500 ppm polyacrylamide polymer, Alcoflood 935, in different salinity brines after aging at 50 °C.**

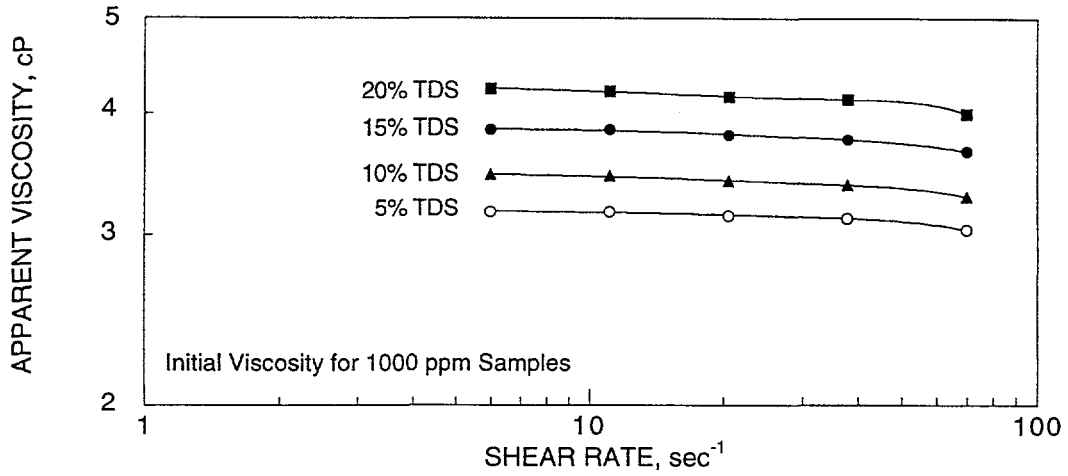

FIGURE A-7 **Initial viscosity of 1000 ppm polyacrylamide polymer, Alcoflood 935, in different salinity brines.**

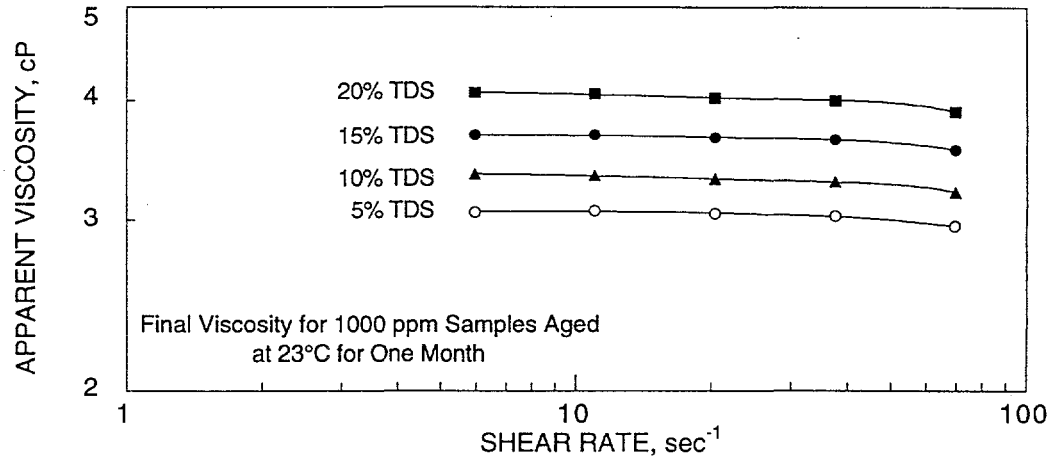

FIGURE A-8 **Apparent viscosity of 1000 ppm polyacrylamide polymer, Alcoflood 935, in different salinity brines after aging at ambient temperature.**

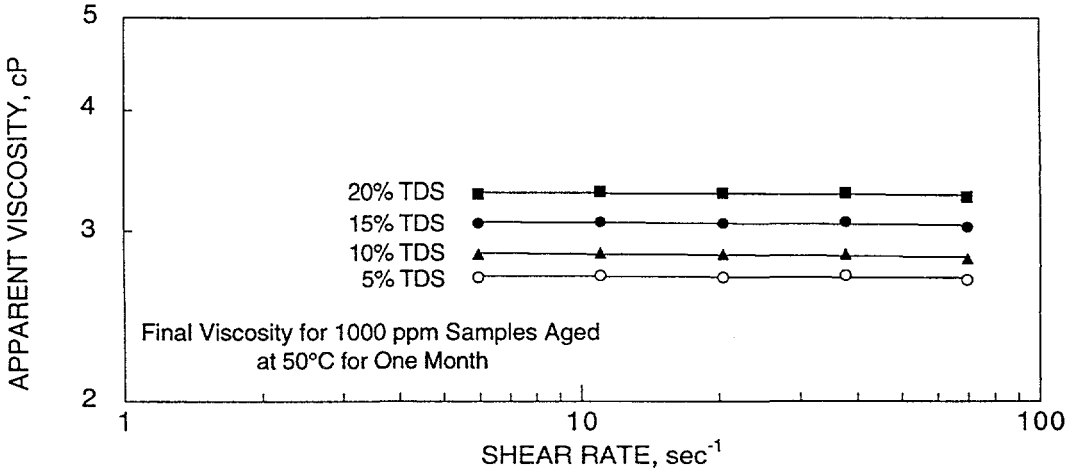

FIGURE A-9 **Apparent viscosity of 1000 polyacrylamide polymer, Alcoflood 935, in different salinity brines after aging at 50 °C.**

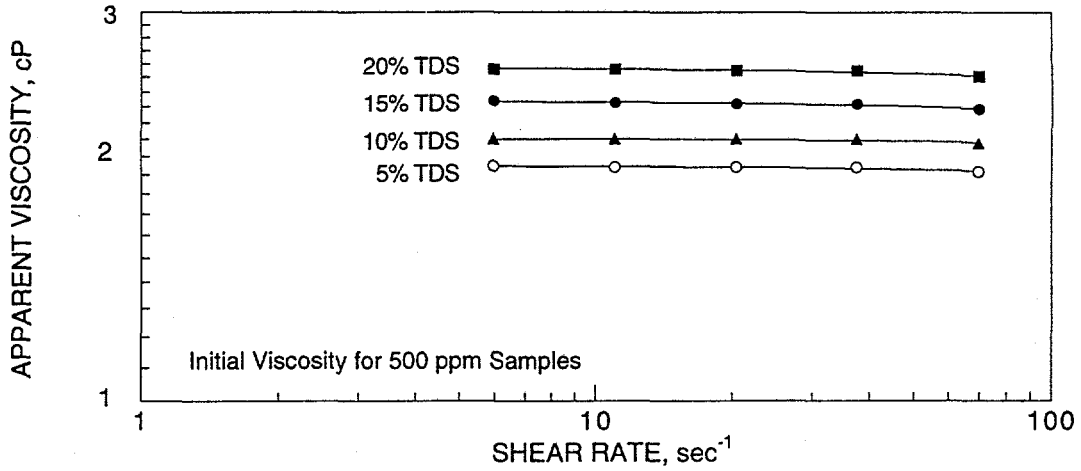

FIGURE A-10 **Initial viscosity of 500 ppm polyacrylamide polymer, Alcoflood 935, in different salinity brines.**

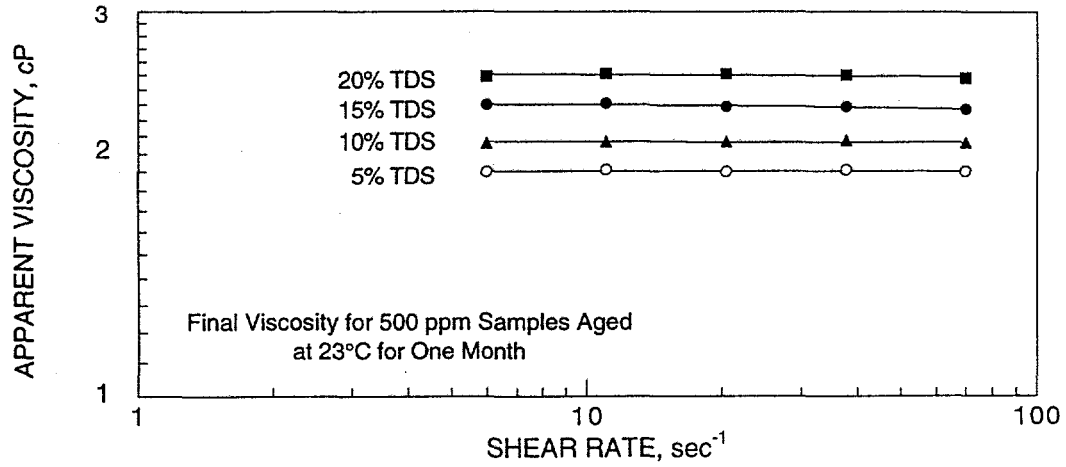

FIGURE A-11 **Apparent viscosity of 500 polyacrylamide polymer, Alcoflood 935, in different salinity brines after aging at 50 °C.**

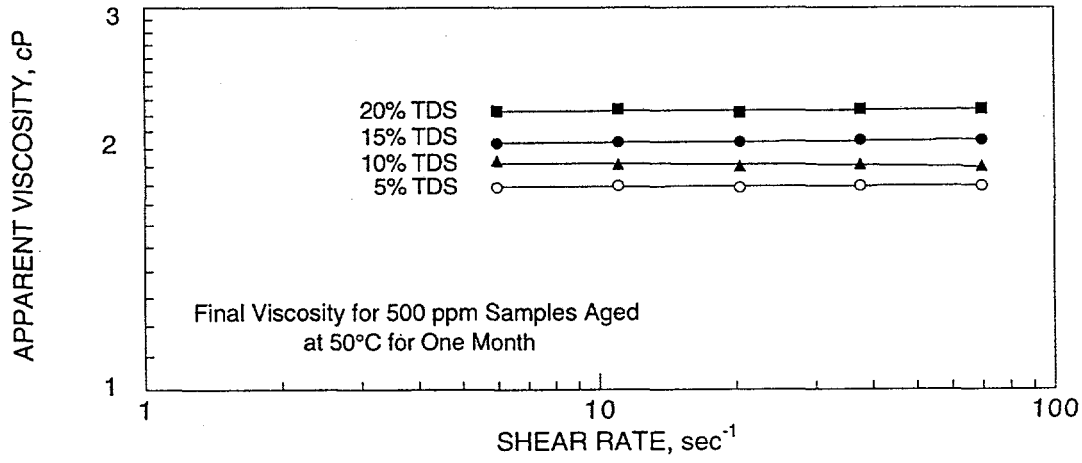

FIGURE A-12 **Apparent viscosity of 500 polyacrylamide polymer, Alcoflood 935, in different salinity brines after aging at 50 °C.**

Figures A-13 to A-15 show the apparent viscosities for the various polymers used in the mobility control study. Polymer preparation procedures make solutions with comparable viscosity from batch to batch.

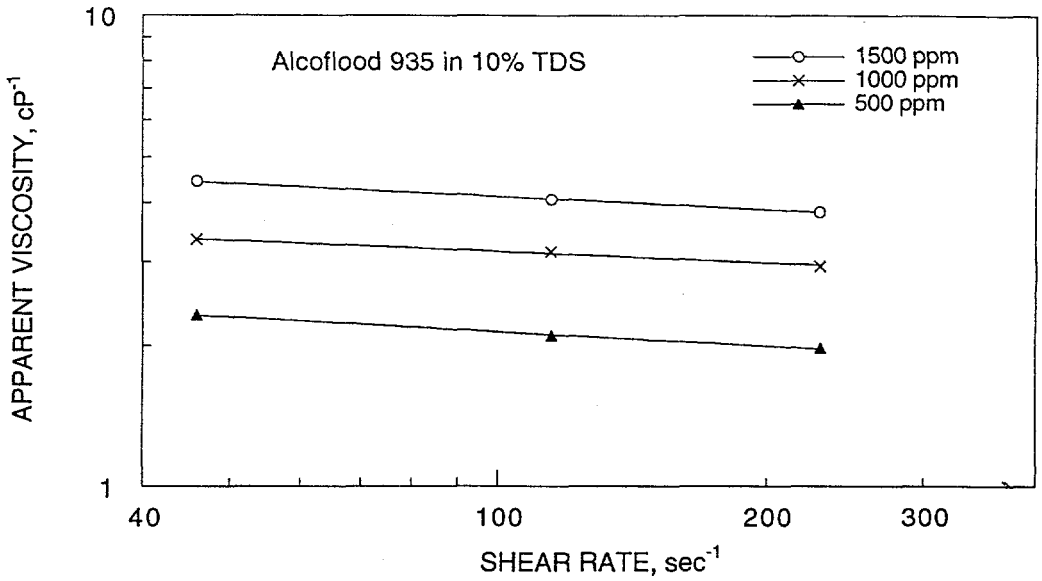

FIGURE A-13 **Apparent viscosity at ambient temperature of polyacrylamide polymer, Alcoflood 935 used in the polymer mobility control study. Viscosities agree with initial viscosity values measured in the polymer degradation studies.**

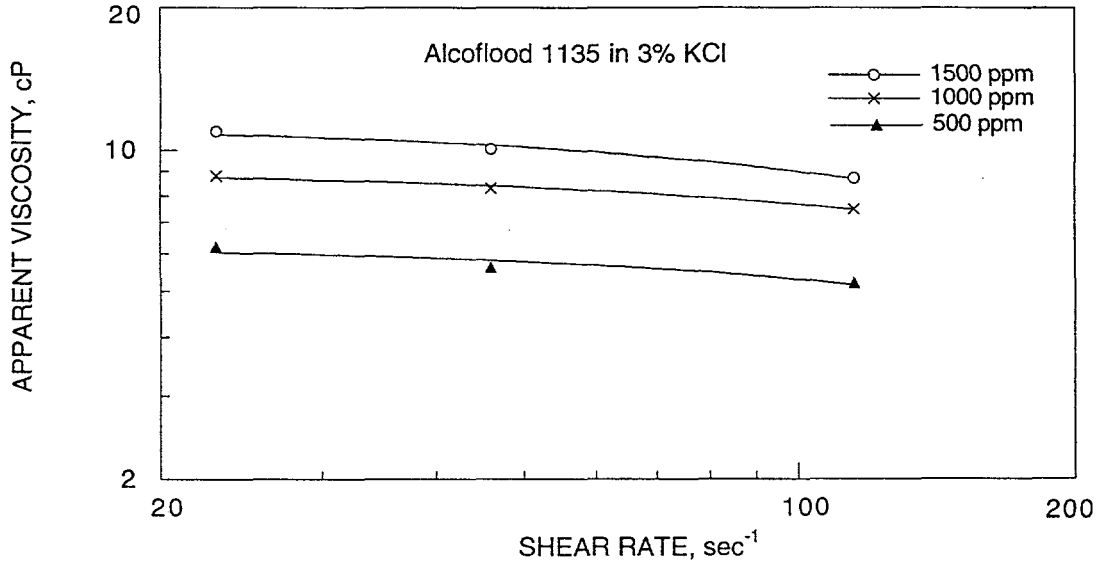

FIGURE A-14 **Apparent viscosity at ambient temperature of polyacrylamide polymer, Alcoflood 1135 used in the polymer mobility control study.**

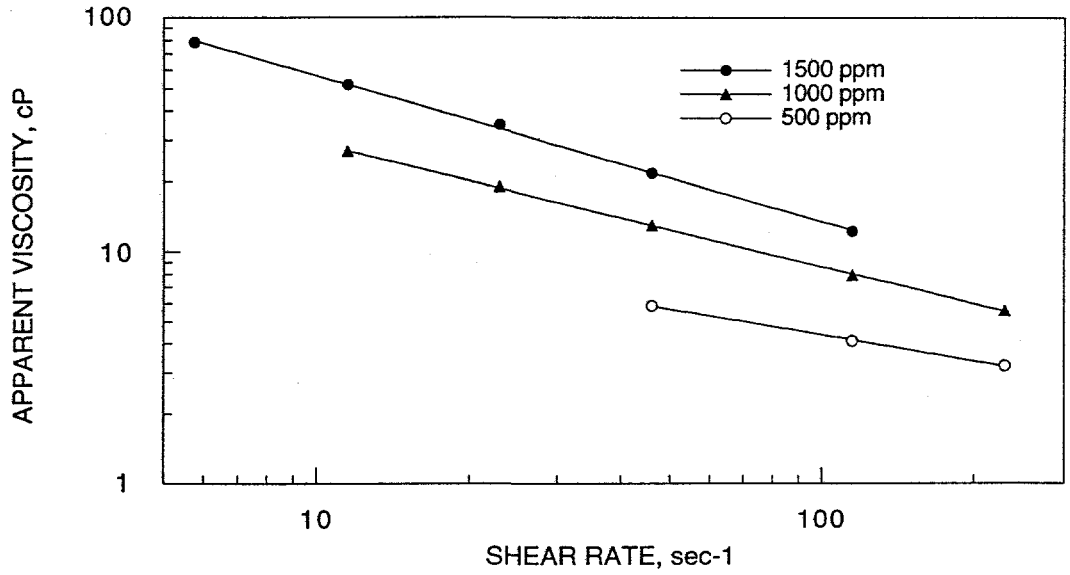

FIGURE A-15 Apparent viscosity at ambient temperature of Xanthan biopolymer, Flocon 4800C used in the polymer mobility control study.

☆U.S. GOVERNMENT PRINTING OFFICE: 1995 - 660-029/20062